Study and development of physical models to evaluate biological effects of ion therapy : the study of local control of prostate cancer

Marie-Anne Chanrion

Université Claude Bernard Lyon 1 et Universität Duisburg-Essen

THÈSE

Pour obtenir le grade de **DOCTEUR DE L'UNIVERSITÉ DE LYON**
Spécialité : **Physique**
de l'**École Doctorale de Physique et d'Astrophysique de Lyon**

et le grade de **DR. RER. MEDIC DE L'UNIVERSITÄT DUISBURG-ESSEN**
de la **Medizinischen Fakultät der Universität Duisburg-Essen**

Arrêté ministériel : 7 août 2006 et 6 janvier 2005 relatif à la cotutelle internationale de thèse

Présentée par

Marie-Anne Chanrion

Thèse dirigée conjointement par **Michaël Beuve et Wolfgang Sauerwein**

préparée à l' **UMR 5822, CNRS/IN2P3, Institut de Physique Nucléaire de Lyon; Université Lyon 1, Université de Lyon, Villeurbanne, France**

et à la **Klinik und Poliklinik für Strahlentherapie, NCTeam, Universität Duisburg-Essen, Universitätsklinikum Essen, Essen, Germany**

Study and development of physical models to evaluate biological effects of ion therapy: the study of local control of prostate cancer.

Numéro d'ordre: 304 - 2014
Thèse soutenue le Jeudi 18 décembre 2014

Jury composé de :

M. HERAULT Joël, Rapporteur
Mme TOMA-DAŞU Iuliana, Rapporteure
Mme JELEN Urszula, Examinatrice
Mme WITTIG Andrea, Examinatrice
M. SAUERWEIN Wolfgang , Co-Directeur de thèse
M. BEUVE Michaël , Co-Directeur de thèse

Contents

Acknowledgments

THANKS! I would like to warmy thank all the members of the jury who have accepted to examine my thesis: Joël Herault, Iuliana Toma-Daşu, Urszula Jelen and Andrea Wittig.

I would like to thank the institutions that hosted me for this PhD work: the Radiotherapy Department of University of Marburg directed by Prof. Dr. Rita Engenhart-Cabillic and the CAS-Phabio group directed by Dr. Denis Dauvergne from IPNL of University Lyon 1. Thank you for your continuous support!

I would like to express my sincere gratitude to my supervisors: Michaël Beuve et Wolfgang Sauerwein. Thank you for your mentorship, scientific advices, and support. Beyong science, thank you very much for your patience and understanding!

Muchas gracias to Alina Santiago who shared, almost everyday, my joys, pains, excitements, weariness, with whom I had very interesting scientific conversations, but not only scientific!!! Muito obrigada to Micaela Cunha with whom I mostly shared the office in Lyon and grazie mille to Caterina Monini: it was always great to be with you two!

A general thank you for all my collegues in Marburg, Lyon, Essen, everybody from the staff (administration and IT) that made everything working for this collaboration! A particular thank goes to Sylvie Flores from the doctoral school directed by Christophe Dujardin: thank you for your support.

I would like to thank everybody with whom I spent the last years: flatemates, old and not-so-old friends from Marburg, Lyon and elsewhere!! Thank you for all the good moments! Each of them counts in my heart!

Great thanks to my family and our friends!

Abstract

External beam radiotherapy (EBRT) is a therapy technique aiming at treating locoregional tumors with high efficiency. However, many tumors remain uncontrolled. Newest EBRT techniques always aim at increasing the dose to the tumor while sparing the surrounding healthy tissues. Carbon-ion beam therapy is one of these promising techniques. The number of clinical centres offering carbon-ion beam radiotherapy has been increasing over the world for the last decade. This keen interest spread after very promising results from pilot projects at Berkeley (USA), Chiba (Japan) and Darmstadt (Germany). The theoretical advantages of carbon-ions are better spatial selectivity in dose deposition and better efficiency in cell killing. They have thus the potential to increase the control of tumors, particularly for unresectable radioresistant tumors.

In high linear-energy-transfer (LET) radiations, such as carbon-ion beams, biological effects vary along the ion track, hence, to quantify them, specific radiobiological models are needed. There exist several radiobiological models based on very different theoretical approaches and approximations. They were created and improved in each of the pilot institutions. At the current state of knowledge, no convergence between the model results seems to be possible in the very near future. Clinically employed radiobiological models are the Local Effect Model (LEM) developed in Germany and implemented in CE-certified treatment planning systems, the National Institute of Radiological Science (NIRS) model employed in Japanese centres with passive beam delivery systems and the microdosimetric kinetic model (MKM) in Japanese centres with active scanning beam delivery systems.

Mathematical models can be used to predict, for instance, Tumor Control Probability (TCP) and then evaluate treatment outcomes. For a given radiation dose delivered in a defined schedule, TCP models calculate the level of tumor control.

In the first step, this work studies the influence of the LEM (first version) input parameters on the TCP predictions in the specific case of prostate cancer. Several published input parameters and their combination were tested. Their influence on the dose distribution calculated in a water phantom and in a patient geometry was evaluated. Changing input parameters induced clinically significant modifications of mean dose, spatial dose distribution, and TCP predictions. TCP predictions were found more sensitive to the parameter threshold dose (D_{t}) than to the biological parameters α and β.

In the second step, methods for evaluation, comparison and optimization of clinical protocols are presented. For defined boundary conditions, "optimized" D_{t} are proposed for the treatment of prostate cancer.

The theoretical methodologies developed in this thesis can only be validated when they will be challenged with clinical results from on-going trials. More generally, the improvement of radiobiological models and the comparison of clinical results from different institutions will be only achieved when more patient outcome data with well-defined patient groups, fractionation schemes, well-defined end-points and harmonized reporting will be available.

Résumé

La radiothérapie externe est un traitement anticancéreux locorégional efficace et curatif. Néanmoins, il y a toujours des malades qui meurent de tumeurs locales non-contrôlées. Les nouvelles techniques en radiothérapie visent toujours à trouver un moyen d'augmenter la dose à la tumeur tout en réduisant au minimum la dose aux tissus sains adjacents. Une des dernières techniques innovantes est l'hadronthérapie par ions carbone. Ces dix dernières années ont vu augmenter le nombre de nouveaux centres d'hadronthérapie dans le monde avec des faisceaux d'ions carbone, forts des résultats promettant des projets pilotes Berkeley (USA), Chiba (Japon) et Darmstadt (Allemagne). Les avantages théoriques des ions carbone sont: une meilleure balistique et une meilleure efficacité dans la destruction des cellules tumorales. Ainsi cette technique a le potentiel d'augmenter le contrôle des tumeurs, particulièrement pour celles inopérables et radiorésistantes. Les effets biologiques varient le long de la trajectoire des ions de haut TEL (Transfert d'Énergie Linéique) comme les ions carbone. Ainsi des modèles radiobiologiques sont nécessaires pour quantifier les effets biologiques. Il existe plusieurs modèles radiobiologiques qui reposent sur des approches et des approximations théoriques différentes. Ces modèles ont été développés au sein de chacune des institutions où se déroulaient les projets pilotes. Au stade actuel des connaissances, il semble peu probable d'atteindre une rapide convergence des résultats produits par ces différents modèles. Parmi les modèles radiobiologiques utilisés en clinique, il y a le Local Effect Model (LEM), développé en Allemagne et implémenté dans les systèmes de planification de traitement certifiés CE, le modèle de la National Institute of Radiological Science (NIRS), employé dans les centres japonais d'hadronthérapie possédant un système d'irradiation passif, et le Microdosimetric Kinetic Model (MKM) employé dans les centres japonais d'hadronthérapie possédant un système d'irradiation actif en mode pencil beam scanning.

Les modèles mathématiques peuvent être utilisés, par exemple, pour la prédiction de la Probabilité de Contrôle Tumoral (PCT) permettant ainsi d'évaluer les résultats cliniques d'un traitement. Pour une dose délivrée, avec un fractionnement et un étalement défini, les modèles de PCT calculent le niveau de contrôle tumoral.

Dans un premier temps, ce travail étudie l'influence des paramètres d'entrée du LEM (version I) sur les prédictions de PCT pour le cas spécifique d'une tumeur de la prostate. Plusieurs publications ont proposé des valeurs pour les paramètres d'entrée du LEM I et la combinaison de ces paramètres est testée. Ainsi leur influence sur la distribution de dose calculée dans un fantôme d'eau et dans une géométrie patient a été évaluée. Le changement des paramètres d'entrée a permis de mettre en évidence des modifications significatives sur les distributions de dose en termes de dose moyennes mais également de PCT. De plus, les prédictions de PCT sont apparues plus sensibles au paramètre dose seuil (D_{t}) qu'aux paramètres biologiques α et

β.
Dans un second temps, des méthodes pour l'évaluation, la comparaison et l'optimisation des protocoles cliniques sont présentés. Dans des conditions bien définies, des valeurs "optimisées" de D_{t} sont proposées pour le traitement du cancer de la prostate.
Les méthodes théoriques développées dans cette thèse pourront être validées ou non lorsqu'elles seront confrontées aux futurs résultats cliniques. Plus généralement, l'amélioration des modèles radiobiologiques et des méthodes de comparaison des résultats cliniques entre les institutions nécessite plus des résultats cliniques avec des cohortes bien définies de patients, des plans de traitements identiques, des endpoints bien définis et enfin des rapports de traitement harmonisés.

Introduction and project context

Introduction and project context

Cancer is a disease due to the uncontrolled growth and spread of cells. In the treatment of cancer, external beam radiotherapy (EBRT) with photons or electrons is a modality of choice with surgery and chemotherapy. EBRT aims at inactivating cancer cells by targeting the cancer cell DNA or the direct cancer cell environment. In the same time, surrounding healthy cells should be spared as much as possible. To obtain this differential effect, several strategies may be implemented by taking advantage of either better spatial selectivity in dose deposition or better efficiency in cell killing. One possibility for increasing the ballistic selectivity is to resort to light ions. Ions have the advantage of depositing the maximum of energy at the end of their range. The linear energy transfer (LET, expressed in keV/μm) is the energy transferred per unit distance along the trajectory of a charge particle and increases along the ion path until reaching a maximum near the Bragg-peak. Biological experiments have demonstrated that light ions have a better cell killing efficiency than photons or electrons. This means, that for the same dose deposited, more cells are killed with a light ion beam. Furthermore, the increase in cell killing efficiency has also been found to be strongly correlated with LET: it increases with the LET until the latter reaches a defined maximum. After the maximum, the cell killing efficiency decreases due to the overkill effect. Clinical photon and proton beams are considered to be low-LET radiations, while clinical carbon-ion and neutron beams are considered to be high-LET radiations. Hence, carbon-ion EBRT has the theoretical advantage of offering both the ballistic selectivity and a LET high enough for a high cell killing efficiency around the Bragg-peak. To benefit from both advantages it is preliminary necessary to know the dose distribution and to predict the cell lethal damages. Radiobiological models aim at quantifying these lethal events along the ion track. They require, as any model, input parameters. Consequently, the determination of appropriate input parameters is mandatory to optimize carbon-ion therapy.

This doctoral research has been realized under a “cotutelle”, administrated jointly by University of Lyon 1 and University of Duisburg-Essen. It is funded by University of Marburg, and the traveling costs between the institutions are funded by the French-German University (Deutsch-Französische Hochschule/Université Franco-Allemande). This collaboration gathers Prof. Michaël Beuve (Lyon), Prof. Andrea Wittig (Marburg) and Prof. Wolfgang Sauerwein (Essen) around the topic of radiobiological modeling of therapeutic carbon-ion beams. Radiobiological modeling for carbon-ion beams needs interdisciplinary knowledge: physics, biology and medicine, and particularly expertise in high-LET radiations. The university hospital of Essen has treated cancer patients with neutron beams since the 80s, and still refer some patients to neutrontherapy in South Africa (iThemba labs), or to protontherapy in France (Nice). In Lyon, several scientific teams (engineers, biologists, physicists and computer scientists) are involved in the research phase for the project of particle therapy center ETOILE. The Marburg

ion therapy center (MIT) will soon be opening and will treat patients with a clinical treatment planning system (TPS) based on the radiobiological local effect model (LEM). This work takes part of the pre-clinical research and aims at answering the following questions:

- What are the influences of the radiobiological model LEM parameters for tumor control probability predictions?
- What are the possible methods to optimize clinical protocols in carbon-ion therapy for prostate cancer?

After introducing physical and biological concepts of radiobiological modeling for particle therapy, the influence of the LEM input parameters on the prediction of tumor control probability for prostate cancer will be studied. It will be followed by the presentation of strategies to optimize clinical protocols for prostate cancer. Finally, a general discussion will end the manuscript.

Part A

General concepts and state of the art

I

Physics

Contents

1 Ion interactions with matter

Ions can interact with the surrounding matter with multiple processes and the energy loss to the matter can be transferred either to electrons or to nuclei. The average energy loss of a charged particle in a medium per unit length is called the stopping power. At therapeutic energies ($\sim 10^2$ MeV/n) there is a predominance of the interaction between the incident particle and electrons (dominance of the electronic stopping power). At the lowest energies, the interaction between the incident particle and nuclei through elastic collision (nuclear stopping power) has to be considered in the calculation of the total stopping power. Towards the end of the ion's range, the energy loss increases to a maximum: the Bragg-peak. A relatively large fraction of the incident carbon ions undergo inelastic nuclear reactions resulting in their break into fragments and the breaking of atomic nuclei of the matter. Some of these ion fragments carry a large part of the incident ion energy and may travel a little further, depositing dose behind the Bragg-peak. Figure I.1 depicts depth dose distributions of three carbon-ion beams.

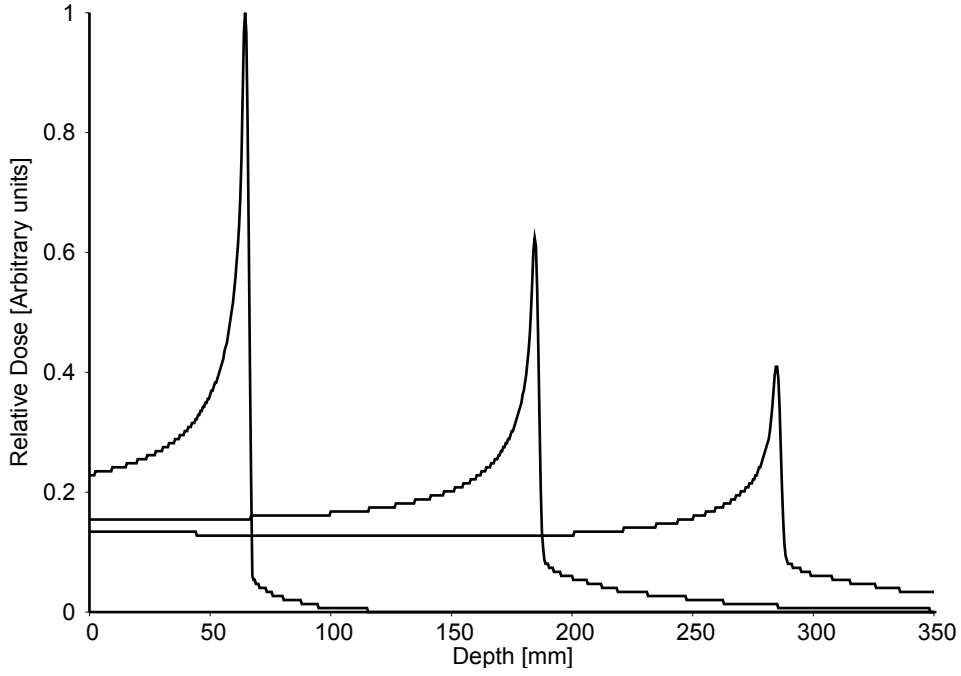

Figure I.1: Transversal depth dose distribution in water of single spot of carbon-ion (FWHM = 5 mm) beam calculated with TRiP98 for three beams of initial energy of 51, 170 and 241 MeV/n.

2 LET

The LET is defined as "the mean energy, dE, lost by a charged particle owing to collisions with electrons in traversing a distance dl in matter" (Beringer *et al.* (2012)). The units are J/m but it is generally given in kiloelectron volt per mircrometer (keV/μm). The International Commission on Radiation Units and Measurements (ICRU) defined the LET as a "restricted stopping power": only the energy losses with energy lower than a defined cut-off Δ are consid-

ered. Consequently, the energy transferred to the medium around the particle:

$$\mathrm{LET}_{\Delta} = \frac{\mathrm{d}E_{\Delta}}{\mathrm{d}l} \tag{I.1}$$

$\mathrm{d}E_{\Delta}$ is the energy lost by a charged particle due to electronic collisions when traversing the distance $\mathrm{d}l$. When no cut-off is applied, the LET is said to be "unrestricted" or stopping power. Generally, radiations considered as low-LET radiations (LET $< 10\ keV/\mu$m) are X-rays, gamma rays or light charged particles (*e.g.* electrons). When interacting with the surrounding medium, these radiations set in motion electrons ionizing the matter. Other radiations like neutrons (producing charged recoil-ions) or heavy charged particles (directly ionizing) are considered to be high-LET radiations (LET $> 10\ keV/\mu$m). The difference between low- and high-LET radiations is on the distribution of ionizing events at the molecular scale: for low-LET, sparse events are distributed far apart, and, on the contrary, there are densely spaced distributed for high-LET radiations (Beringer *et al.* (2012)).

3 Accelerator

The ideal medical accelerator should be compact. It should be possible to change quickly the beam energy and intensity. Furthermore, the beam line should be reliable and, last not least, with a cost as minimal as possible. The conventional photon radiotherapy is the modality of choice in EBRT and requires a "simple" and compact linear accelerator. Light particles like proton or carbon-ions require however more complex technologies to accelerate particles to some hundreds of MeV/n. Clinical proton beams can be obtained either by synchrotron or cyclotron, however, for dual-beam machines (proton and carbon), a synchrotron is recommended. With a synchrotron, the beam energy can be changed without having to degrade the beam with physical materials (Wambersie *et al.* (1992)).
The first proton therapy treatment was delivered at the Berkeley Lab in 1954 using a 184-inch cyclotron. In the 70s, treatments with heavier ions were delivered using the Bevalac synchrotron (Berkeley Lab (2010)). Europe's first proton therapy program ran from 1957 to 1976 in Uppsala (Sweden). After US and Europe, Japan started ion therapy with a proton beam in 1979 at the National Institute of Radiological Sciences in Chiba (NIRS). In 1994 the world's first medical synchrotron accelerator started treating patients. Until March 2014, 8227 patients received treatment with carbon beam at NIRS (NIRS (2014)). In 1997, the German Clinical Pilot Project started at the heavy ion physics research center Helmholtzzentrum für Schwerionenforschung (GSI) in Darmstadt (Germany). This project aimed at treating cancer patients with carbon-ions using the synchrotron beam of the facility. The pilot project ended in 2010, 440 patients were treated. The technical and clinical experience from the pilot project was a prerequisite for the design of the dedicated clinical particle therapy center of Heidelberg where treatments started in 2009. From physics research centers, particle therapy treatments are now delivered in medical based facilities. For carbon-ion therapy this transfer of technology has allowed the emergence of new designs of synchrotron accelerators: from the injection linac to the beam extraction.

4 Beam delivery

The rationale behind the use of ion beams in radiation therapy lies in their physical property of depositing most of the dose at a well-defined depth, the Bragg peak. In order to irradiate an extended target volume, multiple individual Bragg peaks of single narrow mono-energetic beams need to be juxtaposed to form the so-called Spread Out Bragg-Peak (SOBP) (Figure I.2).

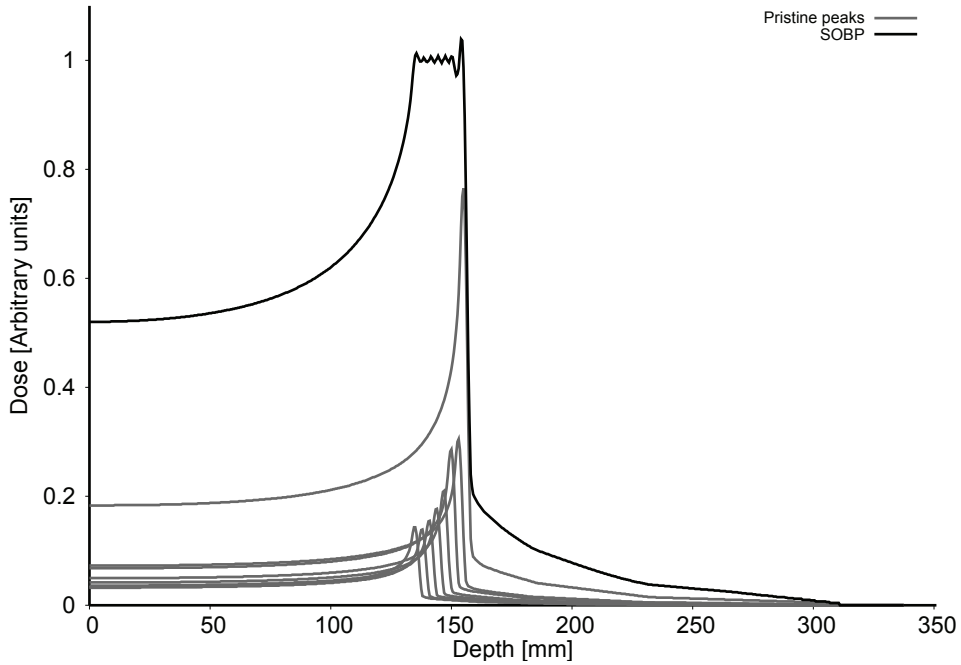

Figure I.2: Example of a spread-out Bragg peak: 8 beams of several energies, called pristine peaks, can be added-up so that the dose in a defined area is homogeneous.

The highest possible degree of target conformation may be achieved with scanning delivery systems (Haberer *et al.* (1993), Pedroni *et al.* (1995), Furukawa *et al.* (2007)). In such systems, the target is sliced into layers of equal beam energy, and each layer is covered by a grid of points receiving successively a dose. The ion beam is deflected by magnetic fields to paint the tumor transversely in a raster fashion, each circular-shaped pencil beam has a Gaussian profile (Figure I.3). The in-depth Bragg peak placing is achieved by either active energy variation at the accelerator level or passive energy variation with range shifter plates. Hence, the active beam delivery allows a control of the beam fluence and energy for each grid point. Historically, two facilities offered this spot scanning system: GSI and Paul Scherrer Institute (PSI) in Switzerland. This technology has been transferred to European particle-therapy center like HIT (Heidelberg, Germany), MIT (Marburg, Germany), CNAO (Pavia, Italy) and MedAustron (Vienna Neustadt, Austria).

The passive beam delivery system uses scattering elements to broaden the beam and to shape it. Range filters, modulators and a collimator finalize the beam shaping. This beam shaping configuration is used at most of Japanese particle therapy facilities. However, a new beam line at NIRS Chiba also offers a pencil beam delivery.

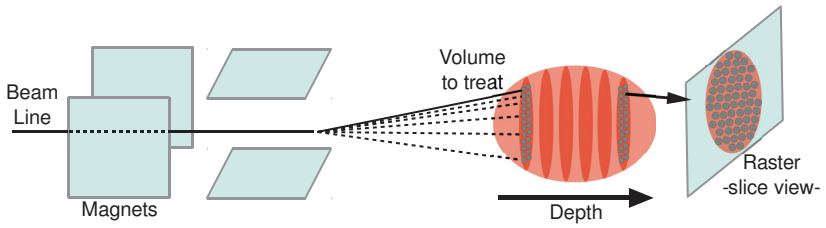

Figure I.3: Schematic representation of the beam spot scanning delivery system. The beam of a defined energy is deviated by magnets in order to "paint" the tumor with dose spots..

The active beam delivery system offers a higher degree of conformation compared to the passive delivering system. However, the dose covering in the target is extremely sensitive to organ movements.

For most facilities, the beam is transported horizontally or with a 45 or 90 degree angle. This angle limitation reduces the possibility of beam geometry optimization to achieve the best dose conformation in the target volume. Ideally, any particle therapy center should have a 360 degrees gantry for the set of the optimal beam angle for the therapy. The main challenge for designing a gantry with 360 degrees rotation is to bend the high energetic carbon-ion beam with a light and low-cost system. Powerful magnets are needed to deflect ion beams. The first rotational isocentric gantry for carbon-ion beam is now operating at HIT. A superconducting gantry is under commissioning at NIRS and planned to be used for patient treatments in March 2015 (Iwata (2013)).

II

Biology

Contents

1 General concepts and definitions

When cells are exposed to ionizing radiation, their structure may be damaged. In particular, when the damages cannot be repaired as well as when they are wrongly repaired, ionizing radiations may cause the cell to die. One aspect of radiobiology is to investigate the dose response relationship at the human, tissue or cell level. The dose response relationship is classically quantified after *in vitro* or *in vivo* experiments. Within a population of tumor cells, some of the cells are considered to be "clonogenic cells". This means that they can produce large amount of daughter cells to maintain or enlarge the cell colony. There also exist stem-like cancer cells in a population of tumor cells. They possess the same ability as normal stem cells: the capacity to produce many differentiated tumor cells. The role of stem-like cancer cells in the cancer resistance or relapse is, however, not clearly known and the subject of scientific discussion.

2 Mechanisms of cell death

After being irradiated, a cell may be damaged in several ways. Very soon after the deposition of energy, so-called "free radicals" may appear and change the chemical state of cells. Some free-radicals are highly reactive and may initiate various events like cell death, mutations or chromosomal aberrations. When DNA molecule is hit, single-(SSB), double-stand break (DSB) or base damages may occur. The mechanisms of cell death are:

- Apoptosis also called the "programmed" cell death. The cell rapidly "kills" itself. This form of death is the "ideal" way to get rid of tumor cells: clean and quick.

- Autophagy. The cell "eats" its own cytoplasm. This can lead to the production of macromolecules and can release energy for other cell to survive; this effect is considered "pro-survival". However, autophagy can also lead to the death, in a similar way as apoptosis.

- Senescence. The cell that undergoes senescence loses its capacity to proliferate permanently. It is an indirect cell death.

- Necrosis is the uncontrolled, irreversible and chaotic form of cell death. Contrary to apoptosis, infection, inflammation or ischemia usually occur when the cell dies through necrosis.

- Mitotic catastrophe/death appears when the cell undergoes mitosis while DNA damages are unrepaired or wrongly repaired. The presence of chromosome aberrations may lead to the loss of proliferation capacity or trigger other form of cell death.

3 Mechanisms of cell repair

Depending on the damage type and severity, several repair mechanisms will act; for instance base excision repair, homologous recombination or non-homologous end joining. More details about these mechanisms can be found in reference textbooks (*e.g.* Joiner and van der Kogel

(2009)). Each mechanism of cell repair acts preferably in a particular phase of the cell cycle. Hence, during the time needed for the reparation, the cell cycle may be paused, which may delay the repopulation.

4 Dose-response to radiation

a) Survival curves

The surviving fraction of cells in an irradiated cell population may be measured and is typically plotted on a logarithmic scale against dose on linear scale: the so-called cell survival curve. With low-LET radiations, the cell survival curve is usually described with a shoulder region at low dose, which then is followed by a linear curve. Contrarily, high-LET radiations do not have a "shoulder region". The efficiency of lethally damaging a cell can be described as the number of cells that die per unit of dose deposited. In particular, with increasing LET, this efficiency increases up to a maximum. From this optimal LET for cell inactivation, the efficiency reduces as the biological effectiveness does. This phenomenon is called "overkill effect" (Joiner and van der Kogel (2009)). Many mathematical models describing cell survival curves have been proposed, the most clinically used being the "linear quadratic model" (LQ). The probability of cell survival S exposed to a macroscopic dose D is:

$$S(D) = exp(-(\alpha D + \beta D^2)) \tag{II.1}$$

The parameters α and β characterize the cellular radiosensitivity to fractionation. In a mechanistic interpretation of the linear quadratic model, α is an estimate of initial lethal damages and β an estimate of sublethal damages (Douglas and Fowler (1976)). α and β parameters depend on kinetic properties of the cells (slow or rapid renewal). They have an influence on the choice and the optimization of the treatment dose needed to obtain the differential effect between tumor and healthy tissues. In the "classic radiobiology" (Bentzen and Joiner (2009)), the α/β ratio is an important parameter to characterize the cell radiosensitivity. It is generally assumed that when this ratio is "high" (>10 Gy), the tissues are mostly tumors and considered as "acutely responding tissues" (*i.e.* early responding tissues). When the ratio is "low" (< 3 Gy), the tissue is generally a healthy tissue with late responding properties. The radiosensitivity can also be characterized for each phase of the cell cycle. For instance, in the S-phase the cells are more resistant while in the G2 phase cells are more sensitive to radiation. Interestingly, high-LET radiations may stimulate the cancer cell to arrest in sensitive phase like in G2 (Maalouf *et al.* (2009)).

b) RBE

To quantify the differences of the cell killing efficiency of low-LET beam *vs* high-LET beam, the relative biological effectiveness (RBE) concept was introduced and applied to cell survival. The RBE is the ratio between the dose needed with a reference low-LET radiation for a defined level of survival and the dose needed with a high-LET radiation to obtain the same level of

survival. Hence, this can be written:

$$RBE = \left.\frac{D_{low-LET}}{D_{high-LET}}\right|_{iso-survival} \tag{II.2}$$

Although, the definition of RBE is simple, the clinical application is not. To quantify RBE in a clinical context, many factors and/or endpoints could be taken into account:

- particle type
- energy
- LET
- total dose
- dose per fraction
- number of fractions
- cell or tissue type
- cell environment
- cell state

Several methods have been developed in the particle therapy centers around the world to calculate RBE in a clinical situation, either using pragmatic conversion models or more theoretical models. These models will be presented in §3 page 22. These models can determinate the carbon-ion beam parameters that will produce a homogeneous distribution of the probability of cell kill in the tumor. Since the RBE depends on many factors and particularly on the LET distribution, the absorbed dose is inhomogeneously distributed in the tumor, as illustrated in Figure II.1.

c) The cell hyper-radiosensitivity

At lower doses ($\lesssim$ 10 cGy), dose-response analyses on several cell lines have identified a cell hypersensitivity to radiation called hyper-radiosensitivity (HRS). Today's consensus to explain HRS is that, the protective strategy adopted by a cell population is the removal of only few cells with risk of mutation (Martin *et al.* (2013)). This mechanism prevents the entire population of genomic instability. Contrarily, at higher dose, the whole population becomes a population at risk of mutation. Hence, the protective strategy for the cell population is to start repair mechanisms to attempt the preservation of each individual of the population. Many mechanisms to explain HRS remain to be elucidated.

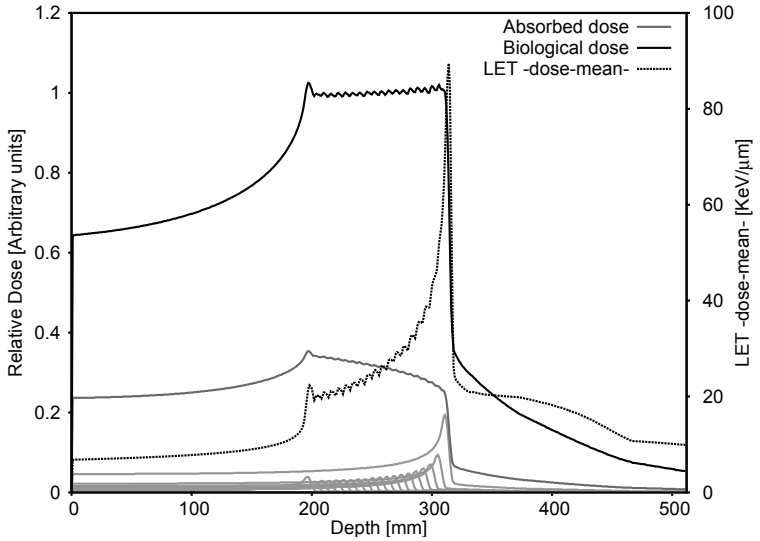

Figure II.1: Transversal dose deposition in water for a SOBP of 60 mm. For a prescribed dose defined, TRiP98 calculates the SOBP of absorbed carbon-ion made of several mono-energetic pristine peaks (in light grey). The prescribed biological dose is 3.3 Gy for an endpoint "late toxicity to the brain" with LEM I (α= 0.1 Gy^{-1}, β= 0.05 Gy^{-2}, D_{t}= 30 Gy and r_{nucl}=5 μm). The LET increases towards the distal part of the SOBP.

III

Biophysics

Contents

1 Mixed field

Along the carbon-ion track, inelastic nuclear interactions of the incident ions with matter lead to nuclear fragmentation and, thus, to the production of numerous recoil ions. The build-up of secondary charged particles, which results in a mixed radiation field, has to be considered in the dose algorithm and later in the calculation of biological effects.

Online monitoring of the beam delivery in a patient potentially takes advantage of these nuclear reactions to detect prompt gamma rays and particle radiations but also induced positron activity. In the mixed radiation field of particle T and energy E, each pair of (T_i, E_i) contributes to the dose with a fraction f_i, which varies from one voxel to another.

The biological effects are related to the dose deposited calculated each voxel. For that reason, the dose-average LET has to be calculated in each voxel (Kanai *et al.* (1997), Krämer and Scholz (2006)). The dose average LET is a distribution generally expressed (ICRU (1970)):

$$\overline{LET}_{Dp} = \frac{\int_0^\infty L^2 t(L)\,\mathrm{d}L}{\int_0^\infty L t(L)\,\mathrm{d}L} \tag{III.1}$$

with $t(L)\,\mathrm{d}L$ representing the fraction of total track lenght, T, having values of LET between L ans $L + \mathrm{d}L$. For carbon-ion EBRT, each radiation component j, of any type and energy, is taken into account to calculate the dose average LET in pixel p. Hence the previous equation can be re-written:

$$\overline{LET}_{Dp} = \frac{\int_j r_j LET_j\,\mathrm{d}j}{\int_j r_j\,\mathrm{d}j} \tag{III.2}$$

Where r_j is the weighting factor and $\mathrm{d}j$ is the dose, for each radiation component j.

Calculating the biological response to such a mixed-radiation field is complex and time consuming. An approximation was proposed by several authors to simplify the calculation of biological effects in a mixed-radiation field. It is detailed in §b) page 23.

2 Track structure and radial dose

For each ion in the beam, electrons of the medium are ejected around the ion trajectory; inducing a distribution of excitations and ionizations. This distribution is referred as "track structure". In Figure 4, the track structure of carbon-ions is depicted: the core track where the delta-electron are ejected, and the penumbra where delta-electrons interact with the medium. Models developed for calculating biological effects of ions often use amorphous track structure models to compile and add-up the hundreds of thousands of particles track and to calculate the energy deposition. Some aspects of the track structure can be represented by radial dose models. For each track, the radial dose $D(r)$ is calculated. The radial dose is the average dose expected at a certain point from the center of the ion trajectory. Several radial dose models exist to calculate the radial dose distribution.

Historically, Katz and Sharma (1974) proposed the use of a track theory for heavy particles therapy. Later, this application of the track theory was used by Waligòrski *et al.* (1986) for the calculation of the radial dose in the frame of cell inactivation calculation. Other authors described the radial dose: Scholz and Kraft (1996) proposed that λ would be a normalization constant and r the radial distance. The integral over the whole track yields to the LET. Hence,

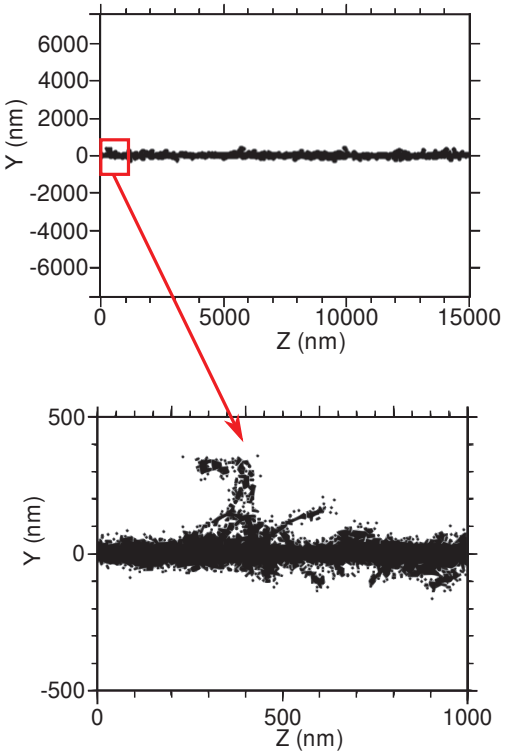

Figure III.1: Track structure of carbon-ion of 2 MeV/n beam. On the top the track is recorded along 15 μm. On the bottom, a zoom on the first micrometers is depicted. Ionizations appear on the core of the ion trajectory. The penumbra region is the region where the delta electrons interact: ionizations are less densely spaced distributed [figure adapted from Colliaux (2009)].

for $r < r_{min}$, the radial dose distribution is a constant. The radial dose distribution was described by Elsässer and Scholz (2007).

$$D(r) = \begin{cases} \lambda LET/r_{min}^2 & \text{if } r < r_{min} \\ \lambda LET/r^2 & \text{if } r_{min} \leq r \leq r_{max} \\ 0 & \text{if } r > r_{max} \end{cases} \tag{III.3}$$

where λ is a normalization constant and r the radial distance to the ion trajectory. r_{min} is the radius, at which the dose decreases and r_{max} the radius, at which the dose is negligible. Generally, $r_{min} = 10$ nm (Elsässer and Scholz (2007)). The total dose contribution around the track can be expressed:

$$S_e = \int_0^{r_{max}} 2\pi D(r) r \, \mathrm{d}r = \int_0^{r_{min}} 2\pi a r \, \mathrm{d}r + \int_{r_{min}}^{r_{max}} 2\pi \frac{a r_{min}^2}{r^2} \, \mathrm{d}r \tag{III.4}$$

Another track structure model is the Kiefer-Chatterjee model. As explained by Kase *et al.* (2008), this model mixes models for accounting for the penumbra : the Kiefer model (Kiefer and Straaten (1986)) and for the core radius : the Chatterjee model (Chatterjee and Schaefer (1976)). The core radius, R_c (μm), is expressed with the ion velocity relative to the light velocity:

$$R_c = 0.0116\beta_{ion} \tag{III.5}$$

The penumbra radius, R_p, is:

$$R_p = 0.0616\left(\frac{E}{A}\right)^{1.7} \tag{III.6}$$

With E the energy, A the mass.
Consequently, the penumbra dose D_p and the constant core dose D_c read:

$$D_p(r) = 1.25 \times 10^{-4}\left(\frac{z^*}{\beta_{ion}}\right)^2 r^{-2}, D_c = \frac{1}{\pi R_c^2}\left(\frac{LET_\infty}{r} - 2\pi K_p \ln\left(\frac{R_p}{R_c}\right)\right) \tag{III.7}$$

With z^* the effective charge (in the Barkas expression), β_{ion} is the ions velocity relative to the velocity of light in vacuum (Sakama *et al.* (2005)).

The radial dose is an average quantity. In the track core, the number of events and the energy transfer is high enough to quantify this radial dose. In this case, the radial dose gives a "fair" feature of the particles trajectory. On the contrary, in the track penumbra, events are very inhomogeneous distributed : there are regions with no events and regions with big clusters. In this case, using an average dose for describing such distribution of events seems limited. Another limitation of simple radial dose models is that stochastic effects are ignored. This can lead to inaccuracy in some dose deposition calculation (Beuve *et al.* (2009)).

3 Biophysical models for ion therapy

a) Rationale and history

The search for dose-response models for high-LET beam has raised several propositions of models in the past 40 years. The biological endpoint has often been defined with x-ray and *in vitro* experiments. Hence, for practical reasons, the RBE is defined has the dose in photons divided by the dose of ions needed for the same level of survival probability. In *in vitro* experiments, the iso-biological effect is usually taken at 10% survival:

$$RBE = \left.\frac{D_{RX}}{D_{ion}}\right|_{10\%survival} \tag{III.8}$$

Several biophysical models from clinical, mechanistic and microdosimetric approaches were developed for modeling RBE in various high-LET treatments. Neutron therapy was one of the first clinical high-LET treatments offered to large cohort of patients. As reported by Cárabe-Fernández (2007), in 1972, Kellerer and Rossi (1972) measured RBE values for several biological endpoints and for several high-LET. Kellerer and Rossi (1972) theorized their observations in the "theory of dual radiation action" (TDRA). The theory is based on the hypothesis that lesions are created from pairs of sub-lesions together with microdosimetric considerations and

the quantification of the radial dose. When pairs of sub-lesions occur in a defined "sensitive site", they will be responsible of the observed biological effect. In the TDRA model, the biological effects are hence correlated with the energy deposited in a defined "sensitive site".

At Berkeley, the SOBP was obtained by degrading the beam with ridge filters specially shaped for a particular treatment. In order to understand the biological response for many energy configurations, an extensive cell study was performed. The biological equivalence of the ion beam with the photon beam was obtained at 66% survival and for 2 Gy per fraction (Schardt *et al.* (2010)).

At NIRS, where carbon-ion therapy started, the approach chosen is based on their clinical experience with therapeutic neutron beams and dose-response models of few well-known *in vitro* cell lines (Kanai *et al.* (1999)).

Later, the LEM and the modified MKM were developed for calculating lethal damages of ions under several conditions of irradiation. The scientific community continues to improve or develop new models, for instance the "probabilitstic two-stage model" by Kundrát and co-workers (Kundrát *et al.* (2005)) or the "Nanox" model developed at my host institute (Beuve (2012)). In the following, only biophysical models implemented in clinical treatment planning systems (TPS) and used for patient treatments will be presented.

b) The NIRS model

In Japan, the NIRS launched the heavy-ion medical accelerator complex (HIMAC) where they initiated carbon-ion therapy in 1994. The NIRS radiobiological model aims at designing a carbon-ion beam, delivered passively through ridge filters, in order to achieve a uniform biological response in the SOBP. This model is based on establishing equivalence between carbon and neutron clinical beam. This equivalence is found after two steps:

- First RBE renormalization: human salivary gland (HSG) cells are the reference biological system. This cell line has a moderate radiosensitivity and can be considered representative for various cell lines. Same biological response is found between a carbon-ion beam with LET$\sim$ 80 keV/μm and a neutron beam with the same LET.
- Second RBE renormalization: At this LET point, the RBE is renormalized to account for the RBE of HSG cells and the RBE found by clinical experience with neutron beams.

Practically how can an absorbed dose distribution be calculated with the NIRS radiobiological model?

1) The clinical dose is chosen by a radiation oncologist. This dose is historically expressed in the unit "GyE", the E stands for equivalent. The figure given in GyE is known from past experience of neutron therapy at NIRS.
2) The clinical dose is converted to a biological dose. The RBE of clinical neutron therapy was estimated to be 3 and, under the same conditions, the RBE of HSG cells was estimated to be $\sim$2. This step is the second RBE normalization.
3) *In vitro* experiments with HSG cells were performed with several SOBP widths. For each SOBP width, the equivalent LET point (LET$\sim$ 80 keV/μm) is found applying the mixed field approximation (Kanai *et al.* (1997)). This step is the first RBE renormalization.

In the SOBP of carbon-ion beam, several particles of several energy and LET affect the cell inactivation. The mixed field LET, L_{mix} is:

$$L_{mix} = \sum_i f_i Li \tag{III.9}$$

with $f_i = d_i/D$, the fraction of the dose of the ith monoenergetic beam: $D = \sum_i d_i$ the total dose of the beam and d_i is the radiation dose of the ith monoenergetic beam. L_i is the dose-averaged LET. According to Lam (1989), the RBE in a mixed field can be calculated:

$$RBE_{mix} = \sum_i f_i RBE_i \tag{III.10}$$

Combining this hypothesis and the Zaider and Rossi's formalism on LQ survival equation in a mixed field:

$$S_{mix}(D) = e^{\left(-\alpha_{mix}D - \beta_{mix}D^2\right)} \tag{III.11}$$

with

$$\alpha_{mix} = \sum_i f_i \alpha_i \tag{III.12}$$

and,

$$\sqrt{\beta_{mix}} = \sum_i f_i \sqrt{\beta_i} \tag{III.13}$$

Hence, for several SOBP size the clinical RBE is tabulated (III.1).

Table III.1: Table of Clinical RBE at the middle of several SOBP widths (Kanai *et al.* (1999))

SOBP width (mm)	Clinical RBE
30	2.8
40	2.6
60	2.4
80	2.3
120	2.1

As described Kanai *et al.* (1999), the two-steps renormalization is kept constant even when "the schedule or the fraction size are changed".

This NIRS approach has been used since 1994. With the implementation of active beam delivery at NIRS, another radiobiological model is used: the modified microdosimetric kinetic model (modified MKM).

c) The modified MKM

The MKM was first proposed by Hawkins (Hawkins (1994), Hawkins (2003)). It is based on microdosimetric quantities measured with proportional counter and on the statistical aspect of dose deposition. Later Kase *et al.* (2006) proposed a modified version for the purpose of carbon-ion therapy at NIRS. The MKM can be described in several steps:

1) *The surviving fraction of cells for any radiation is predicted from the specific energy z contained in a domain (=subcellular structure).*
The cell survival probability is:

$$S = e^{-\overline{L}_{nucl}} \tag{III.14}$$

with $\overline{L}_{nucl}$, the average number of lethal lesions in the cell nucleus. The specific energy of the domain, z, is a microdosimetric quantity and a stochastic variable L_{nucl} is the sum of lesions in all domains. For any radiation type, L_{nucl} is:

$$L_{nucl} = N(A\overline{z} + B\overline{z}^2) \tag{III.15}$$

With N the number of domains in a nucleus. The number of events in a domain follows a Poisson distribution, hence:

$$L_{nucl} = (\alpha_0 + \beta z_{1D})D + \beta D^2 \tag{III.16}$$

With D the absorbed dose and z_{1D} the mean energy for a single event in a domain, the calculation of the cell survival probability requires also α_0 the initial slope of the surviving fraction curve at LET = 0, and β from the LQ model.

2) *calculating z_{1D}.*
One method to calculate the specific energy z, is to resort to a radial dose model. In Kase *et al.* (2008) the Kiefer-Chatterjee model is used (see §2 page 20)

3) *accounting for saturation effects.*
z_{1D} increases linearly with LET and hence would increase with RBE. Considering overkilling effect, the definition of a z_{sat} to account for this saturation effect is needed:

$$z_{sat} = \frac{z_0^2}{z}\left(1 - exp\left(\frac{-z}{z_0^2}\right)\right) \tag{III.17}$$

z_0 is the saturation coefficient (Inaniwa *et al.* (2010)):

$$z_0 = \frac{(R_n/r_d)^2}{\sqrt{\beta(1 + (R_n/r_d)^2)}} \tag{III.18}$$

with R_n and r_d the radii of the cell nucleus and the domain respectively. Hence, z_{1D} that will account for saturation will be named z^*_{1D} :

$$z^*_{1D} = \frac{\int_0^\infty z_{sat}\ z\ f_1(z)\mathrm{d}z}{\int_0^\infty z f_1(z)\mathrm{d}z} \tag{III.19}$$

with $f_1(z)$ the probability density of z deposited by a single energy-deposition event of the domain.

4) *HSG survival in a carbon-ion beam.*
The MKM was adapted to predict HSG cell survival from the NIRS carbon-ion beam. The β was set to 0.0615 Gy^{-2}. From a cell experiment with a mono-energetic 290 MeV/n, α was found to be equal to 0.282 Gy^{-1} and z^*_{1D} was measured: 3.43 Gy. From these values,

the α_0 could be calculated: $\alpha_0 = \alpha - \beta z^*_{1D} = 0.0708$ Gy (Inaniwa *et al.* (2010)). In the treatment planning system of NIRS, $r_d = 0.32$ μm and $R_n = 3.9$ μm.

Finally, this model is implemented in the NIRS spot-scanning treatment planning system for calculating RBE. At the end of 2011, the first patients were treated at NIRS with the spot-scanning beam and this new treatment planning system (Mori *et al.* (2012)). The use of a radial dose model has the advantage of speeding the calculations. However it lacks in properly describing high levels of dose fluctuation, inherent to ionizing radiations (see §2 page 20).

d) The GSI/HIT approach: the LEM

At the GSI the active beam scanning system was implemented to allow a better dose conformity. With this technique the biological effectiveness is unique for each spot scan and voxel. For that reason, a mathematical radiobiological model rather than a table of RBE was preferred. The Local Effect Model (LEM) was developed for that purpose.

i Summary of LEM

The idea of the LEM is that, the cell inactivation after an ion irradiation is determined by the spatial local dose distribution inside the cell nucleus. The local dose is calculated with a radial dose model and is considered in a subvolume. In this subvolume, lethal effects are calculated independently of the radiation quality with the the LQ-L model parameterized for the cell response to photons (α, β and D_{t} , see §1 page 30). Finally, subvolumes, where the biological damages are calculated, are integrated to estimate a total survival probability.

ii Details of LEM

1) Considering that the distribution of lethal events follow Poisson statistics, the cell survival probability is:
$$S(D) = e^{-N_{lethal}(D)} \tag{III.20}$$

2) The dose-response of a cellular system exposed to ions of particular type and energy is:
$$-\,ln(S) = \alpha_z D_z + \beta_z D_z^2 \tag{III.21}$$
where D_z is the specific energy deposited in the cell nucleus by a particular ion type and energy. α_z and β_z are intrinsic radiosentivity parameters for single monoenergetic particle at the specific energy D_z.

3) The local dose is calculated with a radial dose model (see §2 page 20).

4) With the local dose in the three dimensions $d(x, y, z)$, the average number of lethal events can be calculated:
$$N_{ion} = \int_{V_{nucleus}} \mathrm{d}V \nu_{ion}[d(x, y, z)] \tag{III.22}$$
with ν_{ion} the lethal event density.

5) From the hypothesis that the local dose can be directly related to the macroscopic dose D (hence neglecting stochastic effects), the ν_{ion} can be related to the lethal event density

of the radiation of reference, X-ray :

$$\nu_{ion}(d) = v_x(d) = -\frac{\ln(S_x)}{V} \tag{III.23}$$

6) Finally, considering that the sensitive sites are homogeneously distributed over the cell nucleus:

$$N_{ion} = -\int_{V_{nucleus}} \mathrm{d}V \frac{\ln(S_x)}{V} \tag{III.24}$$

with $\ln(S_x)$ calculated with the LQ-L model (see §1 page 30).

For a set of 4 input parameters: α, β, D_t and r_nucl, LEM I provides an initial calculation of α_z/α for single monoenergetic particle. So called "look-up tables" contain these input parameters together with table of α_z/α for each pair of particle type and energy (Scholz *et al.* (1997), Krämer and Scholz (2000), Krämer and Scholz (2006), Elsässer (2012)).

After observing some discrepancies with *in vitro* experiments, the LEM was updated (Elsässer (2012)). The last version of the LEM is the fourth version and takes into account the spatial distribution and density of double strand breaks (DSB). Although the LEM IV seems to be more accurate for predicting lethal damages in *in vitro* experiments (Friedrich *et al.* (2012), Grün *et al.* (2012)), the demonstration of this improvement in the context of a clinical treatment remains to be done (Gillmann *et al.* (2014)).

IV
Clinics

Contents

1 General concepts and the 4 R's of radiobiology

The 4 R's of radiobiology where proposed by Withers (1975) to describe important factors for improving the differential effect in EBRT: optimizing the repair periods for healthy tissues while holding the repopulation of cancer cells at minimum:

- Recovery: soon after radiation, sublethal damages may be recovered so that the probability of cell survival of a tissue will increase.

- Redistribution: Before irradiation, each cell is in a particular phase of the cell cycle; the distribution of the cell phases in the cell population is hence defined. During and soon after irradiation, some cells paused their cell cycle; the distribution of cell phases in the cell population has hence changed from the original distribution before irradiation. Long after irradiation, the distribution of the cell phases from the surviving cell population will have the same distribution as before irradiation.

- Repopulation: after irradiation, surviving clonogenic cells may reduce the depopulation by repopulating or reducing cell loss.

- Reoxygenation: due to the chaotic tumor vasculature, most of tumor cells are hypoxic. In the tumor there are few aerobic cells and they are more radiosensitive. Soon after the irradiation, most of them will be killed: the tumor will be mostly composed of hypoxic cells and the hypoxic fraction is at its maximum. From this maximum, the hypoxic fraction will decrease; aerobic cells will re-appear, causing the slow reoxygenation of the tumor. Fast reoxygenation also happens soon after the irradiation: some vessels that were occluded in and around the tumor may re-open and oxygenate the hypoxic cells.

The importance of repair time has been historically shown when sterilization of rams could be achieved without extensive skin reaction: the total dose was delivered in several fractions extended over a certain period of time (Hall and Giaccia (2012)). Following the same principle, a total therapeutic dose is given in multiple fractions of doses. The optimization of the fractionation scheme results from a compromise between the 4 R's considering the tumor type and the surrounding healthy tissues.

Clinical protocols with different fractionation schemes may need to be compared. For this purpose, the concept of biologically effective dose (BED) was developed: it "indicates quantitatively the biological effect of any radiotherapy treatment" (Fowler (2010)). Based on the LQ model and on the assumption that the α/β ratio is known for the tumor, the BED reads:

$$BED = nd\left(1 + \frac{d}{\frac{\alpha}{\beta}}\right) \tag{IV.1}$$

n and d are the total number of fractions and the dose per fraction, respectively. In the course of a radiotherapy treatment, clonogens repopulate, hence the strict application of the linear quadratic approach for counting the survival must take the fractionation scheme into account, and the properties of tumor cells to proliferate. The LQ model can be adapted to take into account proliferation factors that increases cell survival so that the BED now read:

$$BED = nd\left(1 + \frac{d}{\frac{\alpha}{\beta}}\right) - \ln(2)\frac{T - T_k}{\alpha T_{pot}} \tag{IV.2}$$

T_{pot} is the average doubling time of the tumor cells, T is the overall time and T_k is the time at which accelerated proliferation begins after the start of the treatment. When most tumor cells arrest in a cell cycle after irradiation, the repopulation starts with a delay which can be taken into account in some models with the time factor T_k. Finally, the number of days during the radiotherapy treatment where repopulation occurs $(T - T_k)$ is multiplied by the rate of repopulation per day. These time factors may or may not be considered in everyday clinical practice and by some authors in TCP studies (see §2 page 32).

For decades, the reference dose per fraction was 2 Gy. For this reason, it is very convenient to renormalize a delivered dose, which was not given in 2 Gy/fraction, to an equivalent total dose in 2 Gy/fraction that would give the same probability of cell survival (Fowler (2010)):

$$EQD2 = \frac{BED}{1 + \frac{2}{\alpha/\beta}} \tag{IV.3}$$

The LQ model has been extensively used to adapt fractionation and compare clinical schedules. Whether the original LQ model has or not radiobiological parameters with strict mechanistic explanation gave rise to several discussions in the scientific community (Zaider (1998) *vs* Sachs and Brenner (1998)). New radiotherapy techniques deliver the dose in many beam ports or continuously around the tumor (*ie* tomotherapy), hence a significantly large amount of healthy tissue receives very low doses. It remains a challenge to compare dose-volume histograms (DVH) from these healthy regions with DVHs obtained from conventional treatment knowing that the HRS may have to be considered. When hypofractionnated treatments are delivered, i.e. when the dose per fraction is considerably higher than 2 Gy/fraction, the calculation of the cell survival probability with the LQ is questioned. Year after year, it becomes more obvious that extrapolation techniques like EQD2 for comparing treatments with standard fractionation and hypo- or hyper- fractionation may "potentially compromise the patient safety" and hence "should only be attempted with a great care" (Bentzen and Joiner (2009)). Since the standard LQ model was found not appropriate for calculating survival probability at very high dose per fraction, new models were proposed such as the linear-quadratic-linear model (Guerrero and Li (2004), Carlone *et al.* (2005), Wang *et al.* (2007), Astrahan (2008)). In particular, in the Astrahan formulation, the LQ-L model reads:

$$S(D) = \begin{cases} e^{-(\alpha D + \beta D^2)} & \text{if } D < D_t \\ e^{-(\alpha D_t + \beta D_t^2 + s_{max}(D - D_t))} & \text{if } D \geq D_t \end{cases} \tag{IV.4}$$

where α and β are the input parameters for the linear quadratic model to calculate the cell survival probability to irradiation with low-LET photons; D_{t} is a threshold dose, defined as the dose at which the survival curve is supposed to become purely exponential; $s_{max} = \alpha + 2\beta D_t$ is the final slope at $D > D_t$.

2 TCP models

Clinical radiobiology aims at understanding the relationship between a distribution of dose in a defined clinical protocol (fractionation, beam geometry, etc) and the clinical outcomes. The mathematical dose-response model for the tumor is the tumor control probability (TCP) and for the healthy tissue, the normal tissue complication probability (NTCP). The TCP-NTCP trade-off will define the therapeutic window of a therapy. In the following, only TCP mathematical models will be presented. In 1936, Holthusen (1936) demonstrated the sigmoid shape of the dose response for both tumor and normal tissues. Later mathematical models were developed for describing quantitatively the tumor dose response.
The sigmoid shape of the dose response can suggest a statistical behavior of the tumor control in a patient cohort, and hence the probability of tumor control reflects the heterogeneity of the clinical response among patients. For that reason, two mathematical approaches can be chosen for describing the tumor control probability: one that fits the tumor local control clinical data with empirical methods and one based on the mechanistic interpretation of the linear quadratic model. In both approaches, a defined number of parameters have to be fitted or estimated. The meaning of these parameters and their values has been discussed by several authors (Bentzen and Tucker (1997), Daşu *et al.* (2003)). The tumor control is theoretically obtained when all clonogenic cells of a tumor have been inactivated. Three TCP models are mainly used: Poisson, logistic and probit. While the theoretical poissonian model is based on radiobiological parameters, the logistic and probit models are empirical approaches. The probit and logistic models take few parameters and are thus easier to apply to a large clinical data set in order to approximate the sigmoid curve. The poissonian approach has a phenomenological and radiobiological background, which means that some of its intrinsic parameters could be estimated experimentally.

a) Poisson model

i Concept

The number of surviving cells after radiation can be considered as a stochastic process that follows a Poisson distribution (Munro and Gilbert (1961)). Models using Poisson statistics to predict the probability of complete tumor inactivation at certain cell survival level (*i.e.* certain dose level) have been developed. The general formula describing the probability of surviving cells is:

$$P(n) = \frac{e^{-N_s} N_s^n}{n!} \tag{IV.5}$$

Where n is the number of surviving cells and N_s is the expected number of surviving cells. In the case of tumor control, the endpoint is the inactivation of the tumor and then, n equals zero.

$$P(n) = \frac{e^{-N_s} N_s^0}{0!} = e^{-N_s} \tag{IV.6}$$

This probability corresponds to the classical TCP definition:

$$TCP = e^{-N_s} \tag{IV.7}$$

The number of surviving cells is known by applying the LQ model and assuming a homogeneous cell-response and cell-concentration distribution over the tumor volume:

$$TCP(D) = e^{-N_s} = e^{-N_0 e^{-\alpha D - \beta D^2}} \tag{IV.8}$$

With N_0 the initial number of clonogenic cells or stem-like cancer cells. This equation reproduces the sigmoid curve of the clinical tumor control, using values of alpha and beta obtained from *in vitro* assays or from clinical data analysis. However N_0 is not precisely known. The TCP formula can be modified to take into account different phenomenological and radiobiological parameters like: radiosensitivity distribution, inhomogeneities in the dose distribution, variation in tumor volume and in clonogenic cell density. There exist two main extensions of the poissonian TCP model: one for analyzing local control of a cohort of patients (inter-patient heterogeneity) and one for analyzing the local control of a tumor with a distribution of parameters (intra-patient heterogeneity). In the first case, the inter-patient heterogeneity can be explained by the fact that each tumor is unique and that treatments are not exactly identical between patients. In the second case, the distribution of radiosensitivity in a tumor, for instance enhanced by the oxygen distribution, explains the distribution of surviving probabilities. Theoretically, the best model would take into account both inter-and intra- patient heterogeneity parameters. To account for the increase of survival probability in the course of a radiotherapy treatment, time factors may be included in the cell survival probability equation like explained in §1 page 30. The typical TCP equation with repopulation factors reads:

$$TCP(D) = e^{-N_0 e^{-nd(\alpha+\beta d)+\frac{ln(2)}{T_{pot}}(T-T_k)}} \tag{IV.9}$$

T_{pot} is the average doubling time of the tumor cells, T is the overall time and T_k is the time at which proliferation begins after the start of the treatment. n and d are the total number of fractions and the dose per fraction, respectively.
A more exact formulation of TCP was published by Warkentin *et al.* (2005):

$$TCP(D) = e^{-N_0 e^{-nd(\alpha+\beta d)+\frac{ln(2)}{T_{pot}} max\left(T-T_k,0\right)}} \tag{IV.10}$$

With $max\left(T-T_k, 0\right)$ is equal to $T - T_k$ if $T > T_k$ and 0 otherwise.

ii Radiosensistivity distribution

To account for intra- or inter-patient heterogeneity, the distribution of one or several of the TCP parameters (α, β, N_0) has been proposed (Webb and Nahum (1993), Roberts and Hendry (1998)). Depending on the authors, these distributions where either purely gaussian (or normal) or log-gaussian (or log-normal) (Roberts and Hendry (2007)). In case of inter-patient heterogeneity, the standard deviation (σ) is either determined by biopsies, biological images or obtained by fitting procedures. For instance, with gaussian distribution of alpha parameters; the TCP equation reads:

$$\overline{TCP} = \sum_i g(\alpha_i) TCP_i \tag{IV.11}$$

As $g(\alpha)$ follows a Gaussian distribution:

$$g(\alpha) = \frac{1}{\sigma\sqrt{2\pi}} e^{-\frac{(\alpha-\overline{\alpha})^2}{2\sigma^2}} \tag{IV.12}$$

With σ the standard deviation and $\overline{\alpha}$ the mean. Finally, considering heterogeneity for alpha, but homogeneity in beta and proliferation time, the TCP can be expressed:

$$g(\alpha) = \frac{1}{\sigma\sqrt{2\pi}} e^{-\frac{(\alpha_i-\overline{\alpha})^2}{2\sigma^2}} \tag{IV.13}$$

In meta-analysis of clinical local control, like performed by Scholz *et al.* (2006), the previous TCP formula was used (Eq. IV.10).

b) Logistic model

The sigmoid shape of the dose response can be described by the logistic model. The logistic model was historically introduced in tumor growth modeling. It relies on the assumption that a population cannot grow infinitely because of their restricted environment, which defines the upper limit to the number of individuals. Hence, when the population gets closer to the upper limit, the rate of growth diminishes. In the case of tumor inactivation, at the time of observation, the application of the logistic model has to be redefined: the logistic model describe the growth of "the probability P of the cell to die" in respect to the dose applied. The mathematical formulation is hence:

$$\frac{\mathrm{d}P}{\mathrm{d}D} = f(P) \text{ with : } P(0) = 0 \text{ and } f(0) = 0 \tag{IV.14}$$

The value at zero assumes that if no tumor cells are killed there will be no tumor control. The function $f(P)$, can be re-written as:

$$f(P) = Pg(P) \tag{IV.15}$$

The most resistant tumor cells reduce the rate of tumor cells inactivation so that the "growth" of the probability of the cell to die diminishes with the increase of dose. This is located at the upper level of tumor control. Since $g(P)$ represents the rate of growth, $g'(P) < 0$. One can consider $g(P)$ as a linear function:

$$g(P) = a - bP \tag{IV.16}$$

With a and b positive constants. Hence:

$$\frac{\mathrm{d}P}{\mathrm{d}D} = f(P) = Pg(P) = P(a - bP) \tag{IV.17}$$

Then, the logistic function for tumor control probability can be written as:

$$P = \frac{exp(u)}{1 + exp(u)} \tag{IV.18}$$

Taking into account the integration steps, u can be defined as $u = a + a'D$, where D is the total dose and a' on of the integration constants. In the logistic equation, D_{50} can be introduced, the dose at which $P = 0.5$:

$$P = \frac{exp(a'D_{50} + a)}{1 + exp(a'D_{50} + a)} = 0.5 \tag{IV.19}$$

In this case, $D_{50} = \frac{-a}{a'}$. More generally, the dose response gradient gamma is usually calculated at 50% or 37% probability. In the literature, the dose response gradient is defined in two manners:

- Normalized: $\gamma = D\frac{\mathrm{d}P}{\mathrm{d}D}$
- Not normalized: $\gamma = \frac{\mathrm{d}P}{\mathrm{d}D}$

c) Probit model

The probit model is often used for describing the sigmoid shape of the NTCP curve, based on the cumulative distribution function of the normal distribution. In the Lyman-Kutcher-Burman (LKB) model, it takes two parameters $TD50$ and m, for describing the position of sigmoid at the probability 50% and the steepness of the sigmoid (Allen Li *et al.* (2012), Källman *et al.* (1996)). It can be expressed either with the error function:

$$TPC(D) = \frac{1}{2}\left(1 - \mathrm{Erf}\left(\sqrt{\pi}\gamma\left(1 - \frac{D}{D_{50}}\right)\right)\right) \tag{IV.20}$$

Or, in the LKB model,

$$NTCP(D) = \frac{1}{\sqrt{2\pi}}\int_{-\infty}^{t} e^{\frac{x^2}{2}}\mathrm{d}x \tag{IV.21}$$

with

$$t = \frac{D - TD_{50}}{mTD_{50}} \tag{IV.22}$$

3 Prescribing and reporting in carbon-ion therapy

a) Treatment planning systems

New treatment planning systems have been specifically created for carbon-ion therapy. In Japan, the initial TPS was specially designed to calculate treatment plans for passive beam delivery coupled with the radiobiological model from NIRS. In Germany, the initial TPS was designed for active scanning-beam delivery coupled with the LEM.

i Passive beam delivery: example of HIPLAN

HIPLAN (Endo *et al.* (1996)) is the TPS used at NIRS for carbon-ion therapy delivered with the passive beam line. It contains libraries of standard beams calculated with the NIRS radiobiological model. The TPS calculates the beams properties (wobbling conditions, range shifter thickness, field size, *etc.*) to achieve the desired dose distribution. Hence, the libraries contain information for several possible SOBP to cover the target volume.

ii Active scanning-beam delivery: example of TRiP98

The TPS TRiP98 (TReatment planning for Particles, 1998 version) was developed at the GSI for the German Clinical Pilot Project (Krämer and Scholz (2000), Krämer *et al.* (2000)). TRiP98 was designed for carbon-ion radiotherapy with a scanned beam delivery system, it also allows inverse planning. On the basis of a prescribed dose in photon therapy, a cell survival probability can be calculated. Subsequently, TRiP98 calculates a set of beam parameters leading to the same cell survival probability per fraction for a carbon-ion treatment. Taking into account the transport of carbon-ions in tissue and the biological response that they induce, TRiP98 calculates the carbon-ion absorbed dose per fraction in each voxel. To be precise, the survival probability is calculated using the mixed field approximation explained in §1 page 20. This approximation has the advantage to significantly reduce the computing time to calculate the biological response. The LEM I is implemented in TRiP98 and so-called "look-up tables" are a prerequisite for calculating and optimizing of carbon-ion treatment plans (see §d) page 26).

b) Dose reporting

i Definition

The choice of a unit or a broadly accepted denomination when describing a dose that would have been calculated according to a "radiobiological model" has been under debate for several years. Historically, it started when biological factors were introduced in conventional photon radiotherapy for taking into account late- and early-reacting tissues. That way, new fractionation schemes could be inter-compared. In 1982 Barandsen introduced the "biologically effective dose" (Fowler (1989)) or also called "extrapolated tolerance dose" for calculating "biological effects" and/or normalized them with parameters from the fractionation scheme and from the α/β ratio. This concept has been a little updated and is now called "the equieffective dose", *EQDX*, and is defined in the last report from ICRU committee on "Bioeffect Modeling and Biologically Equivalent Dose Concepts in Radiation Therapy" as :

> the total absorbed dose delivered by the reference treatment plan (fraction size X) that leads to the same biological effect as a test treatment plan that is conducted with absorbed dose per fraction d and total absorbed dose D according to a relation adapted from the Withers formula

(Bentzen *et al.* (2012)). This equation is used daily for calculating the extra daily dose to give to a patient treatment when a fraction was missed along the treatment course for instance. This "equieffective dose" has the unit of Gray. Fowler proposed to add a subscript to the unit "Gy" depending on the endpoint taken into consideration: late- and early-reacting tissues (usually, the α/β ratio equals to 3 or 10 respectively). That way the α/β ratio used for the re-normalization is known and there is the same meaning under "equieffective dose" (or, in the wording of Fowler, "biologically effective dose"). This nomenclature would look like: "Gy_3" or "Gy_{10}" for instance (Fowler (1989), Fowler (2006)).

With the advent of new radiation therapy techniques characterized by high linear energy transfer (LET), the term "relative biological effectiveness" must be clearly defined for each treatment type (particle, energy), treatment system delivery, tumor or healthy tissue type. At

NIRS, treatments were calculated in term of "Gray Equivalent", which is the absorbed dose (in unit of Gray) multiplied by an ion "weighting factor, W_i" calculated at some defined endpoints. In this W_i, the relative biological effectiveness (RBE) is included -alone- in the W_i and a list of its values was tabulated depending of the ridge filter used (see §b) page 23). For several years this "Gray Equivalent" was written *GyE*. Since standard definition of unit forbid to append a symbol to a standard unit, some authors report "Gray Equivalent" with a space between the unit Gray and the *E*: *Gy E*.

In 1997, the German carbon-ion clinical pilot project started. The radiobiological model used was the LEM I. The first clinical results of this pilot project were also reported in *GyE* or cobalt-gray-equivalent *CGE* or later in *Gy E* (Schulz-Ertner *et al.* (2003), Schulz-Ertner *et al.* (2007), Combs *et al.* (2010)). First clinical studies were delivered in "3 GyE" per fraction using the following input parameters for the LEM I : α= 0.1 Gy^{-1}, β= 0.05 Gy^{-2}, D_t= 30 Gy and r_{nucl}=5 μm.

In 2007, the IAEA and the ICRU delivered a report called "Dose Reporting in Ion Beam Therapy" aiming at harmonizing dose reporting so that "the treatments [are] reported in a similar/comparable way in all centers so that the clinical reports and protocols can be understood and interpreted without ambiguity by the radiation therapy community in general" (IAEA and ICRU (2007)). Some of the conclusions and recommendations are:

- The reporting of physical doses alone is not sufficient, and biologically effective dose distributions and DVH (dose volume histogram) data have to be reported as well,
- It is advisable to report the α/β values for the dose limiting toxicity and to optimize the plans according to this biological endpoint. The estimated α/β value for the specific tumor cell type and an additional treatment optimization for this endpoint might be reported as well, in cases where α/β ratios for the dose-limiting toxicity and the specific tumor cell type are expected to differ substantially,
- The isoeffective dose, as introduced here for radiation therapy applications, is the dose expressed in Gy that, delivered under reference conditions, would produce the same clinical effects as the actual treatment, in a given system, all other conditions being identical. The reference treatment conditions are: photon irradiation, 2 Gy per fraction, 5 daily fractions a week. The isoeffective dose D_{IsoE} is the product of the physical quantity of absorbed dose D and a weighting factor W_{IsoE}. W_{IsoE} is an inclusive weighting factor that takes into account all factors that could influence the clinical effects (dose per fraction, overall time, radiation quality, biological system and effects, and other factors).
- The numerical value of W_{IsoE} is selected by the radiation oncology team for a given patient (or treatment protocol), and it is part of the treatment prescription. Evaluation of the influence of radiation quality on W_{IsoE} raises complex problems because of the clinically significant RBE variations with biological effect (late versus early reactions), and the position at depth in the tissues which is a problem specific to ion beam therapy. *IsoE* is written as a subscript or, eventually, can be written in parentheses: W_{IsoE} or $W(IsoE)$ and D_{IsoE} or $D(IsoE)$.
- Confusion exists between the term "equivalent dose" as used in the present context of particle therapy and the term equivalent dose as defined by the ICRP, for radiation

> protection applications, with a totally different meaning. The special unit for the equivalent dose defined by the ICRP is the Sievert, Sv.
>
> - As mentioned, the unit commonly used is the GyE, but this practice has to be discouraged [...] neither subscript nor letter/symbol may be added to the recommended symbols of units, such as GyE.

This report had the merit to clarify certain points, however it failed to define precisely the $W(IsoE)$ for carbon-ion therapy, where on top of a "equieffective dose" calculation represented by the subscript *iso*, comes a "radiobiological model" that calculates RBE with different endpoints depending on the institution that provided the treatment.

In 2008, the IAEA and ICRU published the technical reports series no 461; "Relative Biological Effectiveness in ion beam therapy" that contained a section called "Quantities and units", which "discusses the definitions of some terms and recommended symbols" (IAEA and ICRU (2008)). In this report the "isoeffective dose weighting $W(IsoE)$" is defined and some particularities, when taking into account RBE, are discussed. It is suggested to report all parameters in the RBE and isoeffective dose calculation. A proposition for the isoeffective dose weighting factor is given:

$$\mathrm{W_{IsoE}}\left(\mathrm{C+; SOBP = 6\ cm; RBE = 3; }\alpha/\beta_{\mathrm{photons,early}} = 10\ \mathrm{Gy; 0.6\ Gy/d}\right)$$

And a full example for reporting dose in a clinical study is also given:

> the patient received 20 Gy (60 Gy (IsoE))" : with the implicit understanding that the 20 Gy absorbed dose from ions produces a biological effect equivalent to that produced by an absorbed dose of 60 Gy of photons given under reference conditions of 2 Gy/d of photon radiation over the same treatment time

After some years, it became evident that the "Japanese GyE" and the "German GyE" were not directly comparable because of the wide differences of the endpoints used (IAEA and ICRU (2007)). A new denomination started to appear in publications of carbon-ion therapy: "relative biological effectiveness (RBE)-weighted dose" expressed in *GyRBE* or *Gy(RBE)*. This nomenclature came mostly from the community using the LEM for calculating biological effects in the carbon-ion therapy treatment. Today, it seems that most publications from NIRS with the NIRS radiobiological model report doses with *GyE* and publications where the LEM is used report dose with *Gy(RBE)*.

In the near future ICRU committees should release reports on the issue of reporting carbon-ion treatment doses: "Prescribing, recording, and reporting Ion-beam Therapy" and also on bioeffect modeling: "Bioeffect modeling and equieffective dose concepts in radiation therapy" ICRU (2014).

ii Radiobiological models comparison and conversion

At the world level, it is very important to be able to compare clinical data between carbon-ion treatments. Up to now, the LEM and the NIRS model have been implemented in particle therapy TPS for several years and long term clinical outcome is available. Since, the dose reported from institutions using these two different models is known to be different (IAEA and

ICRU (2007)), several methods have been proposed to convert a NIRS-model-based prescribed total dose into a LEM-based prescribed total dose (Matsufuji *et al.* (2007), Mizoe *et al.* (2008), Steinsträter *et al.* (2012), Fossati *et al.* (2012)). These methods have been principally based on the study of physical dose distributions between European and Japanese centers in order to map the RBE between institutions. After defining boundary conditions, Mizoe *et al.* (2008) concluded that the NIRS physical dose was 15% higher than the GSI physical dose. The boundary conditions were:

- SOBP = 60 mm
- Prescribed dose in both models (NIRS model and LEM): 4 Gy
- Target: chordoma [1]
- Distal energy: 290 MeV/n

In the IAEA report 2007, Matsufuji *et al.* (2007) tried also to quantify the difference between NIRS and LEM dose with a different method and different boundary conditions. The dose averaged LET and the physical dose were calculated for a prescribed dose of 3.3 Gy with the LEM, chordoma parameters and parallel opposed fields. From this information the NIRS biological model was applied. The conclusion is that the biological dose recalculation with the NIRS model is 20% lower than prescribed dose with the LEM. Later, Steinsträter *et al.* (2012) published a more detail analysis to map "RBE-weighted dose" between NIRS and LEM models. After reconstructing the physical dose distribution used at NIRS for several SOBP and distal energy, factors to convert the biological dose from LEM to NIRS were calculated. Simultaneously, Fossati *et al.* (2012) published a similar analysis and concluded with similar conversion factors. In the design of clinical protocol and trials, the CNAO clinical team has used the conversion factors published to reproduce NIRS most recent clinical protocols (NIRS and MedAustron (2013)).

4 Prostate cancer

First clinical results with carbon-ion beams are available (Ishikawa *et al.* (2012)) for prostate cancer. Recently, clinical trials started at HIT and CNAO (NIRS and MedAustron (2013)). Prostate cancer was chosen as an example of a slowly growing tumor surrounded by radiosensitive structures (i.e. the rectum and bladder; Nikoghosyan *et al.* (2004)). To the best of our knowledge, for all carbon-ion treatments for prostate cancer delivered in Europe, treatment planning was based on the LEM I with input parameters validated during the German Clinical Pilot Project and determined for the endpoint "late toxicity to the brain". So far, no clinically-validated LEM input parameters for prostate cancer have been published and tested.

[1] With the LEM I, the "chordoma" endpoint corresponds to the endpoint "late toxicity to the brain" : α= 0.1 Gy^{-1}, β= 0.05 Gy^{-2}, D_t= 30 Gy and r_{nucl}=5 μm

Bibliography

Allen Li, X., Alber, M., Deasy, J., Jackson, A., Ken Jee, K., *et al.* (2012). The use and qa of biologically related models for treatment planning. Technical Report 166, AAPM. c)

Astrahan, M. (2008). Some implications of linear-quadratic-linear radiation dose-response with regard to hypofractionation. *Med Phys*, 35(9):4161–4172. 1

Bentzen, S. and Joiner, M. (2009). *Basic Clinical Radiobiology 4th edition*, chapter 9: The linear-quadratic approach in clinical practice. Hodder Arnold, Great Britain. a), 1

Bentzen, S. M., Dörr, W., Gahbauer, R., Howell, R. W., Joiner, M. C., *et al.* (2012). Bioeffect modeling and equieffective dose concepts in radiation oncology–terminology, quantities and units. *Radiother Oncol*, 105(2):266–268. i

Bentzen, S. M. and Tucker, S. L. (1997). Quantifying the position and steepness of radiation dose-response curves. *Int J Radiat Biol*, 71(5):531–542. 2

Beringer, J., Arguin, J. F., Barnett, R. M., Copic, K., Dahl, O., *et al.* (2012). Review of particle physics. *Phys. Rev. D*, 86. 2, 2

Berkeley Lab (2010). `http://newscenter.lbl.gov/2010/10/18/ion-beam-therapy/` (accessed 2014.09.30). The promise of ion beam cancer therapy. 3

Beuve, M. (2012). `http://hal.archives-ouvertes.fr/hal-00949676` (accessed 2014.09.29). Toward the nanox model. a)

Beuve, M., Colliaux, A., Dabli, D., Dauvergne, D., Gervais, B., *et al.* (2009). Statistical effects of dose deposition in track-structure modelling of radiobiology efficiency. *Nuclear Instruments and Methods in Physics Research Section B: Beam Interactions with Materials and Atoms*, 267(6):983 – 988. Proceedings of the Seventh International Symposium on Swift Heavy Ions in Matter. 2

Cárabe-Fernández, A. (2007). *A theoretical investigation of the radiobiological rationale for high-LET radiotherapy*. PhD thesis, University of London Imperial College of Science, Technology and Medicine Department of Medicine Division of Surgery, Oncology, Reproductive Biology and Anaesthetics (SORA). a)

Carlone, M., Wilkins, D., and Raaphorst, P. (2005). The modified linear-quadratic model of guerrero and li can be derived from a mechanistic basis and exhibits linear-quadratic-linear behaviour. *Phys Med Biol*, 50(10):L9–13; author reply L13–5. 1

Chatterjee, A. and Schaefer, H. J. (1976). Microdosimetric structure of heavy ion tracks in tissue. *Radiat Environ Biophys*, 13(3):215–227. 2

Colliaux, A. (2009). *Implication de loxygène et des anti-oxydants dans le processus de radiolyse de leau induit par lirradiation aux ions de haute énergie : simulations numériques pour la radiobiologie*. PhD thesis, Université Claude Bernard Lyon 1. III.1

Combs, S. E., Ellerbrock, M., Haberer, T., Habermehl, D., Hoess, A., *et al.* (2010). Heidelberg ion therapy center (hit): Initial clinical experience in the first 80 patients. *Acta Oncol*, 49(7):1132–1140. i

Daşu, A., Toma-Daşu, I., and Fowler, J. F. (2003). Should single or distributed parameters be used to explain the steepness of tumour control probability curves? *Phys Med Biol*, 48(3):387–397. 2

Douglas, B. G. and Fowler, J. F. (1976). The effect of multiple small doses of x rays on skin reactions in the mouse and a basic interpretation. *Radiation Research*, 66(2):401–426. a)

Elsässer, T. (2012). *Ion Beam Therapy: Fundamentals, Technology, Clinical Applications*, chapter Modeling Heavy Ion Radiation Effects, pages 117–133. Biological and Medical Physics, Biomedical Engineering. Springer. ii

Elsässer, T. and Scholz, M. (2007). Cluster effects within the local effect model. *Radiat Res*, 167(3):319–329. 2, 2

Endo, M., Koyamaito, H., ichi Minohara, S., Miyahara, N., Tomura, H., *et al.* (1996). Hiplan-a heavy ion treatment planning system at himac. *The Journal of JASTRO*, 8(3):231–238. i

Fossati, P., Molinelli, S., Matsufuji, N., Ciocca, M., Mirandola, A., *et al.* (2012). Dose prescription in carbon ion radiotherapy: a planning study to compare nirs and lem approaches with a clinically-oriented strategy. *Phys Med Biol*, 57(22):7543–7554. ii

Fowler, J. F. (1989). The linear-quadratic formula and progress in fractionated radiotherapy. *The British Journal of Radiology*, 62(740):679–694. i

Fowler, J. F. (2006). Development of radiobiology for oncology-a personal view. *Phys Med Biol*, 51(13):R263–R286. i

Fowler, J. F. (2010). 21 years of biologically effective dose. *Br J Radiol*, 83(991):554–568. 1, 1

Friedrich, T., Scholz, U., Elsässer, T., Durante, M., and Scholz, M. (2012). Calculation of the biological effects of ion beams based on the microscopic spatial damage distribution pattern. *Int J Radiat Biol*, 88(1-2):103–107. ii

Furukawa, T., Inaniwa, T., Sato, S., Tomitani, T., Minohara, S., *et al.* (2007). Design study of a raster scanning system for moving target irradiation in heavy-ion radiotherapy. *Med Phys*, 34(3):1085–1097. 4

Gillmann, C., Jäkel, O., Schlampp, I., and Karger, C. P. (2014). Temporal lobe reactions after carbon ion radiation therapy: comparison of relative biological effectiveness-weighted tolerance doses predicted by local effect models i and iv. *Int J Radiat Oncol Biol Phys*, 88(5):1136–1141. ii

Grün, R., Friedrich, T., Elsässer, T., Krämer, M., Zink, K., *et al.* (2012). Impact of enhancements in the local effect model (lem) on the predicted rbe-weighted target dose distribution in carbon ion therapy. *Phys Med Biol*, 57(22):7261–7274. ii

Guerrero, M. and Li, X. A. (2004). Extending the linear-quadratic model for large fraction doses pertinent to stereotactic radiotherapy. *Phys Med Biol*, 49(20):4825–4835. 1

Haberer, T., Becher, W., Schardt, D., and Kraft, G. (1993). Magnetic scanning system for heavy ion therapy. *Nuclear Instruments and Methods in Physics Research Section A: Accelerators, Spectrometers, Detectors and Associated Equipment*, 330:296 – 305. 4

Hall, E. and Giaccia, A. (2012). *Radiobiology for the Radiologist*. Wolters Kluwer Health. 1

Hawkins, R. B. (1994). A statistical theory of cell killing by radiation of varying linear energy transfer. *Radiat. Res.*, 140(3):366–374. c)

Hawkins, R. B. (2003). A microdosimetric-kinetic model for the effect of non-poisson distribution of lethal lesions on the variation of rbe with let. *Radiat Res*, 160(1):61–69. c)

Holthusen, H. (1936). Erfahrungen über die vertrglichkeitsgrenze fr röntgenstrahlen und deren nutzanwendung zur verhütung von schäden. *Strahlenther Onkol*, 57:254269. 2

IAEA and ICRU (2007). Iaea-tecdoc-1560: Dose reporting in ion beam therapy. Technical report, INTERNATIONAL ATOMIC ENERGY AGENCY, Vienna. i, ii

IAEA and ICRU (2008). Technical reports series no. 461: Relative biological effectiveness in ion beam therapy. Technical report, INTERNATIONAL ATOMIC ENERGY AGENCY, Vienna. i

ICRU (1970). Task group dose as a function of let: Linear energy transfer: report 16. Technical report, International Commission on Radiation Units and Measurements, Washington. 1

ICRU (2014). `www.icru.org/content/uncategorised/current-program-of-the-icru` (accessed 2014.09.30). The international commission on radiation units and measurements; current activities of icru. i

Inaniwa, T., Furukawa, T., Kase, Y., Matsufuji, N., Toshito, T., *et al.* (2010). Treatment planning for a scanned carbon beam with a modified microdosimetric kinetic model. *Phys Med Biol*, 55(22):6721–6737. c), c)

Ishikawa, H., Tsuji, H., Kamada, T., Akakura, K., Suzuki, H., *et al.* (2012). Carbon-ion radiation therapy for prostate cancer. *Int J Urol*, 19(4):296–305. 4

Iwata, Y. (2013). `accelconf.web.cern.ch/AccelConf/pac2013/talks/frxb1_talk.pdf` (accessed 2014.09.20). Superconducting rotating-gantry and other developments at himac. 4

Joiner, M. and van der Kogel, A. (2009). *Basic Clinical Radiobiology Fourth Edition*. Hodder Education. 3, a)

Källman, P., Agren, A., and Brahme, A. (1996). Radiation dose in radiotherapy from prescription to delivery. IAEA-TECDOC 896, International Atomic Energy Agency, Vienna. c)

Kanai, T., Endo, M., Minohara, S., Miyahara, N., Koyama-ito, H., *et al.* (1999). Biophysical characteristics of himac clinical irradiation system for heavy-ion radiation therapy. *Int J Radiat Oncol Biol Phys*, 44(1):201–210. a), III.1, b)

Kanai, T., Furusawa, Y., Fukutsu, K., Itsukaichi, H., Eguchi-Kasai, K., *et al.* (1997). Irradiation of mixed beam and design of spread-out bragg peak for heavy-ion radiotherapy. *Radiat Res*, 147(1):78–85. 1, b)

Kase, Y., Kanai, T., Matsufuji, N., Furusawa, Y., Elsässer, T., *et al.* (2008). Biophysical calculation of cell survival probabilities using amorphous track structure models for heavy-ion irradiation. *Physics in Medicine and Biology*, 53(1):37. 2, c)

Kase, Y., Kanai, T., Matsumoto, Y., Furusawa, Y., Okamoto, H., *et al.* (2006). Microdosimetric measurements and estimation of human cell survival for heavy-ion beams. *Radiat Res*, 166(4):629–638. c)

Katz, R. and Sharma, S. C. (1974). Heavy particles in therapy: an application of track theory. *Physics in Medicine and Biology*, 19(4):413. 2

Kellerer, A. M. and Rossi, H. H. (1972). The theory of dual radiation action. *Current Topics in Radiation Research Quarterly*, 8(2):85–158. a)

Kiefer, J. and Straaten, H. (1986). A model of ion track structure based on classical collision dynamics (radiobiology application). *Physics in Medicine and Biology*, 31(11):1201. 2

Krämer, M., Jäkel, O., Haberer, T., Kraft, G., Schardt, D., *et al.* (2000). Treatment planning for heavy-ion radiotherapy: physical beam model and dose optimization. *Phys Med Biol*, 45(11):3299–3317. ii

Krämer, M. and Scholz, M. (2000). Treatment planning for heavy-ion radiotherapy: calculation and optimization of biologically effective dose. *Phys Med Biol*, 45(11):3319–3330. ii, ii

Krämer, M. and Scholz, M. (2006). Rapid calculation of biological effects in ion radiotherapy. *Phys Med Biol*, 51(8):1959–1970. 1, ii

Kundrát, P., Lokajícek, M., and Hromcíková, H. (2005). Probabilistic two-stage model of cell inactivation by ionizing particles. *Phys Med Biol*, 50(7):1433–1447. a)

Lam, G. K. (1989). On the use of effective dose in the treatment planning of high linear-energy-transfer radiation. *Med Phys*, 16(5):687–691. b)

Maalouf, M., Alphonse, G., Colliaux, A., Beuve, M., Trajkovic-Bodennec, S., *et al.* (2009). Different mechanisms of cell death in radiosensitive and radioresistant p53 mutated head and neck squamous cell carcinoma cell lines exposed to carbon ions and x-rays. *Int J Radiat Oncol Biol Phys*, 74(1):200–209. a)

Martin, L. M., Marples, B., Lynch, T. H., Hollywood, D., and Marignol, L. (2013). Exposure to low dose ionising radiation: Molecular and clinical consequences. *Cancer Lett*, 338(2):209–18. c)

Matsufuji, N., Kanai, T., Kanematsu, N., Miyamoto, T., Baba, M., *et al.* (2007). *IAEA-TECDOC-1560: Dose Reporting in Ion Beam Therapy*, chapter Treatment planning and dosimetric requirements for prescribing and reporting ion-beam therapy: the current chiba approach, pages 169–180. IAEA, Vienna. ii

Mizoe, J., Ando, K., Kanai, T., Matsufuji, N., and Tsujii, H. (2008). *Technical reports series No. 461: Relative biological effectiveness in ion beam therapy*, chapter Clinical RBE determination scheme at NIRS-HIMAC, pages 135–152. IAEA, Vienna. ii

Mori, S., Shibayama, K., Tanimoto, K., Kumagai, M., Matsuzaki, Y., *et al.* (2012). First clinical experience in carbon ion scanning beam therapy: retrospective analysis of patient positional accuracy. *J Radiat Res*, 53(5):760–768. c)

Munro, T. R. and Gilbert, C. W. (1961). The relation between tumour lethal doses and the radiosensitivity of tumour cells. *Br J Radiol*, 34:246–251. i

Nikoghosyan, A., Schulz-Ertner, D., Didinger, B., Jkel, O., Zuna, I., *et al.* (2004). Evaluation of therapeutic potential of heavy ion therapy for patients with locally advanced prostate cancer. *Int J Radiat Oncol Biol Phys*, 58(1):89–97. 4

NIRS (2014). `http://www.nirs.go.jp/ENG/core/cpt/cpt01.shtml` (accessed 2014.09.30). Research center for charged particle therapy. 3

NIRS and MedAustron, editors (2013). *Proceedings: NIRS and MedAustron Joint Symposium on Carbon Ion Radiotherapy*. ii, 4

Pedroni, E., Bacher, R., Blattmann, H., Böhringer, T., Coray, A., *et al.* (1995). The 200-mev proton therapy project at the paul scherrer institute: conceptual design and practical realization. *Med Phys*, 22(1):37–53. 4

Roberts, S. and Hendry, J. (2007). *Radiobiological modelling in radiation oncology*, chapter Inter-tumour heterogeneity and tumour control, pages 169–95. British Institute of Radiology. ii

Roberts, S. A. and Hendry, J. H. (1998). A realistic closed-form radiobiological model of clinical tumor-control data incorporating intertumor heterogeneity. *Int J Radiat Oncol Biol Phys*, 41(3):689–699. ii

Sachs, R. K. and Brenner, D. J. (1998). The mechanistic basis of the linear-quadratic formalism. *Med Phys*, 25(10):2071–2073. 1

Sakama, M., Kanai, T., Kase, Y., Komori, M., Fukumura, A., *et al.* (2005). Responses of a diamond detector to high-let charged particles. *Phys Med Biol*, 50(10):2275–2289. 2

Schardt, D., Elsässer, T., and Schulz-Ertner, D. (2010). Heavy-ion tumor therapy: Physical and radiobiological benefits. *Rev. Mod. Phys.*, 82:383–425. a)

Scholz, M., Kellerer, A. M., Kraft-Weyrather, W., and Kraft, G. (1997). Computation of cell survival in heavy ion beams for therapy. the model and its approximation. *Radiat Environ Biophys*, 36(1):59–66. ii

Scholz, M. and Kraft, G. (1996). Track structure and the calculation of biological effects of heavy charged particles. *Advances in Space Research*, 18(1-2):5 – 14. 2

Scholz, M., Matsufuji, N., and Kanai, T. (2006). Test of the local effect model using clinical data: tumour control probability for lung tumours after treatment with carbon ion beams. *Radiat Prot Dosimetry*, 122(1-4):478–479. ii

Schulz-Ertner, D., Nikoghosyan, A., Hof, H., Didinger, B., Combs, S. E., *et al.* (2007). Carbon ion radiotherapy of skull base chondrosarcomas. *Int J Radiat Oncol Biol Phys*, 67(1):171–177. i

Schulz-Ertner, D., Nikoghosyan, A., Thilmann, C., Haberer, T., Jkel, O., *et al.* (2003). Carbon ion radiotherapy for chordomas and low-grade chondrosarcomas of the skull base. results in 67 patients. *Strahlenther Onkol*, 179(9):598–605. i

Steinsträter, O., Grün, R., Scholz, U., Friedrich, T., Durante, M., *et al.* (2012). Mapping of rbe-weighted doses between himac- and lem-based treatment planning systems for carbon ion therapy. *Int J Radiat Oncol Biol Phys*, 84(3):854–860. ii

Waligòrski, M., Hamm, R., and Katz, R. (1986). The radial distribution of dose around the path of a heavy ion in liquid water. *International Journal of Radiation Applications and Instrumentation. Part D. Nuclear Tracks and Radiation Measurements*, 11(6):309 – 319. 2

Wambersie, A., Chauvel, P., Gademann, G., Gerard, J., and Sealy, R. (1992). Commission of the european communities, concerted action: Cancer treatment with light ions in europe-eulima, final report-part 1: General feasibility study, socio-economic study. Technical report, EC, rue de la Loi, 200, 1049 Brussels, 1992. 3

Wang, J., Mayr, N., and Yuh, W. (2007). A generalized linear-quadratic formula for high-dose-rate brachytherapy and radiosurgery. *International Journal of Radiation Oncology Biology Physics*, 69(3):S619–S620. 1

Warkentin, B., Stavrev, P., Stavreva, N. A., and Fallone, B. G. (2005). Limitations of a tcp model incorporating population heterogeneity. *Phys Med Biol*, 50(15):3571–3588. i

Webb, S. and Nahum, A. E. (1993). A model for calculating tumour control probability in radiotherapy including the effects of inhomogeneous distributions of dose and clonogenic cell density. *Phys Med Biol*, 38(6):653–666. ii

Withers, H. R. (1975). Cell cycle redistribution as a factor in multifraction irradiation. *Radiology*, 114(1):199–202. 1

Zaider, M. (1998). There is no mechanistic basis for the use of the linear-quadratic expression in cellular survival analysis. *Med Phys*, 25(5):791–792. 1

Part B

Influence of Local Effect Model Parameters for Tumor Control Probability predictions for prostate cancer

I

Introduction

Radiobiological models are essential for the prescription of a carbon-ion treatment. Several approaches exist, but, in European carbon-ion therapy centers, only one approach is implemented in CE-certified TPS: the LEM I. From the physical properties of the specific ion radiation, the LEM calculates the survival probabilities of the cell or tissue type under study, provided that some determinant input parameters are initially defined. So far, only one set of LEM I input parameters is approved for treatments. It corresponds to the "chordoma" endpoint also described as "late toxicity to the brain" and with input parameters $\alpha = 0.1$ Gy^{-1}, $\beta = 0.05$ Gy^{-2}, $D_{\mathrm{t}} = 30$ Gy and $r_{\mathrm{nucl}} = 5$ μm, this endpoint will be called LEM $\mathrm{I}_{ref.}$ in the remainder.

Biological effects of high-LET radiations together with a precise dose deposition make carbon-ion beams favorable for highly-conformal treatments of hypoxic, slowly-growing tumors with high repair capacity. First clinical results support this hypothesis (Tsujii and Kamada (2012)). In particular, prostate cancer, for which first clinical results with carbon-ion beams are also available (Ishikawa *et al.* (2012)), was chosen in this analysis as an example of a slowly-growing tumor surrounded by radiosensitive structures.

Based of the available information, clinically-validated LEM I input parameters have not yet been published for prostate cancer. That is why several published input parameters and their combinations were tested. The objectives of this study were to assess the influence of the LEM I input parameters and their combinations on the dose distribution and on TCP predictions for prostate cancer. Simulations were performed in the case of a cubic water phantom and a patient geometry using the TPS TRiP98.

II

Materials and methods

Contents

1 Nomenclature

Several methods exist for prescribing and reporting the dose in carbon-ion radiotherapy (see §i page 36). Historically, these differences are mainly due to the development of various techniques to deliver a therapeutic carbon-ion beam and due to the experience of the local clinical teams with prescribing a high-LET irradiation. For a defined biological or clinical endpoint and taking into account local technical specificities of the beam delivery, radiobiological models can be used to calculate biological weighting factors as well as the absorbed dose of carbon-ions to be delivered. In accordance with the latest IAEA and ICRU reports (IAEA and ICRU (2008)), we propose the definitions of dose quantities and their abbreviations as reported in table II.1.

Table II.1: Definitions of dose quantities and abbreviations used. In the appendix, additional information is given with respect to some LEM specific dose definitions.

Name	Abbreviation	Unit	Definition
Absorbed dose per fraction in voxel	d_{v}	Gy	Energy deposited per unit of mass in a voxel v for one fraction
Mean absorbed dose per fraction	d_{m}	Gy	Mean of absorbed dose in voxel v over an investigated volume V: $d_m = (1/n_v) \times \sum_v (d_v)$; v in V, n_v number of voxels in V
Mean total absorbed dose	D_{m}	Gy	D_{m}= $d_{\mathrm{m}}\times$ number of fractions
Local dose	-	Gy	the basic dose variable for the calculation of biological effects in the LEM: it corresponds to "the expectation value of the dose deposited at a given point (x,y,z) in the nucleus for a given set of incoming primary photons or particles" (Scholz *et al.* (2008))
Biological dose per fraction in voxel	d_{Bv}	Gy	it corresponds to the dose of photons in voxel v that causes the same biological effects as an absorbed dose d_{v} of carbon-ions
Total biological dose in voxel	D_{Bv}	Gy	D_{Bv}= $d_{\mathrm{Bv}}\times$ number of fractions
Mean total biological dose	D_{Bm}	Gy	average of D_{Bv} in voxel v over an investigated volume V $D_{Bm} = (1/n_v) \times \sum_v (D_{Bv})$ v in V, n_v number of voxels in V
Mean biological dose per fraction	d_{Bm}	Gy	d_{Bm}= D_{Bm}/ number of fractions
Prescribed dose per fraction	d_{Bp}	Gy	prescription for d_{Bv} in each voxel of the target
Threshold dose	D_{t}	Gy	dose at which the survival curve becomes purely exponential: $D_t = (s_{max} - \alpha)/(2 \times \beta)$ applying the modified version of the linear quadratic model (Eq. IV.4)
Dose 50%	D_{50}	Gy	mean absorbed dose D_{m} (in the PTV) necessary to obtain a Tumor Control Probability of 50%

2 Treatment Planning

a) TRiP98 treatment planning system for ions and the LEM

Based on a prescribed dose d_{Bp} in photon therapy, a cell survival probability can be calculated. TRiP98 calculates a set of beam parameters that leads to the same cell survival probability per fraction for a carbon-ion treatment together with the absorbed dose per fraction d_{v} in each voxel v.
In an implementation of the LEM I used for clinical applications, so called "look-up tables" are calculated. They contain the four input parameters of LEM I (α, β, D_{t} and r_{nucl}), and an initial calculation of α_z/α values (see §ii page 26). Consequently, these look-up tables are used by TRiP98 to optimize the beam parameters aiming at distributing the dose d_{Bv} according to the prescription d_{Bp}.

b) LEM I input parameters for prostate cancer

Based on published tumor control data after external beam radiotherapy or brachytherapy, various authors proposed estimations of absolute values of α and β parameters for prostate cancer (Brenner and Hall (1999), Wang *et al.* (2003), Miralbell *et al.* (2012)). Published estimates vary largely, as various mathematical and numerical methods were used, and a comprehensive review of available estimates has been recently published by Oliveira *et al.* (2012). To represent this variability, five different sets of α and β values were analyzed; they were obtained through analysis of clinical tumor control with different TCP models (table II.2). Based of the available information, clinically-validated LEM I input parameters have not yet been published for prostate cancer.
In most publications, threshold doses between 20 and 45 Gy (i.e. -33 % to +50 % compared to the Pilot Project) are reported, some authors assume a threshold between 10 and 60 Gy (i.e. -67 % to +100 % compared to the Pilot Project) (Elsässer and Scholz (2006), Elsässer and Scholz (2007), Elsässer *et al.* (2008), Scholz and Elsässer (2007), Scholz *et al.* (2008), Beuve *et al.* (2008)). For the calculations reported in this study, we used $r_{\mathrm{nucl}} = 5$ μm.
Astrahan (2008) proposed a method to find D_{t} and suggested that $D_t = 2 * \alpha/\beta$. This method to set D_{t} is deduced from dose escalation experiments on cells up to 10 Gy and also that $s_{max}/\alpha \approx 5$. Following Astrahan's suggestion, D_{t} would be between 2.8 or 6.2 Gy.

c) Dose calculation

With TRiP98, treatment plans were generated (1) in a rectangular parallelepiped water phantom and (2) in one example case of a patient with prostate cancer. The rectangular parallelepiped planning target volume (PTV) in the water phantom had a volume of 79 cm^3 (4.45 x 4.45 x 4 cm^3) and was placed at 17.6 cm depth in a water phantom with a size of 35.1 x 35.1 x 16 cm^3. The computed tomography (CT) images of the phantom had a 0.5 x 0.5 mm in slice resolution while the slice thickness was 2 mm. In the patient geometry, the clinical target volume (CTV) was 75 cm^3; the CTV-to-PTV margin was set to 5 mm. The CT-images had a 0.98 x 0.98 mm in slice resolution and a slice thickness of 3 mm. The treatment plans were evaluated only with respect to PTV. In both geometries, TRiP98 planning parameters

were chosen according to previous treatment planning studies (Jelen *et al.* (2012), Chanrion *et al.* (2013)). The raster grid specifying the step size in the x and y direction was set to 2 mm, the energy steps (z direction) to 3 mm in water and the requested full width at half maximum (FWHM) of the spot to 5 mm (delivered: 5.5-5.7 mm). In the process of beam optimization, additional spots are allowed to be delivered outside the target volume in order to ensure PTV coverage. This extension was set to a value corresponding to 0.4 times the local spot FWHM. A double-Gaussian pencil beam model with multiple scattering algorithm (Iancu *et al.* (2009)) was applied for the dose calculation with a cut-off of 1.8 times the FWHM of the local spot size (Krämer and Scholz (2000), M. Krämer (2011)). Different fractionation schedules were investigated with prescribed biological doses d_{Bp} of 2, 4 and 6 Gy. We chose two lateral opposing beams in all treatment plans. This beam geometry (Jäkel *et al.* (2001), Böhlen *et al.* (2012), Friedrich *et al.* (2013)) results in a homogeneous absorbed dose distribution in the target volume for a carbon-ion radiotherapy (see §III for quantification of the dose homogeneity). The absorbed dose in each voxel of the PTV, d_{v}, was averaged and is denominated d_{m}. This mean absorbed dose d_{m} could be considered as a simple and representative indicator to estimate the influence of the LEM I input parameters on the dose distribution. Furthermore, the calculated values of the cell survival probability were also homogeneous in the target and thus the mean cell survival probability could be used for comparison and subsequent TCP calculations. The term *reference plan* is used in this paper for treatment plans prepared with the LEM I input parameters as applied during the German Pilot Project: α= 0.1 Gy^{-1}, β= 0.05 Gy^{-2}, D_{t}= 30 Gy and r_{nucl}=5 μm. This endpoint will be called LEM I$_{ref.}$ in the remainder. Up to now, this set of parameters is the only one used clinically for any tumor type and location.
To assess the influence of the LEM input parameters, we followed these steps:

1) the d_{m} in the PTV calculated for a *reference plan* was compared plans using other sets of input parameters;

2) d_{Bv} was re-calculated with another set of LEM I input parameters, using beam parameters of each of the three *reference plans*. The resulting d_{Bm} were compared;

3) TCP predictions were calculated for all parameters tested.

d) Evaluation of the treatment plans

For steps 1) and 2), distributions of the d_{Bv} were quantitatively evaluated in terms of coverage index (CI-95%) and homogeneity index (HI). The CI-95% index is defined as the percentage of volume receiving 95% of the prescribed biological dose d_{Bp}. The HI index is the difference between near-maximum and near-minimum dose ($\mathrm{D}_{\mathrm{near-max}}$, $\mathrm{D}_{\mathrm{near-min}}$) normalized to the prescription dose. The $\mathrm{D}_{\mathrm{near-min}}$ and $\mathrm{D}_{\mathrm{near-max}}$ were defined at the 98% and 2% volume levels, respectively (ICRU 2007). If CI-95% was <98% and HI>6%, the dose distribution was considered inhomogeneous and plans were excluded from the later TCP analysis.

3 Tumor Control Probability

Following a method proposed by Scholz *et al.* (2006), the calculated mean cell survival probability values in the PTV could be plotted against the mean absorbed dose for the different

LEM I input parameters and treatment-plan scenarios. Six data points were collected from the dose computations: three resulting from computations run for step one (see §c) page 55) and three obtained from computations in step two. With these points, the linear quadratic model could be fitted and estimates of α and β values were obtained. They characterize the response of cells in the PTV to the carbon-ion irradiation and will subsequently be called α_c and β_c. Finally, TCP curves were calculated by replacing α and β parameters of the different TCP equations by α_c and β_c (table II.2).

Table II.2: Overview of published α, β and equations to calculate tumor control probability (TCP) together with their associated parameters values. The 95% confidence interval is given in square brackets when originally given by the author. The percentage of variation compared to the *reference* values from the German Pilot Project are reported in round parenthesis.

publication	α/β	α	β	TCP model	N_0 or K
Brenner and Hall (1999)	1.5 [0.8-2.2] (-25%)	0.036 [0.026-0.045] (-64%)	0.024 (-52%)	$TCP(D) = \exp(-N_0 \exp(-D(\alpha+\beta d)))$ d=2	$N_{0low} = 59$ $N_{0int} = 140$ $N_{0high} = 455$
Wang *et al.* (2003)	3.1 ±0.5 (+55%)	0.15 ±0.04 (+50%)	0.048 (-96%)	$TCP(D) = \exp(-N_0 \exp(-D(\alpha+\beta d)+ (\ln(2)/T_{pot} t(D/d))))$ d=1.7 T_{pot}=42	$N_{0low} = 1.6 \times 10^6$ $N_{0int} = 3.0 \times 10^6$ $N_{0high} = 1.1 \times 10^7$
Miralbell *et al.* (2012) low risk	1.4 [0.9-2.2] (-30%)	0.041 [0.023-0.061] (-59%)	0.029 (-42%)	$TCP(D) = \exp(-\exp(K - \alpha D - \beta D d))$ d=2	5.3
Miralbell *et al.* (2012) intermediate risk	1.4 [0.9-2.2] (-30%)	0.032 [0.019-0.046] (-68%)	0.023 (-54%)	$TCP(D) = \exp(-\exp(K - \alpha D - \beta D d))$ d=2	4.5
Miralbell *et al.* (2012) high risk	1.4 [0.9-2.2] (-30%)	0.019 [0.009-0.031] (-81%)	0.014 (-72%)	$TCP(D) = \exp(-\exp(K - \alpha D - \beta D d))$ d=2	2.8
Pedicini *et al.* (2013) * all risk	2.96 [2.41-3.53] (+48%)	0.16 [0.14-0.18] (+60%)	0.054 (+8%)	$TCP(D) = \exp(-N_0 \exp(-D(\alpha+\beta d)+ (\ln(2)/T_{pot}(T - T_k))))$ d=2 T_{pot}=5.1 T_k=31	6.5×10^6

Abbreviations: d - dose per fraction, D - total dose, T_{pot} - potential doubling time of cell repopulation and t - total treatment time in days (calculated by dividing the total number of fractions by the ratio of treatment days per week), T_k the kick-off time for tumor repopulation, N_0 - initial number of clonogenic cells in the tumor and K - natural logarithm of the initial number of clonogenic cells. * Parameters not used in the sensitivity analysis.

III

Results

Contents

1 Evaluation of the treatment plans

Six of the sixty treatment plans for the phantom geometry and four of the sixty treatment plans for the patient geometry did not fulfill the planning objectives (see §d) page 56) and were excluded from further analysis. For five of the ten discarded plans, both CI-95% and HI did not fulfill the objectives; CI-95% ranged from 66.2% to 90.2% and HI from 22.8% to 33.1%. For the other five discarded plans, although the CI-95% reached the planning objectives, the HI did not and ranged from 6.7% to 8.0%. For all rejected plans, hot and cold spots appeared in the middle of the PTV. We hypothesize a dose optimization algorithm failure for those plans that were calculated with $d_{\mathrm{Bp}} = 2$ Gy with the highest values of D_{t} ($D_{\mathrm{t}} = 45$ and 60 Gy). Indeed, with these input parameters, the relative biological effectiveness (RBE) calculated in the PTV was high (> 6.6) as compared to the published values in the literature (Schulz-Ertner *et al.* (2003), Karger *et al.* (2013)). These RBE values are most likely overestimated, showing the importance of setting an appropriate threshold dose when parameterizing the LEM I with new input values.

2 Absorbed dose

For each set of input parameters (α, β and D_{t}), d_{m} ($\pm$ standard deviation) was calculated at the prescribed biological dose d_{Bp} levels of 2, 4 and 6 Gy. For the *reference plans*, d_{m} was 0.47 ± 0.01 Gy, 1.37 ± 0.02 Gy and 2.63 ± 0.05 Gy for the phantom geometry and 0.50 ± 0.02 Gy, 1.44 ± 0.06 Gy and 2.74 ± 0.10 Gy respectively in the patient geometry. Tested plans, calculated with several LEM I input parameters, led to very different values for d_{m}. Table III.3 summarizes the extreme values, considering two intervals of D_{t} values (20-45 Gy and 10-60 Gy). Depending on the prescribed dose d_{Bp}, the ratio between these extreme values varied from 2.8 to 3.5 for the large interval and from 1.8 to 2.4 for the restricted interval. Table III.2 summarizes these extreme values for the large interval, detailed for each set of α and β values. For all tested α and β values, the D_{t} value strongly influences the calculated d_{m}.

Table III.1: Minimum and maximum mean absorbed dose $d_{\mathrm{m}} \pm$ standard deviation calculated at each prescribed dose level d_{Bp}, for both threshold intervals tested: 20-45 Gy and 10-60 Gy and for all α and β values tested.

	$D_t \in 10-60$ Gy		$D_t \in 20-45$ Gy	
Prescribed dose	Minimum	Maximum	Minimum	Maximum
Phantom geometry:				
$d_{\mathrm{Bp}} = 2$ Gy	0.38 ± 0.01	1.02 ± 0.02	0.30 ± 0.02	0.71 ± 0.01
$d_{\mathrm{Bp}} = 4$ Gy	0.75 ± 0.02	2.59 ± 0.05	0.90 ± 0.02	1.89 ± 0.03
$d_{\mathrm{Bp}} = 6$ Gy	1.52 ± 0.04	4.50 ± 0.07	1.81 ± 0.04	3.41 ± 0.16
Patient geometry:				
$d_{\mathrm{Bp}} = 2$ Gy	0.41 ± 0.02	1.05 ± 0.04	0.31 ± 0.02	0.75 ± 0.03
$d_{\mathrm{Bp}} = 4$ Gy	0.80 ± 0.05	2.66 ± 0.07	0.96 ± 0.06	1.96 ± 0.07
$d_{\mathrm{Bp}} = 6$ Gy	1.62 ± 0.10	4.58 ± 0.10	1.92 ± 0.11	3.52 ± 0.11

Table III.2: Minimum and maximum mean absorbed dose $d_{\mathrm{m}} \pm$ standard deviation in Gy calculated at each prescribed dose level for each α and β value tested and for all threshold doses tested.

	$d_{\mathrm{Bp}} = 2$ Gy		$d_{\mathrm{Bp}} = 4$ Gy		$d_{\mathrm{Bp}} = 6$ Gy	
(α, β)	Minimum	Maximum	Minimum	Maximum	Minimum	Maximum
Phantom geometry:						
(0.036,0.024)	0.31 ± 0.01	0.81 ± 0.02	0.80 ± 0.02	2.30 ± 0.05	1.60 ± 0.03	4.18 ± 0.09
(0.15,0.048)	0.38 ± 0.01	1.02 ± 0.02	1.05 ± 0.02	2.59 ± 0.05	1.98 ± 0.02	4.50 ± 0.07
(0.041,0.029)	0.31 ± 0.01	0.80 ± 0.02	0.80 ± 0.02	2.29 ± 0.05	1.62 ± 0.03	4.19 ± 0.09
(0.032,0.023)	0.30 ± 0.01	0.79 ± 0.02	0.78 ± 0.02	2.28 ± 0.05	1.58 ± 0.03	4.16 ± 0.09
(0.019,0.014)	0.30 ± 0.02	0.78 ± 0.02	0.75 ± 0.02	2.25 ± 0.05	1.52 ± 0.04	4.13 ± 0.09
Patient geometry:						
(0.036,0.024)	0.33 ± 0.02	0.85 ± 0.04	0.85 ± 0.05	2.38 ± 0.08	1.70 ± 0.09	4.30 ± 0.13
(0.15,0.048)	0.41 ± 0.02	1.05 ± 0.04	1.11 ± 0.05	2.66 ± 0.07	2.08 ± 0.09	4.58 ± 0.10
(0.041,0.029)	0.33 ± 0.02	0.84 ± 0.04	0.85 ± 0.05	2.37 ± 0.08	1.72 ± 0.09	4.30 ± 0.12
(0.032,0.023)	0.32 ± 0.02	0.83 ± 0.04	0.83 ± 0.05	2.36 ± 0.08	1.68 ± 0.09	4.28 ± 0.12
(0.019,0.014)	0.31 ± 0.02	0.82 ± 0.04	0.80 ± 0.05	2.33 ± 0.09	1.62 ± 0.10	4.24 ± 0.13

To compare d_{v} distributions with the *reference plans*, dose profiles at the isocenter along the beam axis were divided by the corresponding dose profile of the *reference plans*, and are subsequently called *normalized profiles* (figure III.1). At a first glance, the ratios of dose were constant, indicating that changing the LEM I input parameters led simply to a multiplication of the absorbed dose by a constant factor. However, slightly larger discrepancies occur at the edge of the PTV. These irregularities may be due to the process of plan optimization: with a constraint on homogeneity of the biological dose in the PTV and not at the edges, where a pronounced LET gradient appears.

An analytical expression for d_{m}, as a function of the prescribed d_{Bp}, can be derived based on two hypotheses (see Appendix for mathematical details). First, the energy primarily lost by ions interacting with a cell remains in this cell (i.e. radial extension of ion track smaller than the cell nucleus). Second, overkilling effects were neglected since, in the present study, the dose average LET was always lower than 70 keV/μm in the tumor. Finally, the analytical expression for d_{m} is:

$$d_m = d_{Bp} \cdot \frac{1 + d_{Bp}/\frac{\alpha}{\beta}}{(1-\eta)\frac{s_{max}}{\alpha} + \eta} \tag{III.1}$$

The coefficient η is a number, lower or equal to 1, that characterizes the proportion of lethal events around the ion track and in the cell nucleus. For a mixed field, it is specific to the distribution of ion types and energies in the PTV. This expression can be rewritten as:

$$\frac{\alpha d_{Bp} + \beta d_{Bp}^2}{d_m \alpha} = (1-\eta)\frac{s_{max}}{\alpha} + \eta \tag{III.2}$$

which emphasizes a linear expression of $\frac{-ln(S(d_{Bp}))}{d_m \alpha}$ with s_{max}/α. This hypothetical was tested with the linear expression and values d_{Bp}, D_{t} and d_{m} obtained previously. Through a fitting procedure with nonlinear least-squares using the R statistical environment (R Core Team (2012)), we found a reasonable correlation (figure III.2), supporting the hypothesis that s_{max}/α is a

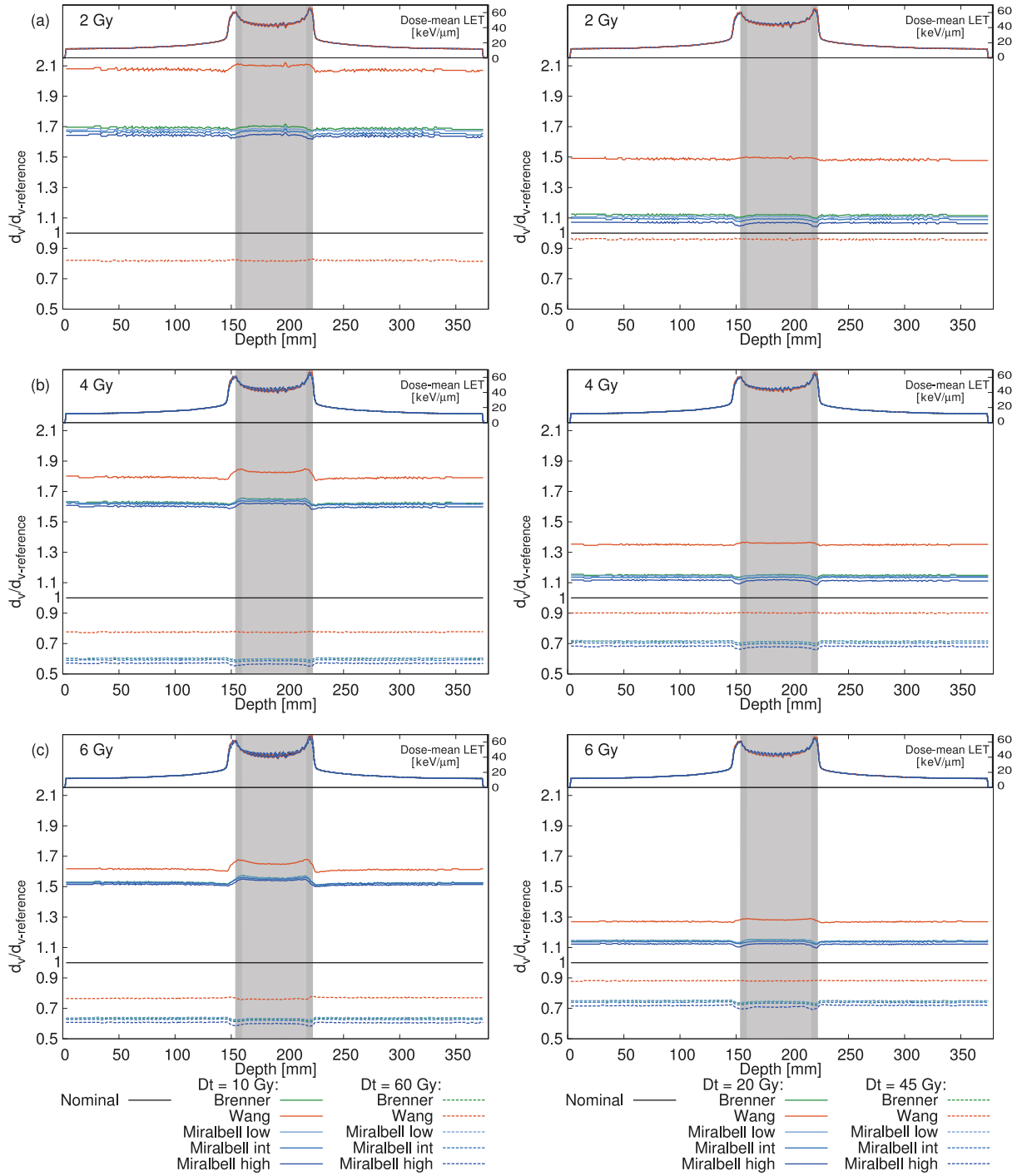

Figure III.1: Normalized profiles of the absorbed dose d_{v} at the isocenter along the beam direction for the patient geometry for the five initial sets of α and β values tested and the three prescribed dose levels: $d_{\mathrm{Bp}} = 2$, 4 and 6 Gy. The left column shows the profiles using $D_t = 10$ or 60 Gy, the right column using $D_t = 20$ or 45 Gy. The PTV area is shown in grey. For each normalized profile, the dose-mean LET profile is presented.

determining parameter in the d_{Bv} calculation by the LEM I. The resulting η equals 0.771 (standard error: $\pm$ 0.003) for the patient geometry and 0.758 ($\pm$ 0.003) for the phantom geometry giving a goodness of fit: $\chi^2_{\mathrm{reduced}} = 3.01$ and 3.18 respectively. With this approach, an estimate of d_{m} can be extracted within conditions close to the ones of the present study ($\alpha/\beta \lesssim 3.1$, $\alpha \lesssim 0.15$; geometry with two opposed fields; PTV volume of the same order of magnitude).

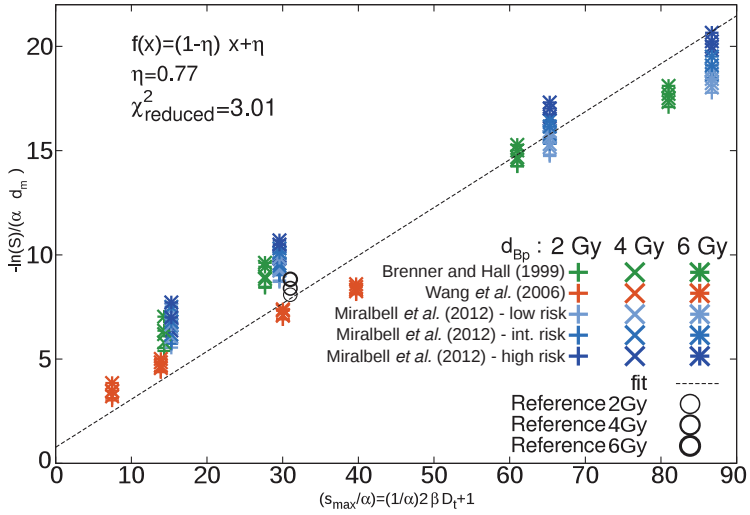

Figure III.2: Patient geometry: results obtained applying equation III.2 for all D_t, d_{Bp} and published α/β used. Results obtained with the reference input parameters are named *reference*. They are given for reference only and were not taken into account in the fitting procedure

Following Astrahan's method, D_t calculated would be between 2.8 to 6.2 Gy, which is lower than values available in the literature in the frame of LEM calculations. With these D_t, in the case of phantom or patient geometry, the $d_m$was calculated, the resulting mean absorbed dose in the PTV with a prescribed biological dose per fraction d_{Bp} (table III.3). In some cases, the prescribed dose d_{Bp} is then higher than D_t (for instance $d_{Bp} = 4$ or 6 Gy).

Table III.3: d_m calculated using specific D_t calculated using Astrahan's method

(α, β)	$d_{Bp} = 2$ Gy	$d_{Bp} = 4$ Gy	$d_{Bp} = 6$ Gy
Phantom geometry:			
(0.036,0.024)	1.47 ±0.03	3.55 ±0.05	5.56 ±0.07
(0.15,0.048)	1.26 ±0.02	3.08 ±0.05	5.20 ±0.07
(0.041,0.029)	1.51 ±0.03	3.58 ±0.05	5.59 ±0.07
(0.032,0.023)	1.50 ±0.03	3.57 ±0.05	5.58 ±0.07
(0.019,0.014)	1.49 ±0.03	3.56 ±0.05	5.57 ±0.07
Patient geometry:			
(0.036,0.024)	1.26 ±0.30	3.04 ±0.71	4.74 ±1.11
(0.15,0.048)	1.08 ±0.26	2.64 ±0.62	4.46 ±1.04
(0.041,0.029)	1.28 ±0.31	3.07 ±0.71	4.76 ±0.12
(0.032,0.023)	1.28 ±0.31	3.06 ±0.71	4.76 ±0.11
(0.019,0.014)	1.27 ±0.31	3.05 ±0.71	4.75 ±0.12

As expected, reducing the D_t leads to an increase of d_m in the PTV and hence an increase of the difference with respect to *reference plans*. However, these new calculations with very low values of D_t show very high inhomogeneous distributions in the patient geometry and the resulting d_m. This makes hard to go further in the analysis since the source of the inhomogeneous

distribution of dose should be firstly studied. Therefore, following the Astrahan's method to calculate D_t is discussed in §1 page 70.

3 Sensitivity of the biological dose d_{Bm}

In order to quantify the consequences of a different tumor response, the d_{Bm} deposited by the three *reference plans* (d_{Bp} = 2, 4 and 6 Gy) was re-calculated without plan re-optimization using the 20 combinations of the LEM I input parameters. The maximum deviations of the re-computed d_{Bm} of the phantom were -45.5%, -26.9%, +35.5% and +51.8% for the threshold doses 10, 20, 45 and 60 Gy, respectively. For the patient geometry, the maximum deviations of the re-computed d_{Bm} were -44.8%, -26.4%, +34.2% and +50.1% for the threshold doses 10, 20, 45 and 60 Gy respectively. These deviations were plotted in a box plot for each α and β value and are shown in figure III.3.

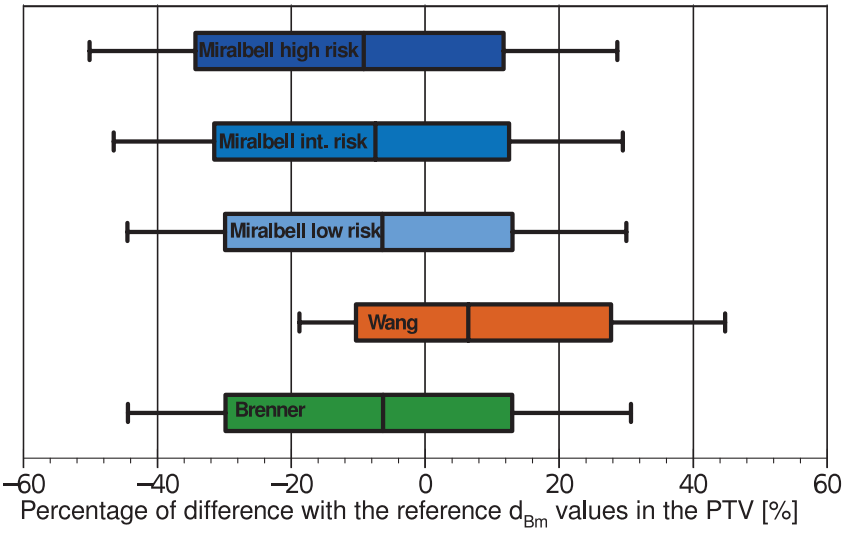

Figure III.3: Box plots of deviations (in %) to the *reference* mean biological dose d_{Bm}calculated in the PTV for each α and β parameter tested in the patient geometry.

The resulting normalized profiles of d_{Bv} at the isocenter along the beam direction in the patient geometry are shown in figure III.4. Contrary to the absorbed dose, normalized d_{Bv} profiles show different sorts of gradient outside, at the border and in the PTV. Using Wang's input parameters for threshold doses $>$ 30 Gy, the deviation from the *reference* profile in the PTV is higher, whereas for threshold doses $<$ 30 Gy, deviations are lower. With Brenner and Miralbell's parameters, profiles are rather flat (except at the target edges), demonstrating a constant variation compared to the *reference* plan. For all input parameters tested, most of the gradients appear at the target edges, where the LET shows significant variations.

4 Tumor Control Probability

The TCP predictions were calculated for each of the five initial sets of α and β using the corresponding TCP model published by each of the authors. Among the TCP models chosen in the present work, only Wang *et al.* (2003) consider a time factor to account for repopulation.

Table III.4: Deviation (in %) to the *reference* mean biological dose d_{Bm} calculated in the PTV for each α, β and D_{t} parameters tested, and for each prescribed dose d_{Bp} : 2, 4 and 6 Gy.

	Brenner and Hall (1999)			Wang *et al.* (2003)			Miralbell *et al.* low risk (2012)			Miralbell *et al.* int risk(2012)			Miralbell *et al.* high risk(2012)		
Phantom geometry:															
d_{Bp}(Gy)	2	4	6	2	4	6	2	4	6	2	4	6	2	4	6
D_{t}(Gy)															
10	-30.9	-29.0	-27.2	-45.5	-37.4	-32.6	-30.2	-28.8	-27.1	-29.7	-28.4	-26.8	-28.8	-27.7	-26.3
20	-6.8	-8.2	-8.3	-26.9	-19.9	-16.4	-6.2	-8.1	-8.5	-5.2	-7.3	-7.8	-3.6	-6.1	-6.8
45	30.3	23.6	20.5	3.1	7.3	8.7	30.5	23.3	20.0	32.3	24.7	21.3	35.5	27.2	23.6
60	45.6	36.7	32.5	15.7	18.6	19.2	45.6	36.1	31.7	47.83	37.9	33.3	51.8	41.1	36.2
Patient geometry:															
d_{Bp}(Gy)	2	4	6	2	4	6	2	4	6	2	4	6	2	4	6
D_{t}(Gy)															
10	-30.7	-28.6	-26.7	-44.8	-36.6	-31.7	-30.0	-28.4	-26.6	-29.5	-28.0	-26.3	-28.7	-27.5	-25.9
20	-7.0	-8.3	-8.4	-26.4	-19.5	-15.9	-6.4	-8.2	-8.5	-5.5	-7.5	-7.9	-4.0	-6.4	-7.0
45	29.4	22.8	19.7	3.1	7.2	8.6	29.7	22.5	19.2	31.3	23.8	20.4	34.2	26.1	22.4
60	44.4	35.6	31.26	15.6	18.3	18.8	44.5	35.1	30.6	46.5	36.7	32.1	50.1	39.6	34.6

For both phantom and patient geometries, calculated D_{50} for all input parameters and for the three clinical prostate cancer risk groups (D'Amico *et al.* (1998)) tested, are presented in table III.5. The TCP curves obtained in the patient geometry are shown in figure III.5.

Table III.5: D_{50} in Gy obtained from the TCP calculations, and calculated from the original photon equations for the different prostate cancer risk groups: low, intermediate (int.) and high. For discarded treatment plans, values are not shown.

	Brenner and Hall (1999)			Wang *et al.* (2003)			Miralbell *et al.* (2012)		
	Low	Int.	High	Low	Int.	High	Low	Int.	High
Photons	52.9	63.2	77.2	62.5	65.2	76.1	57.2	62.4	67.4
Phantom geometry:									
$D_{\mathrm{t}} = 10$ Gy	19.6	23.5	28.7	29.2	30.4	33.0	21.0	22.7	24.0
$D_{\mathrm{t}} = 20$ Gy	12.9	15.4	18.8	20.4	21.2	23.0	13.8	14.8	15.6
$D_{\mathrm{t}} = 45$ Gy	7.8	9.3	11.4	13.0	13.6	14.7	-	8.9	-
$D_{\mathrm{t}} = 60$ Gy	-	-	-	11.1	11.6	12.6	-	-	-
Patient geometry:									
$D_{\mathrm{t}} = 10$ Gy	20.4	24.3	29.7	30.0	31.3	33.9	21.8	23.5	25.0
$D_{\mathrm{t}} = 20$ Gy	13.5	16.2	19.7	21.1	22.0	23.9	14.5	15.5	16.4
$D_{\mathrm{t}} = 45$ Gy	8.2	9.8	12.0	13.6	14.2	15.4	8.8	9.4	9.8
$D_{\mathrm{t}} = 60$ Gy	-	-	-	11.6	-	13.2	-	12.1	-

For a fixed value of dose threshold, the relative differences of D_{50} may be calculated. For the high risk and the low risk prostate cancer groups $(D_{50-high} - D_{50-low})/(D_{50-high} + D_{50-low})$, are very similar for the carbon-ion TCP predictions and for the photon TCP predictions.

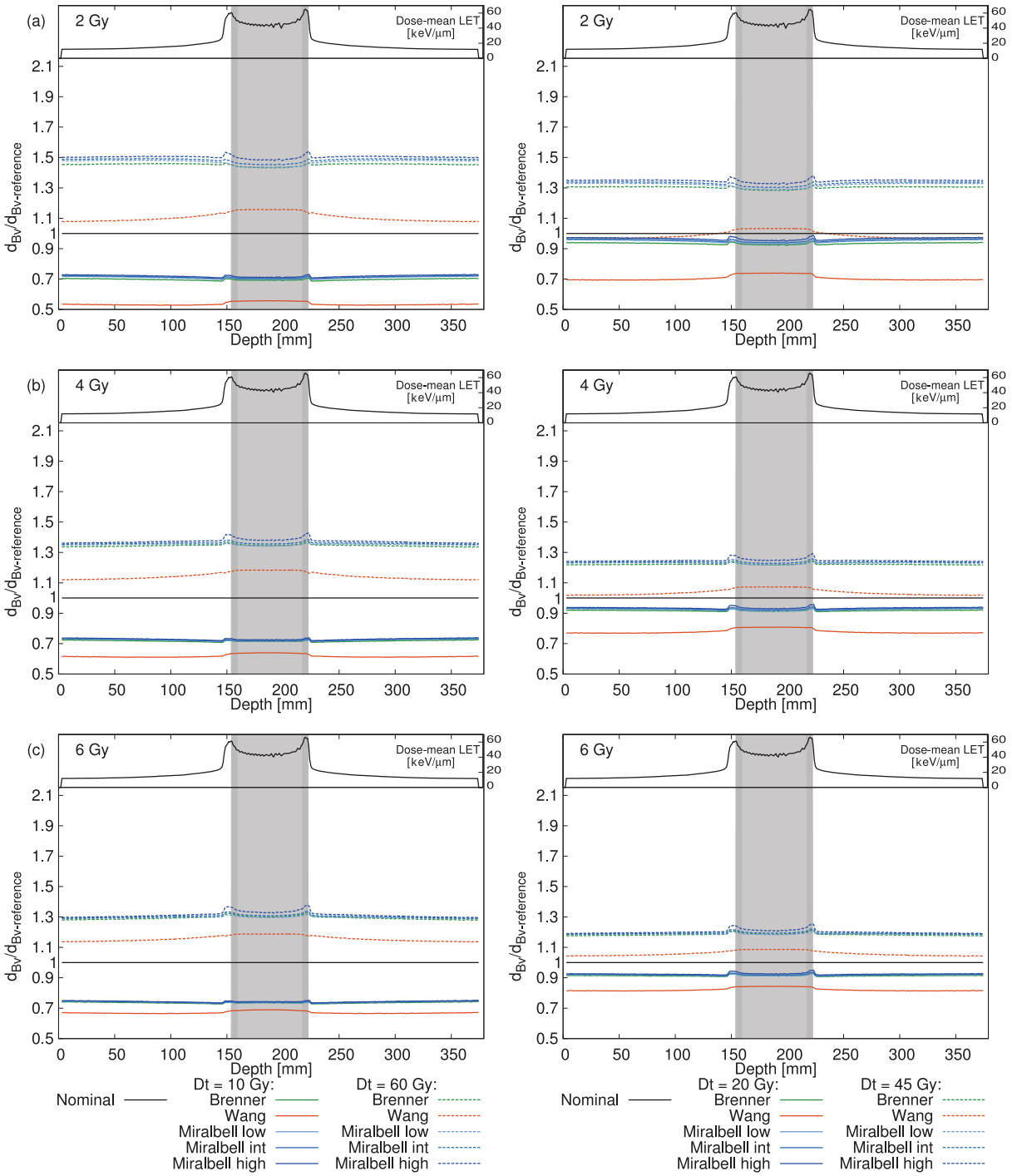

Figure III.4: Normalized profiles of the biological dose d_{Bv} at the isocenter along the beam direction for each of the five initial sets of α and β values tested and the three prescribed dose levels: 2, 4 and 6 Gy. The left column shows the profiles using D_t = 10 or 60 Gy, the right column using D_t = 20 or 45 Gy. The PTV area is shown in grey. For each normalized profile, the dose-mean LET profile is presented.

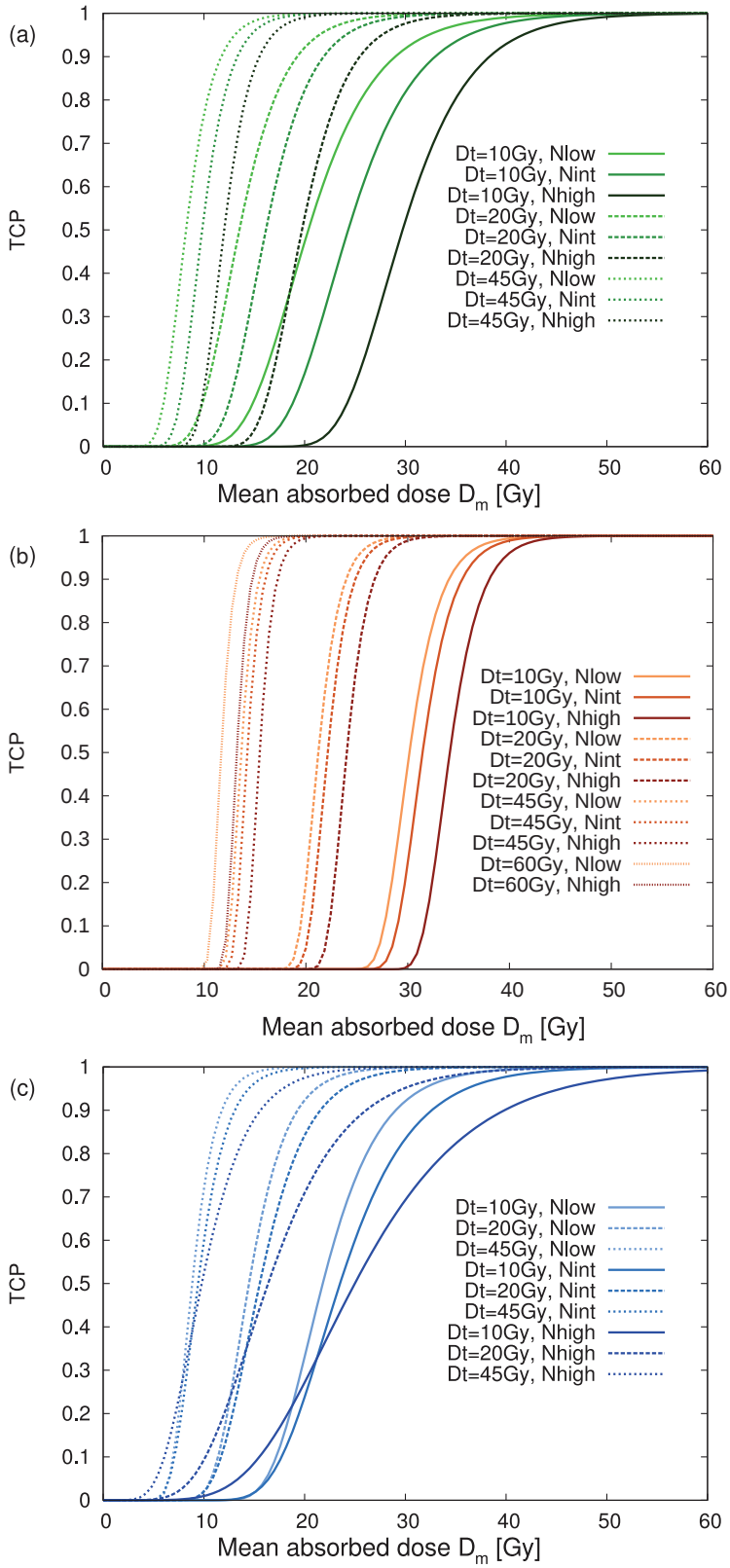

Figure III.5: Tumor control probability for low, intermediate and high risk prostate cancer obtained in the patient geometry for each of the five initial sets of α and β tested using different threshold values and the original TCP models and parameters published by: (a) Brenner and Hall (1999), (b) Wang *et al.* (2003), (c) Miralbell *et al.* (2012)

IV
Discussion

Contents

In this study, the influence of the LEM I input parameters on the calculated absorbed doses (d_{v} and d_{m}), biological doses (d_{Bv} and d_{Bm}) as well as on the resulting TCP predictions, was investigated. Investigating the sensitivity of a radiobiological model to its input parameters in case of carbon-ion therapy was, based of the available information, previously addressed in three papers: Remmes *et al.* (2012), Böhlen *et al.* (2012) and Friedrich *et al.* (2013). Remmes *et al.* focused on the microdosimetric-kinetic model, while Böhlen *et al.* and Friedrich *et al.* investigated the LEM IV. The present study focuses on prostate cancer and investigates the sensitivity of the LEM I predictions to its input parameters (α, β and D_{t}). The choice of these input parameters was based on published and widely accepted values of α, β values and threshold dose (Oliveira *et al.* (2012), Elsässer and Scholz (2006), Elsässer and Scholz (2007), Elsässer *et al.* (2008), Scholz and Elsässer (2007), Scholz *et al.* (2008)). Furthermore, the radiobiological model LEM I is used for clinical purposes at the particle therapy centers of HIT (Heidelberg, Germany) and CNAO (Pavia, Italy) and is intended to be used at the MIT (Marburg, Germany) and Med-Austron (Wiener Neustadt, Austria) facilities. Furthermore, the variation of the predictions of TCP after carbon-ion irradiation using several sets of α and $\beta$was tested; with α and βobtained from TCP analysis of prostate cancer radiotherapy treatments.

1 LEM I input parameters

Aiming at proposing more adequate LEM I input parameters to calculate biological effects of carbon-ion radiotherapy of prostate cancer, we performed a comprehensive literature review to identify clinically accepted α and β values obtained from clinical TCP predictions. Compared to the *reference* LEM I input parameters, the range of variation of α, β and α/β, was [-50%, +81%], [-3%, -72%] and [-55%, +32%], respectively. Friedrich *et al.* (2013) investigated the effects of variation (± 25 % range) of α and β parameters used during the German Pilot Project. Böhlen *et al.* (2012) tested variations of α, β and α/β in a range of ± 5% to ± 50%. A higher amplitude of variation for α, β and α/β was tested to cover the range of published values more extensively.

The α/β ratio can be estimated comparing clinical results obtained with different fractionation schemes, using the BED formalism (Biological Equivalent Dose) and the *fraction-effective* plot (Douglas and Fowler (1976)), but it remains a challenge to establish the absolute values of these parameters (Kal and Gellekom (2003), Carlson *et al.* (2004)). The review of Oliveira *et al.* (2012) illustrates the numerous mathematical and numerical methods that exist and the variability of their deduced estimates. These different models lead to different α and β values even if the same clinical data are used to fit their input parameters (Daşu *et al.* (2003)). Conversely, Pedicini *et al.* (2013) used the same approach as Wang *et al.* (2003), but using a dataset consisting of only radiotherapy results and derived similar estimates for α and β values.

Astrahan (2008) proposed a formula to determine values for the threshold dose D_{t} from *in vitro* cell experiments: $Dt = 2 \times \alpha/\beta$. Following this proposal, D_{t} would be between 2.8 to 6.2 Gy for the sets of α/β tested. These values are lower than those available in the literature for calculations with the LEM and those used for this analysis, hence it would lead into a further increase of the discrepancy as compared to the *reference plans*.

Based of the available information, in all European facilities, treatment plans are calculated using the following LEM I parameters: $\alpha = 0.1$ Gy^{-1}, $\beta = 0.05$ Gy^{-2}, D_{t}=30 Gy, r_{nucl} =5 μm,

irrespective of the tumor entity (e.g. chordoma, tumors in the head and neck region, prostate cancer). The relevance of using such parameters to optimize any carbon-ion treatment plan is not known: clinical results are needed to feedback the LEM and draw conclusions. Interestingly, following Astrahan (2008) proposal, the D_{t} should be 4 Gy when $\alpha = 0.1$ Gy^{-1} and $\beta = 0.05$ Gy^{-2}: this is very different from the values clinically used of 30 Gy. High-LET experiments with *in-vitro* or *in-vivo* systems could help to determine the best combination of input parameters, keeping in mind that these parameters should also be consistent with a specific TCP model. Knowing that different methods to find individual values of α and β and that their result show a large variability, adding a supplementary parameter to calculate biological effects, such as D_{t}, might compensate an initial mis-estimation of those parameters (Böhlen *et al.* (2012), Friedrich *et al.* (2013)).

2 Mean Absorbed Dose d_{m}

When considering all the five sets of α and β values, variations of the D_{t} value led to variations of the calculated d_{m} by a factor of 1.8 to 3.5 with respect to the prescribed biological dose d_{Bp}. The observed impact of the LEM parameters is considerable compared to the accuracy in the dose prescription required in radiotherapy. Fixing a particular value for the α and β couple, led to a variation by a factor of 2 to 3. If, conversely, a fixed value of Dt was given, a maximal variation factor of 1.4 was obtained (table III.2), suggesting, that constraining D_{t} is more important. However, even with D_{t} is fixed, the uncertainties remain clinically significant. To understand better the correlated impact of α, β and D_{t} on the mean absorbed dose d_{m}, an estimate of the biological dose d_{Bp} from an analytical expression of the LEM I predictions was derived (see Appendix) and a linear correlation (equation III.1) was observed. This approach is only valid for conditions close to the ones as described in §c) page 55. Precisely, in this analytical expression, the estimation of d_{m} is, for a given prescription d_{Bp}, a function of only two parameters (α/β) and $(s_{max}/\ \alpha)$, instead of the three parameters α, β and D_{t}. This indicates that, for this study, (α/β) and $(s_{max}/\ \alpha)$ are major parameters for LEM I predictions. This is consistent to *in vitro* experiments, which have shown that the final slope s_{max} of the cell survival curve together with the α value play a major role for irradiation with high-LET ions (Beuve *et al.* (2008)). Furthermore, Scholz and Elsässer (2007) stated that the RBE will increase with s_{max}/α for a given particle type and energy since the highest effectiveness is determined by the final slope of the photon dose response curve. Further studies are needed to evaluate, whether this reduction from three to two parameters can be generalized to other configurations (tumor, geometry, beam setup).

3 Mean Biological Dose d_{Bm}

Until now, exclusively the reference LEM I input parameters have been used for clinical purposes. For the future, other values of LEM input parameters might be used to account for individual tumor radiosensitivity, ideally, patient-specific. For the five sets of α and β values and the four threshold doses tested, the re-computed biological dose was either lower or higher than the prescribed dose level d_{Bp}. Moreover, the distribution of d_{Bm} became inhomogeneous over the PTV. This study shows that, when testing published and clinically accepted α, β and

D_t values to calculate carbon-ion dose distributions, differences in the biological dose calculation ranging from approximately 3% to 50% as compared to the *reference plan* can occur. These differences have only been estimated for prostate cancer, other studies using other sets of LEM I input parameters should be performed to evaluate the differences for other tumor types or to compare radiobiological models (Steinsträter *et al.* (2012), Fossati *et al.* (2012))

4 Phantom geometry vs. patient geometry

The absorbed doses (d_v and d_m), the re-calculated biological dose (d_{Bv} and d_{Bm}), and the TCP predictions were evaluated for two geometries: a rectangular parallelepiped phantom and a prostate cancer patient using a setup with two-opposed fields. No major effect of the geometry was found. This indicates, that the shape of the volume does not quantitatively influence the conclusion derived, at least with similar PTV volumes and depths. Further tests should be performed with very big or very small prostate volumes to verify this conclusion.

5 Tumor Control Probability

One way to ensure that the biological effect calculated by a model is consistent with the observed biological damage, is to correlate the clinically observed local tumor control with the calculated cell survival curves (Scholz *et al.* (2006), Kanai *et al.* (2006), Matsufuji *et al.* (2011)). This work aims at calculating biological effects quantified in terms of TCP predictions for various sets of LEM I input parameters. It should be emphasized here, that this work focuses on sensitivity of the LEM I predictions to its input parameters. It does not give any indication on the reliability of the LEM for biological predictions.

Significantly different TCP curves were obtained testing several combinations of LEM I input parameters for prostate cancer. For the LEM I calculations, the α and β values were consistently associated to each of these TCP models, the impact of the four values of $D_t$was tested. For each TCP model, a parameterization was given according to the prostate cancer risk groups. The ongoing debate on the order of magnitude of α and β parameters versus the number of clonogenic cells estimated in the TCP model (Daşu *et al.* (2003), Daşu (2007)), can have consequences in the estimation of D_{50} and the TCP slope at 50% and thereupon, on the evaluation of α and β parameters. Furthermore, the definition of the clinical end-point to evaluate the local control after external beam radiotherapy and the time of follow-up are different between the five different sets of TCP parameters used in the present study: in Brenner and Hall (1999) the end-point was defined according to the American Society for Therapeutic Radiology and Oncology Consensus Panel definition, in Wang *et al.* (2003) the local tumor control was assessed through prostate biopsies and in Miralbell *et al.* (2012) according to the Phoenix criterion. Consequently, estimates of α and β depend on the TCP model and the clinical end-point used to report local control. Additionally, we observed major changes in the TCP curves due to a modification of the D_t value.

In the past 100 years, radiotherapy has been developed empirically, but also, using radiobiological models. For instance, models like the linear quadratic model have been developed to predict cell survival probability based on biological mechanisms. The interpretation of the linear quadratic model is questioned (Bentzen and Joiner (2009)), but, within defined areas of

application, the linear quadratic model remains a useful model in photon therapy to calculate bioeffects when its parameters are known (i.e. α/β). Exploiting data from conventional radiotherapy experience is useful to deduce key radiobiological parameters, but is not sufficient to predict clinical results of carbon-ion radiotherapy.

Reducing discrepancies of the estimated parameters used for calculation of biological effects induced by carbon-ion, can be achieved by reducing intermediate steps in the radiobiological modeling. For instance, choosing a prescribed dose d_{Bp} corresponds to choosing a desired survival probability calculated with the linear quadratic model. Since survival probability can also be calculated using TCP curves, one could define the survival probability directly from TCP modeling, reducing the sensitivity of d_{m} to the estimated α and β parameters.

We calculated D_{50} for several D_{t} but also the relative difference of D_{50} for the high risk and the low risk cancer groups. These relative differences were very similar between photons and carbon-ions if the dose threshold was fixed to a specific value: in particular for Brenner and Hall, Wang *et al.* this can be proved analytically. This means that, if the α/β and α are fixed between risk groups (Brenner and Hall (1999), Wang *et al.* (2003), Fowler *et al.* (2013)), the value of D_{t} does not modify the relative sensitivity, in terms of TCP predictions, between risk groups. In other words, the free parameter D_{t} impacts on the calculation of survival and biological effects in the same way whatever the risk groups considered. If carbon-ion therapy would reduce the difference in tumor response between risk groups, it would be necessary to adapt the D_{t} value according to the risk. In the framework of this study, it is not possible to conclude whether carbon-ion therapy reduces or not the effects of risk groups. However, when the α/β is fixed but the α changes between risk groups (Miralbell *et al.* (2012)) or when the α/β changes between risk groups (Pedicini *et al.* (2013)), a specific value of D_{t} according to risk groups should only be considered if future clinical observations show a discrepancy.

In vivo studies can be used to discriminate the relevant combinations of α and β values associated with a threshold dose. Karger *et al.* (2013) have estimated D_{50}, RBE and effective α/β for split doses in 1, 2 or 6 fractions of carbon-ion irradiation in a syngeneic rat prostate tumor model (Peschke *et al.* (2011), Karger *et al.* (2013)). They estimated that D_{50} is to 43.7 $\pm$ 2.3 Gy, RBE 2.67 $\pm$ 0.15 and α/β 84.7 $\pm$ 13.8 Gy. Although this study gave estimates and confirmed the effectiveness of carbon-ion radiotherapy, the D_{50} and α/β can hardly be compared with the proposed TCP analysis.

Any radiobiological model to predict high-LET radiobiological effects and clinical outcomes of carbon-ion radiotherapy can be optimized, with a high degree of confidence, only if input parameters are derived and later refined iteratively with feedback of clinical results. Similarly, the input parameters for radiobiological models to predict the effects of carbon-ion radiotherapy have to be estimated from clinical observations or via prospective clinical trials. At the same time, models to calculate biological effects are a prerequisite for designing clinical trials.

6 Conclusion

This study has shown and quantified the high sensitivity of the LEM I predictions to its input parameters in the specific case of prostate cancer. Some first clinical results for prostate cancer

treated with carbon-ion radiotherapy in Japan are available (Ishikawa *et al.* (2012)). This experience is very valuable for the design of treatment protocols in new particle therapy centers in Europe: it may help to find a combination of LEM I input parameters for the treatment of prostate cancer. The next part of this thesis studies possible methodologies for exploiting available clinical results calculated with other radiobiological models and for optimizing upcoming clinical protocols.

Appendix

This appendix details the mathematical steps to obtain an analytical estimation of d_{m}. The radial dose in the LEM was described by Elsässer and Scholz (2007)

$$D(r) = \begin{cases} \lambda LET/r_{min}^2 & \text{if } r < r_{min} \\ \lambda LET/r^2 & \text{if } r_{min} \leq r \leq r_{max} \\ 0 & \text{if } r > r_{max} \end{cases} \tag{A-1}$$

where λ is a normalization constant and r the radial distance to the ion trajectory. a is the constant dose when $r < r_{min}$. r_{min} is the radius, at which the dose decreases and r_{max} the radius, at which the dose is negligible, the total dose contribution around the track can be expressed:

$$S_e = \int_0^{r_{max}} 2\pi D(r) r \, \mathrm{d}r = \int_0^{r_{min}} 2\pi a r \, \mathrm{d}r + \int_{r_{min}}^{r_{max}} 2\pi \frac{a r_{min}^2}{r^2} \, \mathrm{d}r \tag{A-2}$$

After integrating, we obtain:

$$\frac{S_e}{2\pi a} = r_{min}^2 * \left(\frac{1}{2} + \ln\left(\frac{r_{max}}{r_{min}} \right) \right) \tag{A-3}$$

Analytical calculations of the lethal event require the following hypotheses:

- The radius, at which the dose contribution becomes negligible, is assumed to be lower than the nucleus radius: $r_{max} << r_{nucl}$
- Impacts are assumed at a distance: $r < (r_{nucl} - r_{max})$ of the nucleus center
- let r_t be defined such as $D(r_t) = D_t$, when $r_t > r_{min}$

The total number of lethal events can be calculated, when integrating lethal event in the region of the particle track and the cell nucleus:

$$N = \int_0^{r_{max}} -\frac{\ln\Big(S(D(r))\Big)}{A_{nucl}} 2\pi r \, \mathrm{d}r \tag{A-4}$$

In case of higher doses than the LEM specific threshold dose:

$$NA_{nucl} = \int_0^{r_t} \Big(s_{max} D(r) - \beta D_t^2 \Big) 2\pi \ r \, \mathrm{d}r + \int_{r_t}^{r_{max}} \Big(\alpha D(r) + \beta D(r)^2 \Big) 2\pi \ r \, \mathrm{d}r \tag{A-5}$$

With

$$D_t = \frac{a r_{min}^2}{r_t^2} \tag{A-6}$$

The integration of equation A-5 gives:

$$NA_{nucl} = s_{max}S_e + 2\pi a r_{min}^2 \ln\left(\frac{r_{max}}{r_{min}}\left(\sqrt{D_t/a}\right)\right)\left(-2\beta D_t\right) - \beta\pi a^2 \frac{r_{min}^4}{r_{max}^2} \tag{A-7}$$

The last term of the equation is low and can be neglected and finally we have:

$$NA_{nucl} = s_{max}S_e - \left(2\beta D_t\right)\left(2\pi a r_{min}^2 \ln\left(\frac{r_{max}}{r_{min}}\sqrt{D_t/a}\right)\right) \tag{A-8}$$

From equation A-3, we can express:

$$2\pi a = \frac{S_e}{r_{min}^2 * \left(\frac{1}{2} + \ln\left(\frac{r_{max}}{r_{min}}\right)\right)} \tag{A-9}$$

And hence, equation A-8 can be expressed:

$$NA_{nucl} = s_{max}\left[S_e - \left(2\beta D_t\right)\frac{\ln\left(\frac{r_{max}}{r_{min}}\sqrt{D_t/a}\right)}{\frac{1}{2} + \ln\left(\frac{r_{max}}{r_{min}}\right)}\right] \tag{A-10}$$

Saying that:

$$\eta = \frac{\ln\left(\frac{r_{max}}{r_{min}}\sqrt{D_t/a}\right)}{\frac{1}{2} + \ln\left(\frac{r_{max}}{r_{min}}\right)} = \frac{\ln\left(\frac{r_{max}}{r_t}\right)}{\frac{1}{2} + \ln\left(\frac{r_{max}}{r_{min}}\right)} \tag{A-11}$$

and $r_{min}^{'} = r_{min}exp(-\frac{1}{2})$, we have:

$$\eta = \frac{\ln\left(\frac{r_{max}}{r_t}\right)}{\ln\left(\frac{r_{max}}{r_{min}^{'}}\right)} \tag{A-12}$$

And finally,

$$NA_{nucl} = S_e\left(s_{max}(1-\eta) + \alpha\eta\right) \tag{A-13}$$

With the previously mentioned hypotheses we can conclude that:

- $\eta \leq 1$ since $r_t > r_{min}^{'}$
- For high-LET radiations r_t is high (maximum r_{max}) and then $\eta \to 0$. Hence,

$$N = \frac{S_e}{A_{nucl}}s_{max} \tag{A-14}$$

- For low-LET radiations $r_t \to r_{min}^{'}$ and hence $\eta \to 1$

In a mixed field, when neglecting quadratic terms, the survival probability can be approximated:

$$S = exp(-\sum_i F_i\sigma_i) \tag{A-15}$$

With F_i the fluence of (E_i, Z_i) particles and σ_i the lethal cross-section for (E_i, Z_i). The cross-section can be written:

$$\sigma_i = A_{nucl}\Big(1 - e^{n_i}\Big) \tag{A-16}$$

Where n_i is the number of lethal events created by one impact of a particle (E, Z) in the nucleus of area A_{nucl}. Taking equation A-13:

$$n_i = \frac{S_{e(i)}\big(s_{max}(1-\eta_i) + \alpha\eta_i\big)}{A_{nucl}} \tag{A-17}$$

When neglecting the overkilling, σ_i can be expressed:

$$\sigma_i = A_{nucl} n_i \tag{A-18}$$

Hence,

$$S = exp\Big(-\sum_i F_i\sigma_i) = exp\Big(-\sum_i F_i A_{nucl} n_i\Big) = exp\Big(-\sum_i F_i S_{e(i)}\big(s_{max}(1-\eta_i)+\alpha\eta_i\big)\Big) \tag{A-19}$$

Introducing the dose d_i for each particle (E_i, Z_i) in voxel v:

$$S = exp\Big(-\sum_i d_i\big(s_{max}(1-\eta_i) + \alpha\eta_i\big)\Big) \tag{A-20}$$

With $d_v = \sum_i d_{vi}$ and $\overline{\eta_v} = \frac{\sum_i d_i}{d_v}\eta_i$, we can reduce the previous equation to:

$$S = e^{-d_v\left(s_{max}(1-\overline{\eta_v})+\alpha\overline{\eta_v}\right)} \tag{A-21}$$

Which can be re-written:

$$\alpha d_{Bp} + \beta d_{Bp}^2 = d_v\big(s_{max}(1-\overline{\eta_v}) + \alpha\overline{\eta_v}\big) \tag{A-22}$$

And finally,

$$d_v = d_{Bp}.\frac{1 + d_{Bp}/\frac{\alpha}{\beta}}{(1-\eta_v)\frac{s_{max}}{\alpha} + \eta_v} \tag{A-23}$$

In case of a homogeneous dose distribution d_v in the PTV and hence η_v, we can introduce the quantities η and d_{m}, the average of d_{v} in the PTV. Consequently, the previous equation can be written:

$$d_m = d_{Bp}.\frac{1 + d_{Bp}/\frac{\alpha}{\beta}}{(1-\eta)\frac{s_{max}}{\alpha} + \eta} \tag{A-24}$$

Bibliography

Astrahan, M. (2008). Some implications of linear-quadratic-linear radiation dose-response with regard to hypofractionation. *Med Phys*, 35(9):4161–4172. b), 1

Bentzen, S. and Joiner, M. (2009). *Basic Clinical Radiobiology 4th edition*, chapter 9: The linear-quadratic approach in clinical practice. Hodder Arnold, Great Britain. 5

Beuve, M., Alphonse, G., Maalouf, M., Colliaux, A., Battiston-Montagne, P., *et al.* (2008). Radiobiologic parameters and local effect model predictions for head-and-neck squamous cell carcinomas exposed to high linear energy transfer ions. *Int J Radiat Oncol Biol Phys*, 71(2):635–642. b), 2

Böhlen, T. T., Brons, S., Dosanjh, M., Ferrari, A., Fossati, P., *et al.* (2012). Investigating the robustness of ion beam therapy treatment plans to uncertainties in biological treatment parameters. *Phys Med Biol*, 57(23):7983–8004. c), IV, 1

Brenner, D. J. and Hall, E. J. (1999). Fractionation and protraction for radiotherapy of prostate carcinoma. *Int J Radiat Oncol Biol Phys*, 43(5):1095–1101. b), III.5, 5

Carlson, D. J., Stewart, R. D., Li, X. A., Jennings, K., Wang, J. Z., *et al.* (2004). Comparison of in vitro and in vivo alpha/beta ratios for prostate cancer. *Phys Med Biol*, 49(19):4477–4491. 1

Chanrion, M. A., Ammazzalorso, F., Wittig, A., Engenhart-Cabillic, R., and Jelen, U. (2013). Dosimetric consequences of pencil beam width variations in scanned beam particle therapy. *Phys Med Biol*, 58(12):3979–3993. c)

D'Amico, A. V., Whittington, R., Malkowicz, S. B., Schultz, D., Blank, K., *et al.* (1998). Biochemical outcome after radical prostatectomy, external beam radiation therapy, or interstitial radiation therapy for clinically localized prostate cancer. *JAMA*, 280(11):969–974. 4

Daşu, A. (2007). Is the alpha/beta value for prostate tumours low enough to be safely used in clinical trials? *Clin Oncol (R Coll Radiol)*, 19(5):289–301. 5

Daşu, A., Toma-Daşu, I., and Fowler, J. F. (2003). Should single or distributed parameters be used to explain the steepness of tumour control probability curves? *Phys Med Biol*, 48(3):387–397. 1, 5

Douglas, B. G. and Fowler, J. F. (1976). The effect of multiple small doses of x rays on skin reactions in the mouse and a basic interpretation. *Radiat Res*, 66(2):401–426. 1

Elsässer, T., Krämer, M., and Scholz, M. (2008). Accuracy of the local effect model for the prediction of biologic effects of carbon ion beams in vitro and in vivo. *Int J Radiat Oncol Biol Phys*, 71(3):866–872. b), IV

Elsässer, T. and Scholz, M. (2006). Improvement of the local effect model (lem)–implications of clustered dna damage. *Radiat Prot Dosimetry*, 122(1-4):475–477. b), IV

Elsässer, T. and Scholz, M. (2007). Cluster effects within the local effect model. *Radiat Res*, 167(3):319–329. b), IV, 6

Fossati, P., Molinelli, S., Matsufuji, N., Ciocca, M., Mirandola, A., *et al.* (2012). Dose prescription in carbon ion radiotherapy: a planning study to compare nirs and lem approaches with a clinically-oriented strategy. *Phys Med Biol*, 57(22):7543–7554. 3

Fowler, J. F., Toma-Dasu, I., and Dasu, A. (2013). Is the / ratio for prostate tumours really low and does it vary with the level of risk at diagnosis? *Anticancer Res*, 33(3):1009–1011. 5

Friedrich, T., Scholz, U., Elsässer, T., Durante, M., and Scholz, M. (2013). Systematic analysis of rbe and related quantities using a database of cell survival experiments with ion beam irradiation. *J Radiat Res*, 54(3):494–514. c), IV, 1

IAEA and ICRU (2008). Technical reports series no. 461: Relative biological effectiveness in ion beam therapy. Technical report, INTERNATIONAL ATOMIC ENERGY AGENCY, Vienna. 1

Iancu, G., Krämer, M., and Schardt, D. (2009). Scattering implementation in trip. In *Proceedings of the Heavy Ions in Therapy and Space Symposium*, page 58, Cologne, Germany. c)

Ishikawa, H., Tsuji, H., Kamada, T., Akakura, K., Suzuki, H., *et al.* (2012). Carbon-ion radiation therapy for prostate cancer. *Int J Urol*, 19(4):296–305. I, 6

Jäkel, O., Krämer, M., Karger, C. P., and Debus, J. (2001). Treatment planning for heavy ion radiotherapy: clinical implementation and application. *Phys Med Biol*, 46(4):1101–1116. c)

Jelen, U., Ammazzalorso, F., Chanrion, M.-A., Gräf, S., Zink, K., *et al.* (2012). Robustness against interfraction prostate movement in scanned ion beam radiation therapy. *Int J Radiat Oncol Biol Phys*, 84(2):e257–e262. c)

Kal, H. B. and Gellekom, M. P. R. V. (2003). How low is the alpha/beta ratio for prostate cancer? *Int J Radiat Oncol Biol Phys*, 57(4):1116–1121. 1

Kanai, T., Matsufuji, N., Miyamoto, T., Mizoe, J., Kamada, T., *et al.* (2006). Examination of gye system for himac carbon therapy. *Int J Radiat Oncol Biol Phys*, 64(2):650–656. 5

Karger, C. P., Peschke, P., Scholz, M., Huber, P. E., and Debus, J. (2013). Relative biological effectiveness of carbon ions in a rat prostate carcinoma in vivo: comparison of 1, 2, and 6 fractions. *Int J Radiat Oncol Biol Phys*, 86(3):450–455. 1, 5

Krämer, M. and Scholz, M. (2000). Treatment planning for heavy-ion radiotherapy: calculation and optimization of biologically effective dose. *Phys Med Biol*, 45(11):3319–3330. c)

M. Krämer, M. (2011). http://bio.gsi.de/DOCS/TRiP98/DOCS/trip98.html (accessed 2014.10.01). TRiP online documentation. c)

Matsufuji, N., Wada, M., Kase, Y., Uzawa, A., and Ando, K. (2011). Modeling the clinical and biological effect of therapeutic carbon ion beam. In *Proceedings: NIRS-ETOILE 2nd Joint Symposium on Carbon Ion Radiotherapy*. 5

Miralbell, R., Roberts, S. A., Zubizarreta, E., and Hendry, J. H. (2012). Dose-fractionation sensitivity of prostate cancer deduced from radiotherapy outcomes of 5,969 patients in seven international institutional datasets: / = 1.4 (0.9-2.2) gy. *Int J Radiat Oncol Biol Phys*, 82(1):e17–e24. b), III.5, 5

Oliveira, S. M., Teixeira, N. J., and Fernandes, L. (2012). What do we know about the / for prostate cancer? *Med Phys*, 39(6):3189–3201. b), IV, 1

Pedicini, P., Strigari, L., and Benassi, M. (2013). Estimation of a self-consistent set of radiobiological parameters from hypofractionated versus standard radiation therapy of prostate cancer. *Int J Radiat Oncol Biol Phys*, 85(5):e231–e237. 1, 5

Peschke, P., Karger, C. P., Scholz, M., Debus, J., and Huber, P. E. (2011). Relative biological effectiveness of carbon ions for local tumor control of a radioresistant prostate carcinoma in the rat. *Int J Radiat Oncol Biol Phys*, 79(1):239–246. 5

R Core Team (2012). R: A language and environment for statistical computing. http://www.R-project.org (accessed 2014.10.01). ISBN 3-900051-07-0. 2

Remmes, N. B., Herman, M. G., and Kruse, J. J. (2012). Optimizing normal tissue sparing in ion therapy using calculated isoeffective dose for ion selection. *Int J Radiat Oncol Biol Phys*, 83(2):756–762. IV

Scholz, M. and Elsässer, T. (2007). Biophysical models in ion beam radiotherapy. *Advances in Space Research*, 40(9):1381 – 1391. b), IV, 2

Scholz, M., Matsufuji, N., and Kanai, T. (2006). Test of the local effect model using clinical data: tumour control probability for lung tumours after treatment with carbon ion beams. *Radiat Prot Dosimetry*, 122(1-4):478–479. 3, 5

Scholz, M., Weyrather, W., Krmer, M., and Kraft, G. (2008). *Technical reports series No. 461: Relative biological effectiveness in ion beam therapy*, chapter Modelling the increased biological effectiveness of heavy charged particles for tumour therapy treatment planning, pages 93–119. IAEA and ICRU, Vienna. II.1, b), IV

Schulz-Ertner, D., Nikoghosyan, A., Jkel, O., Haberer, T., Kraft, G., *et al.* (2003). Feasibility and toxicity of combined photon and carbon ion radiotherapy for locally advanced adenoid cystic carcinomas. *Int J Radiat Oncol Biol Phys*, 56(2):391–398. 1

Steinsträter, O., Grün, R., Scholz, U., Friedrich, T., Durante, M., *et al.* (2012). Mapping of rbe-weighted doses between himac- and lem-based treatment planning systems for carbon ion therapy. *Int J Radiat Oncol Biol Phys*, 84(3):854–860. 3

Tsujii, H. and Kamada, T. (2012). A review of update clinical results of carbon ion radiotherapy. *Jpn J Clin Oncol*, 42(8):670–685. I

Wang, J. Z., Guerrero, M., and Li, X. A. (2003). How low is the alpha/beta ratio for prostate cancer? *Int J Radiat Oncol Biol Phys*, 55(1):194–203. b), 4, III.5, 1, 5

Part C

Strategies to optimize clinical protocols in carbon-ion therapy for prostate cancer

I

Introduction

The LEM I is the radiobiological model used in CE-certified TPS for carbon-ion therapy. The previous (see B) has shown a significant sensitivity of the LEM I predictions in term of TCP to its input parameters in the specific case of prostate cancer. With the help of available clinical results, the following describes possible methodologies to optimize up-coming clinical protocols for prostate cancer.

The only clinical results from carbon-ion treatments come from Chiba in Japan. Treatments were delivered with the passive irradiation line of carbon-ions and calculated with the NIRS radiobiological model. The dose prescription of these results is given in "Gy E" (see §b) page 36). Since it is known that the "Gy E" from NIRS is different from the "Gy(RBE)" from LEM I, several methods have been proposed to convert a NIRS-model-based prescribed total dose into a LEM-based prescribed total dose (Matsufuji *et al.* (2007), Mizoe *et al.* (2008), Steinsträter *et al.* (2012), Fossati *et al.* (2012)). These methods mostly rely on the comparison of physical dose distributions between European and Japanese centres in order to *map* the relative biological effectiveness (RBE) between institutions. They may be used for European center using the LEM to design new clinical protocols according to the up-to-date protocols of NIRS and, that way, to benefit from their long-term clinical experience.

Previous studies on the LEM have shown that using incorrect input values may lead to incorrect predictions of cell survival (Beuve *et al.* (2008)) and on the prediction of tumor control probability (section B and Chanrion *et al.* (2014)). In particular, the probability of tumor control is more sensitive to the parameter threshold dose (D_{t}) than to the biological parameters α and β.

For evaluation, comparison and optimization of clinical protocols in carbon-ion therapy for prostate cancer, several questions may rise, like:

- Which D_{t} value needs to be set to reproduce the latest TCP results from NIRS when considering a specific TCP model and its parameters for prostate cancer?

- When setting α and β values for prostate cancer, is there any value of D_{t} that leads to a profile of absorbed dose equals to the profile from NIRS when the same prescribed biological dose is planned?

- Some institutions deliver one lateral beam per day and some two lateral beams per day, hence, is there any difference when delivering one lateral field per day or two-opposed lateral fields per day in term of TCP?

Such questions and some others will be addressed for the TCP model and the associated parameter published by Brenner and Hall (1999) for prostate cancer. Although being a relatively old analysis, α and β estimates are obtained from a cohort of patient that did not receive any side treatments like androgen deprivation therapy. After a brief presentation of existing methods to compare NIRS-model-based prescribed total dose into a LEM-based prescribed total dose, our methodology will be presented. In the result section, questions will be addressed and discussed. Finally, a general discussion on all these results is proposed in order to draw strategies to optimize clinical protocols.

II

Materials and methods

Contents

1 Treatment Planning

a) LEM and TRiP98

During the German Clinical Pilot Project one look-up table was used and determined for the endpoint late toxicity to the brain with the following values: $\alpha = 0.1$ Gy^{-1}, $\beta = 0.05$ Gy^{-2}, $r_{\mathrm{nucl}} = 5$ μm and $D_{\mathrm{t}} = 30$Gy. This look-up table will be called LEM $\mathrm{I}_{ref.}$ in the remainder of this manuscript. The same parameters are used daily at the HIT particle therapy center in Germany and at CNAO particle therpy center in Italy. Reported tumors treated with these parameters are: locally advanced adenoid cystic carcinomas, chordomas, chondrosarcomas, osteosarcomas, malignant salivary gland tumors, low grade glioma, primary and recurrent malignant astrocytoma and glioblastoma, and prostate (Combs and Debus (2013)). Finally, in accordance with the latest IAEA and ICRU reports (IAEA and ICRU (2007) and IAEA and ICRU (2008)), the general nomenclature for reporting the dose in carbon-ion radiotherapy in this manuscript is detailed in table II.1. The abbreviation of dose quantity are composed of a subscript that defines how the dose is calculated, the superscript index defines with wich radiobiological model the dose is calculated. The abbreviations of specific reported doses are described in Appendix §7 table III.7.

b) The LEM input parameters for prostate cancer

Amongst many published estimates for α and β parameters for prostate cancer, one combination of α and β extracted from clinical TCP curves have been selected: values from Brenner and Hall (1999). The TCP model associated is presented in table II.2. As previously shown (see section B and Chanrion *et al.* (2014)), for defined clinical end-point (bNED results from NIRS) and a defined TCP model, D_{t} will have to be chosen specifically.

c) Treatment plan simulation

With the TRiP98 TPS, treatment plans were generated with one (left or right) or two lateral beams in one prostate cancer patient. The planning CT was acquired with a voxel size of 0.98 x 0.98 and 3 mm slice thickness. The CTV volume was 45.1 cc. The PTV was defined by uniform 3D CTV expansion of 5 mm. In both geometries, TRiP98 spot parameters were chosen according to previous treatment planning studies (Jelen *et al.* (2012), Chanrion *et al.* (2013)). The raster spot grid pattern specifying the step size in the x and y direction was set to 2 mm, the energy steps (z direction) to 3 mm in water and the minimum full width at half maximum (FWHM) of the spot to 5 mm. In the process of beam optimization, the PTV volume has to be extended to allow additional spots to be delivered outside the target volume and hence to ensure PTV coverage. This extension was set to a value corresponding to 0.4 times the local spot FWHM. A double-Gaussian pencil beam model with multiple scattering algorithm (Iancu *et al.* (2009)) was applied for the dose calculation with a cut-off of 1.8 times the FWHM of the local spot (Krämer and Scholz (2000), M. Krämer (2011)).

Table II.1: Definitions of **general** dose quantities -all expressed in Gy- and abbreviations used. The * symbol should be replaced by the abbreviation of the radiobiological model used to calculate the quantity: NIRS for the NIRS radiobiological model, LEM $I_{ref.}$ when the LEM I with the reference input parameter is used, LEM I_{HSG} for LEM I with human salivary gland (HSG) input parameters (Steinsträter *et al.* (2012), Kanai *et al.* (2006)) and LEM $I_{Brenner\ and\ Hall}$ when the α and β are taken from the estimates published by Brenner and Hall (1999) with $r_{\mathrm{nucl}} = 5\ \mu$m and D_{t} set to a value that has to be precised.

Name	Abbreviation	Definition
Absorbed dose per fraction in voxel	d^*_{v}	energy deposited per unit of mass in a voxel v for one fraction
Mean absorbed dose per fraction	d^*_{m}	mean of absorbed dose in voxel v over an investigated volume V: $d_m = (1/n_v) \times \sum_v (d_v)$; v in V, n_v number of voxels in V
Mean total absorbed dose	D^*_m	$D^*_m = d^*_{\mathrm{m}} \times$ number of fractions
Biological dose per fraction in voxel	d^*_{Bv}	it corresponds to the dose of photons in voxel v that causes the same biological effects as an absorbed dose d^*_{v} of carbon-ions
Total biological dose in voxel	D^*_{Bv}	$D^*_{\mathrm{Bv}} = d^*_{\mathrm{Bv}} \times$ number of fractions
Mean total biological dose	D^*_{Bm}	average of D^*_{Bv} in voxel v over an investigated volume V $D_{Bm} = (1/n_v) \times \sum_v (D_{Bv})$ v in V, n_v number of voxels in V
Mean biological dose per fraction	d^*_{Bm}	$d^*_{\mathrm{Bm}} = D^*_{\mathrm{Bm}}/$ number of fractions
Prescribed dose per fraction	d^*_{Bp}	prescription for d^*_{Bv} in each voxel of the target
Prescribed total dose	D^*_{Bp}	$D^*_{\mathrm{Bp}} = d^*_{\mathrm{Bp}} \times$ number of fractions
Absorbed dose at the middle of the largest SOBP	$d^*_{\mathrm{middle-SOBP}}$	the absorbed dose at the middle of the largest SOBP can either be calculated with the table of clinical RBE for each SOBP width published by Kanai *et al.* (see table III.1 in part A, Kanai *et al.* (1999)): $d^*_{\mathrm{middle-SOBP}} = d^*_{\mathrm{Bp}}/\ RBE_{clinical}$ or by taking the absorbed dose calculated in the voxel at the middle of the largest SOBP of a computed treatment plan.
Total absorbed dose at the middle of the largest SOBP	$D^*_{\mathrm{middle-SOBP}}$	$D^*_{\mathrm{middle-SOBP}} = d^*_{\mathrm{middle-SOBP}} \times$ number of fractions
Threshold dose	D_{t}	dose at which the survival curve becomes purely exponential: $D_t = (s_{max} - \alpha)/(2 \times \beta)$ applying the linear quadratic-linear model

Table II.2: Published α, β and the equation to calculate tumor control probability (TCP) together with its associated parameters.

publication	α/β	α	β	TCP model	N_0
Brenner and Hall (1999)	1.5	0.036	0.024	$TCP(D) = \exp(-N_0 \exp(-D(\alpha + \beta d)))$	$N_{0low} = 59$ $N_{0int} = 140$ $N_{0high} = 455$

Abbreviations: d - dose per fraction, D - total dose, N_0 - initial number of clonogenic cells in the tumor.

2 Clinical experience

a) Converting clinical protocols and radiobiological models

With the development of carbon-ion therapy in Japan and in Europe, it became necessary to find methods for converting radiobiological model between institutions in order to homogenize and clearly define terms like *Relative Biological Effectiveness* and *RBE-weighted dose*, which are later necessary for the comparison of clinical results (see section ii page 38). After defining

boundary conditions (treatment of chordoma tumors with two opposing fields), Mizoe *et al.* (2008) concluded that the NIRS *physical dose* was 15% higher than the GSI *physical dose*, which means that the GSI has consequently a higher *clinical dose* of about 20% compared to the NIRS *equivalent dose*. Later, Steinsträter *et al.* (2012) published a more detail analysis to map "RBE-weighted dose" between NIRS and LEM models. After reconstructing the *physical dose* distribution used at NIRS for several SOBP and distal energy, factors to convert the biological dose from LEM to NIRS were calculated. Simultaneously, Fossati *et al.* (2012) published a similar analysis and concluded with similar conversion factors. In the design of clinical protocol and trials, the CNAO clinical team has used the conversion factors published to reproduce NIRS most recent clinical protocols (NIRS and MedAustron (2013)). For a SOBP of 120 mm, the difference between conversion factor calculated with the Steinsträter's method and the Fossati's method are negligible.

b) Clinical protocols for prostate cancer

In Ishikawa *et al.* (2012) presented results of three clinical protocols of NIRS:

- Protocol 9904: $d_{\mathrm{Bp}}^{\mathrm{NIRS}}$ =3.3 Gy in 20 fractions, hence $D_{\mathrm{Bp}}^{\mathrm{NIRS}}$ =66 Gy (250 patients)
- Protocol 9904-2: $d_{\mathrm{Bp}}^{\mathrm{NIRS}}$ =3.15 Gy in 20 fractions, hence $D_{\mathrm{Bp}}^{\mathrm{NIRS}}$ =63 Gy (216 patients)
- Protocol 9904-3: $d_{\mathrm{Bp}}^{\mathrm{NIRS}}$ =3.6 Gy in 16 fractions, hence $D_{\mathrm{Bp}}^{\mathrm{NIRS}}$ =57.6 Gy (461 patients)

Looking at protocol 9904-3, Fossati *et al.* (2012) concluded that, for single port irradiation of spheres, the physical dose per fraction equivalent to the NIRS dose per fraction of $d_{\mathrm{Bp}}^{\mathrm{NIRS}} = 3.6$ Gy is $d_{\mathrm{Bp}}^{\mathrm{LEM\ I-ref}} = 4.15$ Gy. At HIT the clinical protocol for treating prostate cancer started in May 2011 in the frame of a prospective randomized phase II trial. In this study 92 patients were enrolled with low-risk and intermediate risk cancer patients (NIRS and MedAustron (2013)). The fractionation scheme chosen was 20 fractions of 3.3 Gy (LEM $\mathrm{I}_{ref.}$) following strictly protocol 9904 from NIRS, hence the total dose was 66 Gy (LEM $\mathrm{I}_{ref.}$) (Habl *et al.* (2014)).

c) NIRS clinical results

Clinical results of protocols 9904, 9904-2 and 9904-3 are presented in Ishikawa *et al.* (2012): 927 patients were treated from 2003 to 2012 with a minimum follow-up of 6 months. Patients were separated in risk groups:

- low risk: iPSA < 20 ng/mL and GS ≤ 6 and T-stage $\leq$ T2a
- intermediate risk: iPSA < 20 ng/mL and GS $= 7$ or T-stage $=$ T2b
- high risk: iPSA > 20 ng/mL or GS ≥ 8 or T-stage $=$ T3

Total dose delivered was included between 66.0 or 63.0 Gy (NIRS model) in 20 fractions or 57.6 Gy (NIRS model) in 16 fractions. The reported 5-year biochemical non-evidence of disease (bNED) rates of the low, intermediate and high risk groups were 89.6%, 96.8% and 88.4%, respectively.

d) Determination of NIRS clinical RBE

For the example case of a patient with prostate cancer, the largest SOBP width (longitudinally to the beam) can be found using trip2png, a free software with display and analysis tools developed at our institution (Ammazzalorso *et al.* (2013)), in combination with the software imageJ (Schneider *et al.* (2012)). To find the largest SOBP width, both softwares are used to slice longitudinally to the beam each slice of the CT images. With this information the clinical NIRS RBE can be calculated by interpolation and using the table published by NIRS (see section b) page 23). Hence, the absorbed dose per fraction at the middle of the largest SOBP ($d^{\mathrm{NIRS}}_{\mathrm{middle-SOBP}}$) is calculated by dividing the NIRS prescribed dose by the clinical RBE. Total absorbed dose per fraction are also calculated at the middle of the largest SOBP ($D^{\mathrm{NIRS}}_{\mathrm{middle-SOBP}}$) for the NIRS protocols 9904, 9904-2 and 9904-3.

3 D_{t} value for a tie-in between LEM and NIRS protocols?

With the α and β published by Brenner and Hall, look-up tables are generated for several D_{t}. Treatment plans with the same prescribed dose as the three NIRS protocols are calculated. The D_{t} is allowed to change so that the absorbed dose at the middle of the largest SOBP is the same as published by NIRS, which means that a D_{t} value is found to match both prescribed dose and absorbed dose at the middle of SOBP from NIRS. In the remainder, the method will be called **method A**.

4 Determination of NIRS irradiation fields for HSG cell line

Since NIRS irradiation fields used to treat patients were based on an optimization of absorbed-dose profiles to induce a uniform HSG cell survival, we decided to calculate treatment plans for human salivary gland (HSG) cell lines. From the publication of Steinsträter *et al.* (2012) and Kanai *et al.* (2006), the HSG parameters needed for the LEM look-up tables are: $\alpha = 0.3312$ Gy^{-1}, $\beta = 0.0593$ Gy^{-2}, $D_t = 7.5$ Gy and $r_{nucl} = 5\mu$m. For each beam configuration and each protocol, the $d^{\mathrm{LEM\ I-HSG}}_{\mathrm{Bp}}$ was adjusted so that the obtained absorbed dose $d^{\mathrm{LEM\ I-HSG}}_{\mathrm{middle-SOBP}}$ equals $d^{\mathrm{NIRS}}_{\mathrm{middle-SOBP}}$ at the middle of the largest SOBP. When the goal was achieved, the fields recorded by TRiP98 as "raster files" (M. Krämer (2011)) were stored. They contain the information on the beam spot geometry, fluence and energy needed to achieve an absorbed dose distribution thought to be very close to the distribution of absorbed dose delivered at NIRS for the three protocols and the three beam geometries.
This method was evaluated by comparing the calculated depth dose profile to the dose profile of NIRS published by Fossati *et al.* (2012). For this comparison, a cubic target of 80 mm slide length located at 70 mm depth was considered. The $d^{\mathrm{LEM\ I-HSG}}_{\mathrm{Bp}}$ was adjusted so that the $d^{\mathrm{LEM\ I-HSG}}_{\mathrm{middle-SOBP}}$ equals 1.83 Gy, as published by Fossati *et al.*. The depth dose profile obtained were also compared with the tested LEM $\mathrm{I}_{Brenner\ and\ Hall}$ look-up table and the LEM $\mathrm{I}_{ref.}$.
In summary, dose distributions were computed using:

- the LEM $\mathrm{I}_{ref.}$ and $d^{\mathrm{LEM\ I-ref}}_{\mathrm{Bp}} = 4.60$ Gy.

- the LEM $I_{Brenner\ and\ Hall}$ (method A). $d_{\mathrm{Bp}}^{\mathrm{LEM\ I-BH}}$ was also adjusted to match the NIRS published absorbed dose at the middle of the SOBP. D_{t} equals 18.44 Gy, which correspond to the 9904-3 protocol for high risk patients.

- the LEM I_{HSG} (method B). $d_{\mathrm{Bp}}^{\mathrm{LEM\ I-HSG}}$ was also adjusted so that the absorbed dose at the middle of the SOBP matches with the published NIRS absorbed dose at the middle of the SOBP.

5 Optimizing D_{t} value according to bNED values

LEM look-up tables for several D_{t} using α and β values published by Brenner and Hall were generated. Using the fields saved as "raster files" that reproduce the absorbed dose fields with HSG parameters, the biological dose distributions in the patient CT may be calculated by TRiP98. That way, the predicted survival distribution of such a carbon-ion treatment is obtained. Hence, modifying D_{t} may modify the theoretical TCP. The predicted survival S_i is calculated by TRiP98 in each voxel i. The tumor control probability is calculated according to the model published by Brenner and Hall (see section b) page 88):

$$TCP(D) = exp(-N_0 * \frac{\sum_i S_i^n}{N_v}) \tag{A-1}$$

With N_0 the initial number of clonogenic cells, n the number of fractions and N_v the number of voxel in the PTV. For each risk group and each test LEM table, the calculated $TCP(D)$ is compared with bNED until both are equal. Finally, an "optimized" D_{t} is found for each tumor risk group, each protocol and for each beam configuration when $TCP(D)$ = bNED. In the remainder, the method will be called **method B**.

6 One field one day or two fields per day?

For technical reasons, at NIRS one lateral field is delivered per day. On the contrary, at HIT, both lateral fields are delivered per day. At CNAO, treatments are delivered with one lateral field per day. On the theoretical point of view, it is possible to estimate whether this difference in beam delivery has an impact on the TCP calculation. It could be said that both beam delivery strategies are equivalent in terms of TCP calculation when:

$$\eta = \frac{TCP(n \times d_{opposed-beams})}{TCP(\frac{n}{2} \times d_{left-side} + \frac{n}{2} \times d_{right-side})} \tag{A-2}$$

and $\eta \to 1$.

7 Reproduction of CNAO and HIT treatment protocols

Firsly, treatment plans following strictly the HIT and CNAO protocol are calculated with the LEM $I_{ref.}$. The $d_{\mathrm{Bp}}^{\mathrm{LEM\ I-ref}}$is 3.3 Gy (LEM $I_{ref.}$) for HIT protocol and is $d_{\mathrm{Bp}}^{\mathrm{LEM\ I-ref}}$ = 4.15 Gy (LEM $I_{ref.}$) for CNAO.

With the irradiation fields from the original HIT and CNAO protocols previously calculated and with LEM look-up table LEM $I_{Brenner\ and\ Hall}$, an estimation of the TCP can be calculated and compared with the NIRS bNED published values.

III

Results

Contents

1 One field one day or two fields per day?

The comparison of one field one day and two fields per day for the same dose per fraction was tested on six treatment-plan scenarios calculated with method A and B. In particular, η was calculated for protocol 9904 for low and intermediate cancer risk and protocol 9904-3 for high risk. As an example for protocol 9904 and low risk, η is expressed:

$$\eta = \frac{exp(-N_{0low} * \frac{\sum_i (S_i^{2f})^{20}}{N_v})}{exp(-N_{0low} * \frac{\sum_i (S_i^{Left} \times S_i^{Right})^{10}}{N_v})} \quad \text{(A-1)}$$

With S_i the predicted survival calculated by TRiP98 in each voxel i and N_v the number of voxel in the PTV. Results are presented in table III.1. All values found are close enough to consider that, in the frame of the treatment planning configurations tested (*ie* neglecting the possibility that α and β values are distributed in the tumor), there should not be any difference in the tumor outcome when one lateral field is delivered per day or two opposed lateral fields are delivered per day.

Table III.1: Values of η found for the three risk groups and protocols using treatment plan results with method A and B:

A :	9904 -low risk-	9904 -int. risk-	9904-3 -high risk-
η	1.001	1.002	1.010
B :	9904 -low risk-	9904 -int. risk-	9904-3 -high risk-
η	0.9963	0.9968	0.989

2 Determination of NIRS clinical RBE

For the example case of a patient with prostate cancer, the largest SOBP width (longitudinally to the beam) in the PTV was found to be 68.36 mm. The linear interpolation between the values of clinical RBE (see table III.1) gives a clinical RBE equal to 2.36. This means that the $d^{\text{NIRS}}_{\text{middle-SOBP}}$ and $D^{\text{NIRS}}_{\text{middle-SOBP}}$ should be for the three clinical protocols published by NIRS:

- Protocol 9904: $d^{\text{NIRS}}_{\text{middle-SOBP}} = 1.40$ Gy and $D^{\text{NIRS}}_{\text{middle-SOBP}} = 27.97$ Gy since $d^{\text{NIRS}}_{\text{Bp}} = 3.3$ Gy in 20 fractions.
- Protocol 9904-2: $d^{\text{NIRS}}_{\text{middle-SOBP}} = 1.33$ Gy and $D^{\text{NIRS}}_{\text{middle-SOBP}} = 26.69$ Gy since $d^{\text{NIRS}}_{\text{Bp}} = 3.15$ Gy in 20 fractions.
- Protocol 9904-3: $d^{\text{NIRS}}_{\text{middle-SOBP}} = 1.53$ Gy and $D^{\text{NIRS}}_{\text{middle-SOBP}} = 24.41$ Gy since $d^{\text{NIRS}}_{\text{Bp}} = 3.6$ Gy in 16 fractions.

3 D_t value for a tie-in between LEM and NIRS protocols?

In method A, D_t was adjusted for each treatment protocol and geometry in order to find a combination of LEM parameters that would lead to a matching between the absorbed dose and biological dose calculated with LEM and with the NIRS model. Precisely, several D_t are tested until $d^{\text{LEM I–BH}}_{\text{middle–SOBP}}$ equals to $d^{\text{NIRS}}_{\text{middle–SOBP}}$. The results are presented in table III.2, a difference of 0.01 between $d^{\text{NIRS}}_{\text{middle–SOBP}}$ and $d^{\text{LEM I–BH}}_{\text{middle–SOBP}}$ was considered acceptable. The profiles at the largest SOBP are depicted in figure III.1. For protocol 9904, with two opposed fields per day and for the low and intermediate risks the TCP calculated with the "optimized" D_t are: 97.2% and 93.5% (III.2). For protocol 9904-3 and high risk, the TCP calculated with treatment fields either delivered only on the left or the right hand-side are respectively 67.6 and 67.3 %.

Table III.2: Table of "optimized" D_t, $d^{\text{LEM I–BH}}_{\text{middle–SOBP}}$ and $d^{\text{LEM I–BH}}_{\text{m}}$ for method A. The calculated TCP is also given for low, intermediate and high risk.

		Protocol 9904	Protocol 9904-2	Protocol 9904-3
2f	D_t	16.92±0.45	16.19±0.38	18.60±0.47
	$d^{\text{LEM I–BH}}_{\text{middle–SOBP}}$	1.40	1.34	1.52
	$d^{\text{LEM I–BH}}_{\text{m}}$	1.32±0.05	1.26±0.05	1.44±0.05
	TCP	97.2, 93.5, 80.3	95.1, 88.7, 67.8	95.2, 88.9, 68.3
Left	D_t	16.73±0.54	16.19±0.39	18.56±0.47
	$d^{\text{LEM I–BH}}_{\text{middle–SOBP}}$	1.41	1.33	1.52
	$d^{\text{LEM I–BH}}_{\text{m}}$	1.34±0.10	1.27±0.10	1.44±0.11
	TCP	97.1, 93.3, 79.9	95.0, 88.5, 67.1	95.1, 88.7, 67.6
Right	D_t	16.78±0.51	16.20±0.38	18.44±0.37
	$d^{\text{LEM I–BH}}_{\text{middle–SOBP}}$	1.40	1.33	1.52
	$d^{\text{LEM I–BH}}_{\text{m}}$	1.33±0.11	1.26±0.11	1.44±0.12
	TCP	97.1, 93.2, 79.6	94.9, 88.4, 66.9	95.0, 88.5, 67.3

With this method, the "optimized" D_t is the same for each protocol, which means that the irradiation fields are the same. Consequently, the TCP estimations for low, intermediate or high risk, calculated for each protocol and beam geometry, depend only on the N_0. In the TCP model from Brenner and Hall, the TCP reduces with higher risk when the same dose is delivered. The results presented by NIRS show a different trend: the intermediate risk has the highest bNED compared to the low risk and high risk groups.
A strict tie-in seems hence not possible to reach since a single value of D_t is found per protocol and with this unique value estimations of TCP for each risk group differ from the published bNED.

4 Evaluation of dose profiles

a) Determination of NIRS irradiation fields for HSG cell line

Using a LEM I_{HSG} look up table, treatment plans were calculated: for each beam configuration and each protocol, the $d^{\text{LEM I–HSG}}_{\text{Bp}}$ was adjusted so that the obtained absorbed dose

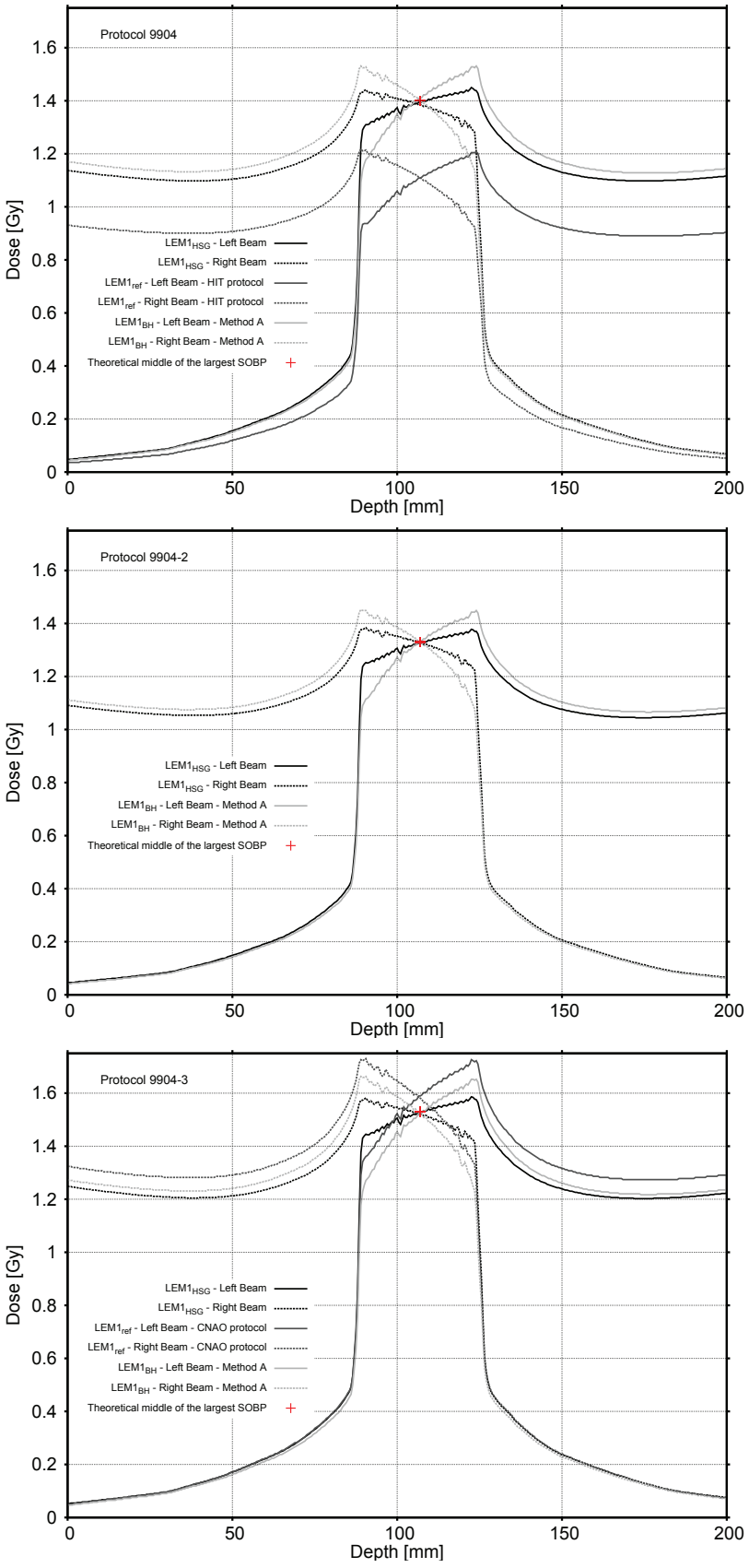

Figure III.1: Profiles of the absorbed dose at the largest SOBP along the beam direction for the patient geometry applying the NIRS protocols 9904, 9904-2 and 9904-3.

$d^{\text{LEM I–HSG}}_{\text{middle–SOBP}}$ equals $d^{\text{NIRS}}_{\text{middle–SOBP}}$ at the middle of the largest SOBP. The results of the adjusted $d^{\text{LEM I–HSG}}_{\text{Bp}}$ for the three protocols and the three beam geometries are presented in table III.3. A difference of 0.01 between $d^{\text{NIRS}}_{\text{middle–SOBP}}$ and $d^{\text{LEM I–HSG}}_{\text{middle–SOBP}}$ was considered acceptable. The profiles found following protocols 9904, 9904-2 and 9904-3 are are depicted in figure III.1 together with profiles previously calculated.

Table III.3: Table of adjusted $d^{\text{LEM I–HSG}}_{\text{Bp}}$that lead to $d^{\text{NIRS}}_{\text{middle–SOBP}}$ with HSG parameters, values of $d^{\text{LEM I–HSG}}_{\text{middle–SOBP}}$together with $d^{\text{LEM I–HSG}}_{\text{m}}$(±standard deviation), calculated for three NIRS protocols and beam geometries are presented. 2f = two laterally opposed fields

		Protocol 9904	Protocol 9904-2	Protocol 9904-3
2f	$d^{\text{LEM I–HSG}}_{\text{Bp}}$	2.00	1.93	2.16
	$d^{\text{LEM I–HSG}}_{\text{middle–SOBP}}$	1.39	1.33	1.52
	$d^{\text{LEM I–HSG}}_{\text{m}}$	1.36±0.03	1.30±0.03	1.49±0.03
Left	$d^{\text{LEM I–HSG}}_{\text{Bp}}$	2.00	1.93	2.17
	$d^{\text{LEM I–HSG}}_{\text{middle–SOBP}}$	1.39	1.32	1.53
	$d^{\text{LEM I–HSG}}_{\text{m}}$	1.36±0.05	1.30±0.05	1.50±0.05
Right	$d^{\text{LEM I–HSG}}_{\text{Bp}}$	2.00	1.92	2.17
	$d^{\text{LEM I–HSG}}_{\text{middle–SOBP}}$	1.39	1.33	1.52
	$d^{\text{LEM I–HSG}}_{\text{m}}$	1.35±0.06	1.29±0.06	1.49±0.06

b) Reproduction of CNAO and HIT irradiation fields

Treatment plans were calculated following CNAO and HIT protocols and using the LEM $\text{I}_{ref.}$(§7). Results are presented in table III.4.

Table III.4: Original CNAO and HIT protocol : Table of $d^{\text{LEM I–ref}}_{\text{middle–SOBP}}$and $d^{\text{LEM I–ref}}_{\text{m}}$ obtained for plans calculated with the LEM $\text{I}_{ref.}$

	Protocol HIT	Protocol CNAO	
	2f	Left	Right
$d^{\text{LEM I–ref}}_{\text{middle–SOBP}}$	1.11	1.59	1.58
$d^{\text{LEM I–ref}}_{\text{m}}$	1.05±0.04	1.51±0.11	1.51±0.12

5 Comparison of absorbed dose profiles

For comparison with Fossati *et al.* published on example of NIRS depth dose profiles, dose distribution using LEM $\text{I}_{Brenner\ and\ Hall}$, LEM $\text{I}_{ref.}$ and LEM I_{HSG} were calculated with:

- $d^{\text{LEM I–ref}}_{\text{Bp}} = 4.60$ Gy.
- $d^{\text{LEM I–BH}}_{\text{Bp}} = 4.05$ Gy. With $D_{\text{t}} = 18.44$ Gy, which corresponds to the 9904-3 protocol for high risk patients.

- $d_{\mathrm{Bp}}^{\mathrm{LEM\ I-HSG}} = 2.50$ Gy.

After retrieving the depth dose profile of NIRS published by Fossati *et al.*, all depth dose profiles could be plot together. They are depicted in figure III.2.

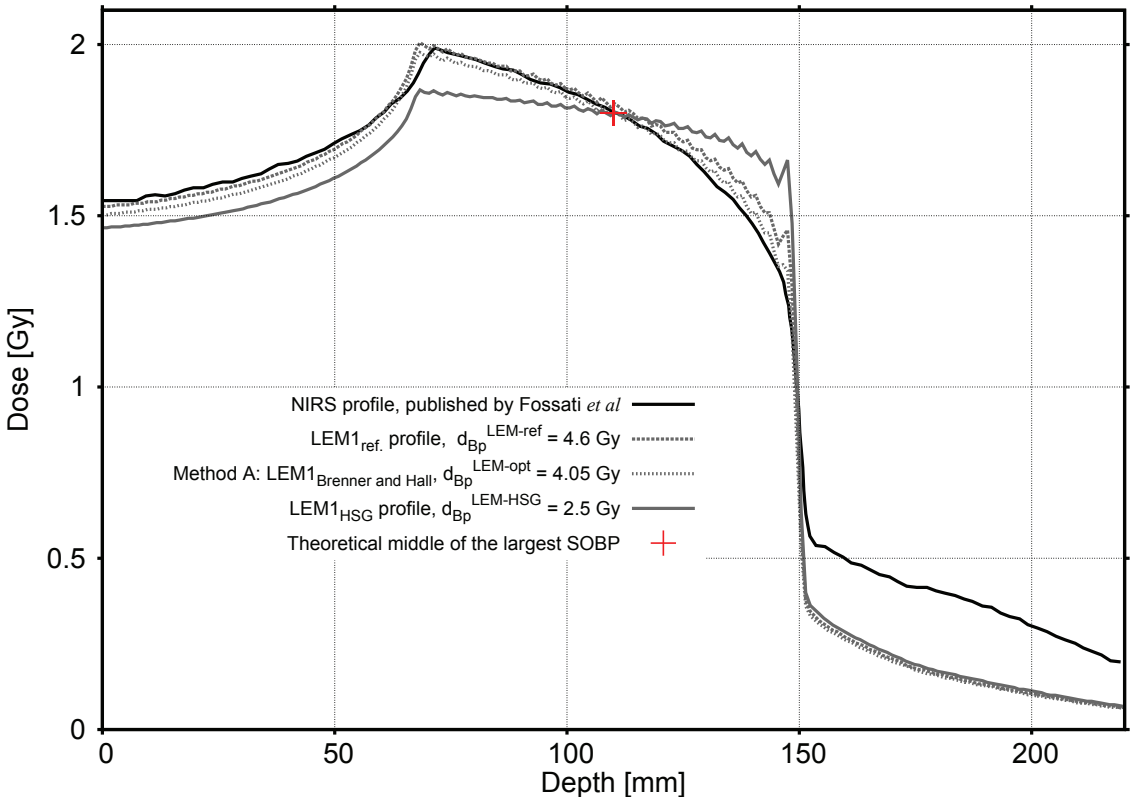

Figure III.2: Absorbed depth dose profile of NIRS originally published by Fossati *et al.* plotted together with the profiles calculated with LEM $\mathrm{I}_{ref.}$, LEM I_{HSG} and LEM $\mathrm{I}_{Brenner\ and\ Hall}$. The middle of the SOBP is shown with a cross tick, this point was used to adjust the prescribed biological dose of all the plans.

In all tested tables, the absorbed dose in the entrance channel (before the SOBP) is lower than the published NIRS profile, in particular using the LEM I_{HSG}. The difference between an active or passive delivery system may explain this difference. The highest absorbed dose point for the theoretical NIRS profile should be located at around 7 cm depth, however there seems to be a little shift towards the entrance channel for all our calculated profiles. The hypothesis for this shift is that during the digitalization of the published NIRS profile. Interestingly is the SOBP profile calculated with LEM I_{HSG}: this profile is rather flat, which differs a lot from the other profiles. Finally, in the tail beyond the SOBP, the absorbed dose of the original profile is higher than all other profiles.
The profile plotted with the HSG is very different from the published NIRS profile. This questions the relevance of using such irradiation fields for the set of D_{t} with bNED results (*i.e.* Method B). Consequently the sensitivity of TCP to the dose profile was tested. With LEM $\mathrm{I}_{Brenner\ and\ Hall}$, for a $D_{\mathrm{t}} = 23.28$ and 23.20 Gy and for the left and right beam respectively, the TCP for high risk was calculated with three different sets of irradiation fields, for which the absorbed dose in the middle of SOBP is very similar.

To study the sensitivity of TCP to the dose profile, two sets of irradiation fields were compared. The first set of irradiation fields was calculated with LEM I_{HSG}: the $d_{\mathrm{Bp}}^{\mathrm{LEM\ I-HSG}}$ is so that the absorbed dose at the middle of the largest SOBP corresponds to $d_{\mathrm{middle-SOBP}}^{\mathrm{NIRS}}$ in the protocol 9907-3 (method B). For the second set, the irradiation fields were calculated with LEM $I_{ref.}$ and following CNAO treatment protocol. In the first case, the TCP is 89.4% in the second case is 91.3%. Absorbed dose profiles and survival profiles at the middle of the largest SOBP are depicted in figure III.3. At the middle of the largest SOBP, the absorbed dose calculated with fields from LEM I_{HSG} is 1.53 Gy and is 1.58 Gy with fields from LEM $I_{ref.}$. The small difference between these two values may explain the difference in the TCP calculated. Furthermore, the mean absorbed dose in the PTV is 1.49±0.03 Gy with LEM I_{HSG} fields and 1.51±0.05 Gy with LEM $I_{ref.}$ fields. Interestingly, the mean biological dose in the target is 3.94±0.08 Gy with LEM I_{HSG} fields and 4.02±0.06 Gy with LEM $I_{ref.}$ fields. From this test, it seems that the the sensitivity of TCP to the dose profile is low. This can be explained by the beam geometry: two-opposed beams are know to lead to rather homogeneous irradiation in the SOBP (Böhlen *et al.* (2012)).

With a reasonable level of confidence, the "optimized" D_{t} values according to bNED values and based on irradiation fields calculated with LEM I_{HSG} could be used to calculate TCP estimates for HIT and NIRS protocols.

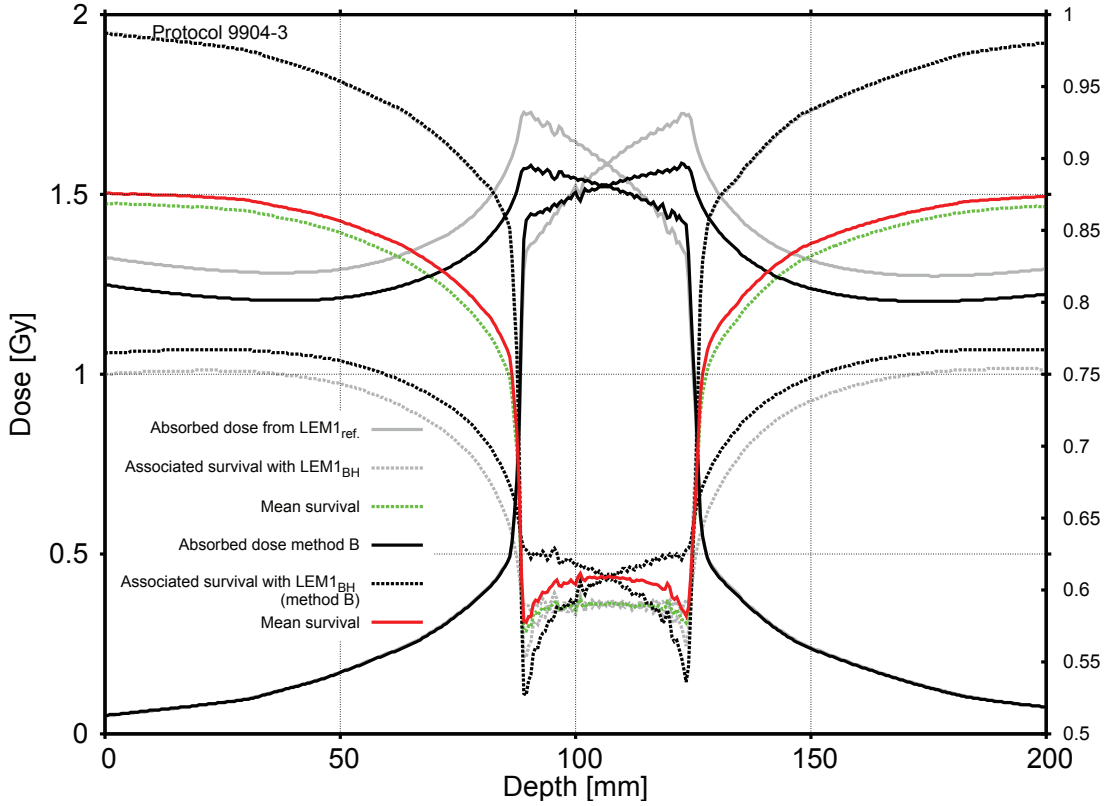

Figure III.3: Profiles of the absorbed dose at the largest SOBP along the beam direction for the patient geometry applying the NIRS protocol 9904-3. The irradiation fields are calculated either with LEM I_{HSG} or with LEM $I_{ref.}$. The survival distribution is calculated with LEM $I_{Brenner\ and\ Hall}$ and the associated profile is depicted for each beam port. The mean survival of both ports is depicted in color for each of the two profiles.

6 Optimizing D_{t} value according to bNED values

In method B, based on the irradiation fields calculated according to LEM I_{HSG}, the D_{t} was adjusted for each treatment protocol, geometry and risk group so that the calculated TCP equals the published bNED by NIRS. The results are presented in table III.5, a difference of 0.1 between bNED and TCP was considered acceptable.

Table III.5: Table of $d_{\mathrm{Bm}}^{\mathrm{LEM\ I-BH}}$ (Gy) obtained with the LEM $\mathrm{I}_{Brenner\ and\ Hall}$ and "optimized" D_{t} (Gy) for each risk group when the absorbed dose fields are calculated with LEM I_{HSG}.

	Protocol 9904			Protocol 9904-2			Protocol 9904-3		
	low	int	high	low	int	high	low	int	high
2f:									
D_{t}	12.02±0.31	19.16±0.10	18.61±0.25	12.96±0.29	20.60±0.09	20.00±0.28	14.72±0.27	23.41±0.15	22.75±0.24
$d_{\mathrm{middle-SOBP}}^{\mathrm{LEM\ I-BH}}$		1.39			1.33			1.52	
$d_{\mathrm{Bm}}^{\mathrm{LEM\ I-BH}}$	2.95±0.05	3.49±0.07	3.46±0.07	2.95±0.06	3.50±0.07	3.46±0.07	3.36±0.06	3.98±0.08	3.94±0.08
TCP	89.6	96.8	88.4	89.6	96.8	88.4	89.6	96.8	88.4
Left:									
D_{t}	12.24±0.32	19.73±0.08	19.12±0.30	13.26±0.30	21.28±0.08	20.65±0.28	14.94±0.26	24.00±0.07	23.28±0.25
$d_{\mathrm{middle-SOBP}}^{\mathrm{LEM\ I-BH}}$		1.39			1.32			1.52	
$d_{\mathrm{Bm}}^{\mathrm{LEM\ I-BH}}$	2.95±0.09	3.52±0.13	3.48±0.13	2.95±0.10	3.52±0.14	3.48±0.13	3.38±0.12	4.01±0.16	3.97±0.15
TCP	89.6	96.8	88.4	89.6	96.8	88.4	89.6	96.8	88.4
Right:									
D_{t}	12.23±0.32	19.70±0.08	19.09±0.30	13.29±0.30	21.30±0.08	20.66±0.28	14.90±0.25	23.85±0.08	23.20±0.25
$d_{\mathrm{middle-SOBP}}^{\mathrm{LEM\ I-BH}}$		1.39			1.33			1.52	
$d_{\mathrm{Bm}}^{\mathrm{LEM\ I-BH}}$	2.95±0.10	3.52±0.13	3.48±0.13	2.95±0.10	3.52±0.13	3.48±0.13	3.38±0.12	4.01±0.16	3.97±0.15
TCP	89.6	96.8	88.4	89.6	96.8	88.4	89.6	96.8	88.4

7 TCP estimates for HIT and NIRS protocols

Using the irradiation fields calculated following CNAO and HIT protocol but applying LEM $\mathrm{I}_{Brenner\ and\ Hall}$ "optimized" with method B, the $d_{\mathrm{Bm}}^{\mathrm{LEM\ I-BH}}$ and the TCP could be calculated (table III.6). The corresponding mean biological dose in the PTV, $d_{\mathrm{Bm}}^{\mathrm{LEM\ I-BH}}$, is also calculated.

Concerning the low risk and following HIT protocol group, the $d_{\mathrm{Bm}}^{\mathrm{LEM\ I-BH}}$ is about 25% less than the theoretical dose prescribed 3.3 Gy. The TCP is 62.2%, which is lower than the published

Table III.6: With the "optimized" D_{t} (Gy), table of predictions of TCP (%) calculated with LEM $\mathrm{I}_{Brenner\ and\ Hall}$ based on the irradiation fields from the original HIT and CNAO protocols. The respective $d_{\mathrm{Bm}}^{\mathrm{LEM\ I-BH}}$ (Gy) are also given.

	Protocol HIT 2f		Protocol CNAO Left	Protocol CNAO Right
	Low risk:	Int risk:	High risk:	
D_{t}	12.02	19.16	23.28 Gy	23.20 Gy
$d_{\mathrm{Bm}}^{\mathrm{LEM\ I-BH}}$	2.50 ±0.03	2.99 ±0.03	4.02 ±0.06	4.02 ±0.06
TCP	62.2	80.3	91.3	

bNED by NIRS of 89.6%.
For the intermediate risk group, the $d_{\mathrm{Bm}}^{\mathrm{LEM\ I-BH}}$ is higher than the $d_{\mathrm{Bm}}^{\mathrm{LEM\ I-BH}}$ obtained for low risk, still, the $d_{\mathrm{Bm}}^{\mathrm{LEM\ I-BH}}$ is about 10% lower than the $d_{\mathrm{Bp}}^{\mathrm{NIRS}}$. The TCP is 80.3%, which is higher than the TCP estimate calculated for low risk (62.2%) but remains lower than the published bNED of NIRS (96.8%).
For CNAO protocol and high risk, the $d_{\mathrm{Bm}}^{\mathrm{LEM\ I-BH}}$ is about 12% higher than the $d_{\mathrm{Bp}}^{\mathrm{NIRS}}$ of 3.6 Gy. The estimation of TCP is 91.3% when following CNAO protocol. The TCP estimate is relatively closed to NIRS published bNED of 88.4%. Finally, the predicted TCP are lower than NIRS published bNED when following HIT protocol for low and intermediate risk cancer, and a bit higher when follow CNAO protocol for high risk cancer.

Appendix

Table III.7: Definitions of **specific** dose quantities -all expressed in Gy- and abbreviations used.

Name	Abbreviation	Definition
NIRS Model		
Prescribed total dose	$D_{\mathrm{Bp}}^{\mathrm{NIRS}}$	Prescribed dose at NIRS with the NIRS model
Prescribed dose per fraction	$d_{\mathrm{Bp}}^{\mathrm{NIRS}}$	$d_{\mathrm{Bp}}^{\mathrm{NIRS}} = D_{\mathrm{Bp}}^{\mathrm{NIRS}}$/ number of fractions
Absorbed dose at the middle of the largest SOBP	$d_{\mathrm{middle-SOBP}}^{\mathrm{NIRS}}$	According to the NIRS radiobiological model, absorbed dose at the middle of the largest SOBP calculated with conversion table of Clinical RBE for each SOBP width published by Kanai *et al.* (): $d_{\mathrm{middle-SOBP}}^{\mathrm{NIRS}} = D_{\mathrm{Bp}}^{\mathrm{NIRS}}/\ RBE_{clinical}$
Total absorbed dose at the middle of the largest SOBP	$D_{\mathrm{middle-SOBP}}^{\mathrm{NIRS}}$	$D_{\mathrm{middle-SOBP}}^{\mathrm{NIRS}} = d_{\mathrm{middle-SOBP}}^{\mathrm{NIRS}}\times$ number of fractions
with the LEM $\mathrm{I}_{ref.}$		
Prescribed total dose	$D_{\mathrm{Bp}}^{\mathrm{LEM\ I-ref}}$	The reference LEM I look-up table is the table with parameters set to: $\alpha = 0.1$, $\beta = 0.05$, $r_{\mathrm{nucl}} = 5$ μm and $D_{\mathrm{t}} = 30$Gy.
Prescribed dose per fraction	$d_{\mathrm{Bp}}^{\mathrm{LEM\ I-ref}}$	
Biological total dose	$d_{\mathrm{Bm}}^{\mathrm{LEM\ I-ref}}$	Mean of Biological dose in the PTV calculated according to the LEM $\mathrm{I}_{ref.}$ model.
Absorbed dose per fraction at the middle of the largest SOBP	$d_{\mathrm{middle-SOBP}}^{\mathrm{LEM\ I-ref}}$	According to the reference LEM I look-up table, the absorbed dose per fraction calculated at the middle of the largest SOBP.
Absorbed total dose at the middle of the largest SOBP	$D_{\mathrm{middle-SOBP}}^{\mathrm{LEM\ I-ref}}$	$D_{\mathrm{middle-SOBP}}^{\mathrm{LEM\ I-ref}} = d_{\mathrm{middle-SOBP}}^{\mathrm{LEM\ I-ref}}\times$ number of fractions
Mean absorbed dose per fraction with the LEM $\mathrm{I}_{ref.}$	$d_{\mathrm{m}}^{\mathrm{LEM\ I-ref}}$	Mean of absorbed dose in the PTV obtained with the LEM $\mathrm{I}_{ref.}$ model (see definition of d_{m}^{*}).
Mean absorbed total dose	$D_{\mathrm{m}}^{\mathrm{LEM\ I-ref}}$	$d_{\mathrm{m}}^{\mathrm{LEM\ I-ref}}\times$ number of fractions
with the LEM I_{HSG}		
Prescribed total dose	$D_{\mathrm{Bp}}^{\mathrm{LEM\ I-HSG}}$	The LEM I look-up table is the table with parameters set to: $\alpha = 0.3312$, $\beta = 0.0593$, $D_t = 7.5$ and $r_{nucl} = 5$.
Prescribed dose per fraction	$d_{\mathrm{Bp}}^{\mathrm{LEM\ I-HSG}}$	$d_{\mathrm{Bp}}^{\mathrm{LEM\ I-HSG}} = D_{\mathrm{Bp}}^{\mathrm{LEM\ I-HSG}}$/ number of fractions
Biological total dose	$d_{\mathrm{Bm}}^{\mathrm{LEM\ I-HSG}}$	Mean of biological dose in the PTV calculated according to the LEM I_{HSG} model.
Absorbed dose per fraction at the middle of the largest SOBP	$d_{\mathrm{middle-SOBP}}^{\mathrm{LEM\ I-HSG}}$	According to the LEM I_{HSG} model, the absorbed dose per fraction calculated at the middle of the largest SOBP.
Absorbed total dose at the middle of the largest SOBP	$D_{\mathrm{middle-SOBP}}^{\mathrm{LEM\ I-HSG}}$	$D_{\mathrm{middle-SOBP}}^{\mathrm{LEM\ I-ref}} = d_{\mathrm{middle-SOBP}}^{\mathrm{LEM\ I-HSG}}\times$ number of fractions
Mean absorbed dose per fraction	$d_{\mathrm{m}}^{\mathrm{LEM\ I-HSG}}$	Mean of absorbed dose in the PTV obtained with the LEM I_{HSG} model (see definition of d_{m}^{*}).
Mean absorbed total dose	$D_{\mathrm{m}}^{\mathrm{LEM\ I-HSG}}$	$d_{\mathrm{m}}^{\mathrm{LEM\ I-HSG}}\times$ number of fractions
with the LEM $\mathrm{I}_{Brenner\ and\ Hall}$		
Prescribed total dose	$D_{\mathrm{Bp}}^{\mathrm{LEM\ I-BH}}$	The LEM I look-up table is the table with parameters set to: $\alpha = 0.036$, $\beta = 0.024$, $r_{\mathrm{nucl}} = 5$ μm. The value of D_{t} is determined based on tests and assumptions, which lead to a so-called "optimized" D_{t}.
Prescribed dose per fraction	$d_{\mathrm{Bp}}^{\mathrm{LEM\ I-BH}}$	$d_{\mathrm{Bp}}^{\mathrm{LEM\ I-BH}} = D_{\mathrm{Bp}}^{\mathrm{LEM\ I-BH}}$/ number of fractions
Mean biological total dose	$d_{\mathrm{Bm}}^{\mathrm{LEM\ I-BH}}$	Mean of biological dose in the PTV calculated according to the LEM $\mathrm{I}_{Brenner\ and\ Hall}$ model with and an "optimized" D_{t}.
Absorbed dose per fraction at the middle of the largest SOBP	$d_{\mathrm{middle-SOBP}}^{\mathrm{LEM\ I-BH}}$	According to the Brenner and Hall LEM I look-up table with an "optimized" D_{t}, the absorbed dose per fraction calculated at the middle of the largest SOBP.
Absorbed total dose at the middle of the largest SOBP	$D_{\mathrm{middle-SOBP}}^{\mathrm{LEM\ I-BH}}$	$D_{\mathrm{middle-SOBP}}^{\mathrm{LEM\ I-ref}} = d_{\mathrm{middle-SOBP}}^{\mathrm{LEM\ I-BH}}\times$ number of fractions
Mean absorbed dose per fraction	$d_{\mathrm{m}}^{\mathrm{LEM\ I-BH}}$	Mean of absorbed dose in the PTV obtained with the LEM $\mathrm{I}_{Brenner\ and\ Hall}$ model with an "optimized" D_{t} (see definition of d_{m}^{*}).
Mean absorbed total dose	$D_{\mathrm{m}}^{\mathrm{LEM\ I-BH}}$	$d_{\mathrm{m}}^{\mathrm{LEM\ I-BH}}\times$ number of fractions

Bibliography

Ammazzalorso, F., Chanrion, M. A., Graef, S., and Jelen, U. (2013). P302: A free software display and analysis tool for photon and particle radiotherapy dose distributions. In *Proceedings:52nd Annual Meeting for the Particle Therapy Cooperative Group (PTCOG)*. d)

Beuve, M., Alphonse, G., Maalouf, M., Colliaux, A., Battiston-Montagne, P., *et al.* (2008). Radiobiologic parameters and local effect model predictions for head-and-neck squamous cell carcinomas exposed to high linear energy transfer ions. *Int J Radiat Oncol Biol Phys*, 71(2):635–642. I

Böhlen, T. T., Brons, S., Dosanjh, M., Ferrari, A., Fossati, P., *et al.* (2012). Investigating the robustness of ion beam therapy treatment plans to uncertainties in biological treatment parameters. *Phys Med Biol*, 57(23):7983–8004. 5

Brenner, D. J. and Hall, E. J. (1999). Fractionation and protraction for radiotherapy of prostate carcinoma. *Int J Radiat Oncol Biol Phys*, 43(5):1095–1101. I, b), II.1

Chanrion, M. A., Ammazzalorso, F., Wittig, A., Engenhart-Cabillic, R., and Jelen, U. (2013). Dosimetric consequences of pencil beam width variations in scanned beam particle therapy. *Phys Med Biol*, 58(12):3979–3993. c)

Chanrion, M.-A., Sauerwein, W., Jelen, U., Wittig, A., Engenhart-Cabillic, R., *et al.* (2014). The influence of the local effect model parameters on the prediction of the tumor control probability for prostate cancer. *Phys Med Biol*, 59(12):3019–3040. I, b)

Combs, S. E. and Debus, J. (2013). Treatment with heavy charged particles: systematic review of clinical data and current clinical (comparative) trials. *Acta Oncol*, 52(7):1272–1286. a)

Fossati, P., Molinelli, S., Matsufuji, N., Ciocca, M., Mirandola, A., *et al.* (2012). Dose prescription in carbon ion radiotherapy: a planning study to compare nirs and lem approaches with a clinically-oriented strategy. *Phys Med Biol*, 57(22):7543–7554. I, a), b), 4

Habl, G., Hatiboglu, G., Edler, L., Uhl, M., Krause, S., *et al.* (2014). Ion prostate irradiation (ipi) - a pilot study to establish the safety and feasibility of primary hypofractionated irradiation of the prostate with protons and carbon ions in a raster scan technique. *BMC Cancer*, 14:202. b)

IAEA and ICRU (2007). Iaea-tecdoc-1560: Dose reporting in ion beam therapy. Technical report, INTERNATIONAL ATOMIC ENERGY AGENCY, Vienna. a)

IAEA and ICRU (2008). Technical reports series no. 461: Relative biological effectiveness in ion beam therapy. Technical report, INTERNATIONAL ATOMIC ENERGY AGENCY, Vienna. a)

Iancu, G., Krämer, M., and Schardt, D. (2009). Scattering implementation in trip. In *Proceedings of the Heavy Ions in Therapy and Space Symposium*, page 58, Cologne, Germany. c)

Ishikawa, H., Tsuji, H., Kamada, T., Akakura, K., Suzuki, H., *et al.* (2012). Carbon-ion radiation therapy for prostate cancer. *Int J Urol*, 19(4):296–305. b), c)

Jelen, U., Ammazzalorso, F., Chanrion, M.-A., Gräf, S., Zink, K., *et al.* (2012). Robustness against interfraction prostate movement in scanned ion beam radiation therapy. *Int J Radiat Oncol Biol Phys*, 84(2):e257–e262. c)

Kanai, T., Endo, M., Minohara, S., Miyahara, N., Koyama-ito, H., *et al.* (1999). Biophysical characteristics of himac clinical irradiation system for heavy-ion radiation therapy. *Int J Radiat Oncol Biol Phys*, 44(1):201–210. II.1

Kanai, T., Matsufuji, N., Miyamoto, T., Mizoe, J., Kamada, T., *et al.* (2006). Examination of gye system for himac carbon therapy. *Int J Radiat Oncol Biol Phys*, 64(2):650–656. II.1, 4

Krämer, M. and Scholz, M. (2000). Treatment planning for heavy-ion radiotherapy: calculation and optimization of biologically effective dose. *Phys Med Biol*, 45(11):3319–3330. c)

M. Krämer, M. (2011). `http://bio.gsi.de/DOCS/TRiP98/DOCS/trip98.html` (accessed 2014.10.01). TRiP online documentation. c), 4

Matsufuji, N., Kanai, T., Kanematsu, N., Miyamoto, T., Baba, M., *et al.* (2007). *IAEA-TECDOC-1560: Dose Reporting in Ion Beam Therapy*, chapter Treatment planning and dosimetric requirements for prescribing and reporting ion-beam therapy: the current chiba approach, pages 169–180. IAEA, Vienna. I

Mizoe, J., Ando, K., Kanai, T., Matsufuji, N., and Tsujii, H. (2008). *Technical reports series No. 461: Relative biological effectiveness in ion beam therapy*, chapter Clinical RBE determination scheme at NIRS-HIMAC, pages 135–152. IAEA and ICRU, Vienna. I, a)

NIRS and MedAustron, editors (2013). *Proceedings: NIRS and MedAustron Joint Symposium on Carbon Ion Radiotherapy*. a), b)

Schneider, C. A., Rasband, W. S., and Eliceiri, K. W. (2012). Nih image to imagej: 25 years of image analysis. *Nat Methods*, 9(7):671–675. d)

Steinsträter, O., Grün, R., Scholz, U., Friedrich, T., Durante, M., *et al.* (2012). Mapping of rbe-weighted doses between himac- and lem-based treatment planning systems for carbon ion therapy. *Int J Radiat Oncol Biol Phys*, 84(3):854–860. I, II.1, a), 4

General discussion

General discussion

The NIRS in Chiba started in 1994 the treatment of cancer patients with carbon-ion radiation therapy. Considering the beam delivery system and the neutron therapy clinical experience, an in-house radiobiological model was developped at NIRS. The NIRS model for the prescription of a carbon-ion dose is a pragmatic approach based on physical parameters: size of SOBP, radiobiological experiments, HSG radiosensitivity and clinical experience of neutrontherapy. This approach has advantages: it depends on few parameters and the clinical implementation is relatively simple. However, the two-steps renormalization of the NIRS model does not include a change in the fraction size or schedule (Kanai *et al.* (1999)). At GSI, where the first european pilot project for carbon-ion therapy started, another radiobiological model was developed: the LEM. The LEM is particularly adapted for the active beam delivery system with spot scanning. Furthermore, with the LEM, the fraction size is taken into account in the calculation of the distribution of lethal effects in a treatment plan. Other radiobiological models like the modified microdosimetric model (Kase *et al.* (2006)) consider the fraction size in the calculation of RBE. This consideration might have encouraged NIRS to recently adopt the MKM for treatments with the active scanning beam delivery system. In the frame of pre-clinical research for the Marburg ion therapy center, this study focuses on the LEM I. To now, LEM I is the only radiobiological model implemented in a CE-certified TPS. This work does not aim at discussing theoretical aspects of LEM, but has concentrated on developping methods for its applications in a clinical context.

In the first part, this study has identified the influence of the radiobiological model LEM parameters for the predictions of tumor control probability. In particular, the focus was on the influence of the LEM I input parameters, for irradiating prostate cancer with scanned carbon-ion beams. Prostate cancer was chosen as an example of a slowly-growing tumor surrounded by radiosensitive structures. The radiobiological parameters α and β may be found with *in vitro*, *in vivo* or with clinical results analyses. A recent estimate of the α/β from a large radiobiological study was recently published (Karger *et al.* (2013)). The value published (84.7 Gy) would require some further analyses and discussion to be directly taken as input for the LEM I. Furthermore, the absolute values of α and β are not given. This is why, for the application of the LEM I in a clinical context, it seems more appropriate to start with estimates of α and β deduced from clinical results analyses. Based on published tumor control data after external beam radiotherapy or brachytherapy and on different TCP models, various authors attempted to estimate absolute values of α and β parameters for prostate cancer. Consequently, published estimates vary largely, as various mathematical and numerical methods were considered. To represent this variability, several sets of α and β values obtained through analysis of clinical

tumor control with different TCP models were used to test different LEM I look-up table with several D_t: 10, 20, 45 and 60 Gy. Absorbed doses, re-calculated biological doses and TCP predictions were analyzed for several TCP models and tumor risk groups. Modifying of the model input parameters influences the spatial (absorbed and biological) dose distribution and consequently, the mean dose in the PTV. TCP predictions were found more sensitive to D_t than to the α, β couple.

When α and β are obtained with TCP modeling, this sensitivity analysis has shown that, α, β, N_0 and D_t need to be considered as a set of indivisible parameters together with the TCP original model.

In the second part, amongst several authors that estimated α and β with a TCP modeling approach, this analysis make use of the estimates published by Brenner and Hall (1999). Their analysis was one of the first to propose a low value of α/β. Although being a relatively old analysis with low D_{50}, α and β estimates were obtained from a cohort of patient that did not receive any side treatments like androgen deprivation therapy. The tendency of a low α/β for prostate cancer has been confirmed by several authors (Oliveira *et al.* (2012)), but how low and with which model α and β estimates should be calculated remain debated today (Vogelius and Bentzen (2013)).
The initial cohort of patients selected by Brenner and Hall has different critera for the assessment of low, intermediate and high risk than NIRS. The criterion of Brenner and Hall is only based on the initial value of the PSA level: when PSA $<$ 10 ng/ml the risk is classified has low, when PSA is between 10 and 20 the risk is classified as intermediate and when PSA $>$ 20 the risk is high. This means that for low and intermediate risk, the patient selection may be different. For high risk, the criterion PSA $>$ 20 dominates, which means that both high risk groups should be similar. Brenner and Hall took a cohort of patients that did not receive at all androgen deprivation therapy (ADT). The α and β values proposed by Brenner and Hall are estimated from a fit of a simple poissonian TCP model and are constant for all risk group, only the N_0 reflects a difference between risk groups. The hypothesis of a unique α/β for all risk groups was also supported by other authors (Fowler *et al.* (2013)). Furthermore, the TCP model used by Brenner and Hall does not include a time factor to account for repopulation. This hypothesis has the merit to simplify the fitting procedure in case those factors are unknown. Otherwise, these time factors should be estimated by other means. To our best knowledge, published estimates in that matter show a large variability and no consensus seem to emerge. In fact, the validity of adding a time factor in a poissonian TCP model has been discussed by several authors (Tucker and Thames (1989), Vogelius and Bentzen (2013)). In particular, when the α/β is determined with a logistic TCP model, Vogelius and Bentzen concluded that the α/β for prostate remains low although an increase was expected when including a time factor. In method A, a D_t was found to try to tie-in LEM and NIRS protocol for both the dose prescribed (for instance, the number of biological dose prescribed: $d_{\mathrm{Bp}}^{\mathrm{NIRS}} = 3.3 = d_{\mathrm{Bp}}^{\mathrm{LEM\ I-BH}}$) and the absorbed dose in the middle of the SOBP. However, with these values, the estimated TCP were not similar to the bNED values published by NIRS. Hence, it seems that a strict tie-in is impossible to find with LEM $\mathrm{I}_{\mathit{Brenner\ and\ Hall}}$. This finding means that the biological prescribed dose should be adapted for each protocol and the figure from a prescribed dose in a NIRS protocol can not be directly "copied" to prescribe a dose based on the LEM I. This conclusion is in accordance with the CNAO approach, detailed in Fossati *et al.* (2012) and in

the proceedings from NIRS and MedAustron (2013). However it is in contradiction with the published clinical trial started at HIT and also described in the proceedings from NIRS and MedAustron (2013).

Method B attempted to take the most of the published clinical experience from NIRS. Firstly, aa method to reproduced irradiation fields from NIRS protocols was proposed. After a bibliography research, no depth dose profiles from NIRS irradiation was found for a depth and SOBP size that corresponded to our example case of a patient with prostate cancer. However, in the paper from Fossati *et al.* (2012) a configuration is depicted. Using the HSG parameters published by Kanai *et al.* (2006) and a proposed D_{t} value published by Steinsträter *et al.* (2012), a LEM I_{HSG} table was created. For the same depth and SOBP as published by Fossati *et al.* (2012), depth dose distributions from NIRS, LEM $\mathrm{I}_{ref.}$ and LEM $\mathrm{I}_{Brenner\ and\ Hall}$ could be compared. The depth dose profile calculated with LEM $\mathrm{I}_{ref.}$ was similar in shape to the original NIRS profile. On the contrary, with the LEM I_{HSG}, the profile was quite different and the gradient of dose was lower than the original profile. Several hypotheses can be formulated to explain this discrepancy. The LEM I has been recently updated, and better survival predictions should be expected from the latest version LEM IV. Furthermore, the parameters used for our LEM I_{HSG} were taken from Steinsträter *et al.* (2012), where they reported a good relative shape of the depth dose profiles calculated with the same HSG parameters but with the LEM IV. They also reported that a scaling was necessary to obtain same absolute dose values. With these considerations, the D_{t} value may have to be changed for LEM I. Another hypothesis is that the α and β parameters used by NIRS for HSG could have different values from what Kanai *et al.* published. In Kase *et al.* (2006), other estimates have been published. Between these published estimates, which set of α and β parameters was and is still being used for clinical treatment planning for prostate cancer at NIRS?

Therefore, the sensitivity of the TCP to the dose profile was studied: a negligible sensibility was found. This can be explained by the beam geometry: two-opposed beams are known to lead to rather homogeneous irradiation in the SOBP (Böhlen *et al.* (2012)). This hypothesis should be however tested with more treatment planning studies including other example cases of a patient with prostate cancer. Finally, with a reasonable level of confidence, the "optimized" D_{t} values according to the published values of bNED and based on irradiation fields calculated with LEM I_{HSG} were found appropriate for the estimation of TCP following HIT and NIRS protocols.

The latest paper from Ishikawa *et al.* (2012) presented bNED for each risk group. Each risk group received one of the three running clinical trials: 9904, 9904-2 or 9904-3. Depending on the risk group and treatment protocol, the values of D_{t} obtained were different: from 12.02 to 24.00 Gy. In all cases, D_{t} was lower than 30 Gy, which is the value of the LEM $\mathrm{I}_{ref.}$. For a protocol and a geometry defined, the lowest D_{t} values were always found for low risk cancer risk, and the highest values of D_{t} were always found for intermediate cancer risk. Furthermore, the obtained $d_{\mathrm{Bm}}^{\mathrm{LEM\ I-BH}}$ were particularly different between low and both intermediate and high risk groups. At NIRS, each risk group received a different treatment: ADT was adapted for each risk group. This means that with this modeling approach, the meaning of an "optimized" D_{t} is unique for each risk group. According to Ishikawa *et al.*, ADT may have increased the bNED for intermediate and high risk patients. Based on results presented, one could conclude that $\mathrm{RBE}_{\mathrm{int.-risk}} > \mathrm{RBE}_{\mathrm{low-risk}}$. However, this is not necessary the case: the combined effect of ADT and carbon-ion therapy has to be taken into account.

Results presented in this thesis showed that D_{t} is unique for each risk group and is an effective value that "contain" the impact of ADT. On the theoretical point of view, this result seems to rise a contradiction. Within the LEM, the definition is linked with the LQ-L model and therefore with the radiosensitivity of cells. Since, it is believed that ADT does not increase the radiosensitivity of cells, the D_{t} should have had the same value for all risk groups.
Theoretically, the TCP should be expressed:

$$TCP(D) = exp(-N_0 * S_{radiation}(D) * S_{ADT}) \tag{III.1}$$

With N_0 the total number of initial cells that have to be inactivated, $S_{radiation}(D)$ the cell survival response to radiation and S_{ADT} the cell survival response to ADT. In practice, S_{ADT} is not known, which means that the TCP can be expressed:

$$TCP(D) = exp(-\widetilde{N_0} * S_{radiation}(D)) \tag{III.2}$$

Where $\widetilde{N_0}$, is the "effective" number of cells that have to be inactivated. However, this quanty is not known. As a consequence and in the frame of the modeling proposed in this thesis, $\widetilde{N_0}$ and the set of D_{t} are correlated. In particular, it seems that the effect of ADT is taken into account in the value of the "optimized" D_{t}.
Acknowledging the limitations of the proposed method for the setting of D_{t}: determination of NIRS clinical RBE, one geometry tested and one α and β couple for the setting of D_{t}, prediction of TCP for HIT and CNAO protocols were tried. From the published CNAO clinical protocol it is known that: $d_{\mathrm{m}}^{\mathrm{LEM\ I-ref}} = d_{\mathrm{m}}^{\mathrm{NIRS}}$(NIRS and MedAustron (2013)). The re-calculation gave TCP = 91.3 %, which is quite similar to published bNED from NIRS high risk cancer. This is coherent with the methodology chosen at CNAO, which reproduces as close as possible the NIRS protocol in term of depth-dose profile, beam ports and ADT. From the HIT clinical protocol, it is known that $d_{\mathrm{m}}^{\mathrm{LEM\ I-ref}} < d_{\mathrm{m}}^{\mathrm{NIRS}}$. For low and intermediate risk, TCP equals respectively 62.2% and 80.3%. Hence, the TCP estimations calculated were lower than bNED published by NIRS.

The "optimized" values of D_{t} proposed in this work seem acceptable within the same irradiation conditions (laterally-opposed fields), with patients gathered in the same risk group and with the same ADT treatment as published by NIRS. These analyses also emphasized the strong interdependence between the LEM input parameter (α, β and D_{t}), the TCP model and the clinical protocol chosen for outcome predictions. Hence, optimum sets of parameters will be only found with more clinical results from carbon-ion therapy and not with conventional radiotherapy. Besides, the impact of ADT on TCP when combined with a radiation therapy needs to be further understood and modeled for both conventional radiotherapy and carbon-ion therapy.

Bibliography

Böhlen, T. T., Brons, S., Dosanjh, M., Ferrari, A., Fossati, P., *et al.* (2012). Investigating the robustness of ion beam therapy treatment plans to uncertainties in biological treatment parameters. *Phys Med Biol*, 57(23):7983–8004. 7

Brenner, D. J. and Hall, E. J. (1999). Fractionation and protraction for radiotherapy of prostate carcinoma. *Int J Radiat Oncol Biol Phys*, 43(5):1095–1101. 7

Fossati, P., Molinelli, S., Matsufuji, N., Ciocca, M., Mirandola, A., *et al.* (2012). Dose prescription in carbon ion radiotherapy: a planning study to compare nirs and lem approaches with a clinically-oriented strategy. *Phys Med Biol*, 57(22):7543–7554. 7

Fowler, J. F., Toma-Dasu, I., and Dasu, A. (2013). Is the alpha/beta ratio for prostate tumours really low and does it vary with the level of risk at diagnosis? *Anticancer Res*, 33(3):1009–1011. 7

Ishikawa, H., Tsuji, H., Kamada, T., Akakura, K., Suzuki, H., *et al.* (2012). Carbon-ion radiation therapy for prostate cancer. *Int J Urol*, 19(4):296–305. 7

Kanai, T., Endo, M., Minohara, S., Miyahara, N., Koyama-ito, H., *et al.* (1999). Biophysical characteristics of himac clinical irradiation system for heavy-ion radiation therapy. *Int J Radiat Oncol Biol Phys*, 44(1):201–210. 7

Kanai, T., Matsufuji, N., Miyamoto, T., Mizoe, J., Kamada, T., *et al.* (2006). Examination of gye system for himac carbon therapy. *Int J Radiat Oncol Biol Phys*, 64(2):650–656. 7

Karger, C. P., Peschke, P., Scholz, M., Huber, P. E., and Debus, J. (2013). Relative biological effectiveness of carbon ions in a rat prostate carcinoma in vivo: comparison of 1, 2, and 6 fractions. *Int J Radiat Oncol Biol Phys*, 86(3):450–455. 7

Kase, Y., Kanai, T., Matsumoto, Y., Furusawa, Y., Okamoto, H., *et al.* (2006). Microdosimetric measurements and estimation of human cell survival for heavy-ion beams. *Radiat Res*, 166(4):629–638. 7

NIRS and MedAustron, editors (2013). *Proceedings: NIRS and MedAustron Joint Symposium on Carbon Ion Radiotherapy*. 7, 7

Oliveira, S. M., Teixeira, N. J., and Fernandes, L. (2012). What do we know about the / for prostate cancer? *Med Phys*, 39(6):3189–3201. 7

Steinsträter, O., Grün, R., Scholz, U., Friedrich, T., Durante, M., *et al.* (2012). Mapping of rbe-weighted doses between himac- and lem-based treatment planning systems for carbon ion therapy. *Int J Radiat Oncol Biol Phys*, 84(3):854–860. 7

Tucker, S. L. and Thames, H. D. (1989). The effect of patient-to-patient variability on the accuracy of predictive assays of tumor response to radiotherapy: a theoretical evaluation. *Int J Radiat Oncol Biol Phys*, 17(1):145–157. 7

Vogelius, I. R. and Bentzen, S. M. (2013). Meta-analysis of the alpha/beta ratio for prostate cancer in the presence of an overall time factor: bad news, good news, or no news? *Int J Radiat Oncol Biol Phys*, 85(1):89–94. 7

Conclusion and perspectives

Conclusion and perspectives

In carbon-ion beams, biological effects vary along the ion track, hence, to quantify them, specific radiobiological models are needed. One of them, the LEM I, is implemented in TPS clinically used in European particle therapy centers. From physical properties of ion radiation, the LEM calculates survival probabilities of the cell or tissue type under study, provided that some determinant input parameters are initially defined. Mathematical models can be used to predict, for instance, TCP and then evaluate treatment outcomes.

Prostate cancer has been treated for several years at NIRS in Japan. Their long-term clinical experience is very valuable for the initiation of clinical trials in European carbon-ion therapy centers. Some very interesting approaches have been published to *map* the RBE between the NIRS model and the LEM. However, the mapping was limited to one set of input parameters for LEM I and only on absorbed dose distribution and not on clinical outcomes.

This work has tried to develop methodologies to, first, evaluate the influence of the LEM I input parameters on the TCP predictions and, secondly, draw strategies to optimize clinical protocols in the specific case of prostate cancer.

First, several published input parameters for LEM I and their combination were tested. Their influence on the dose distribution calculated in a water phantom and in a patient geometry was evaluated using the TPS TRiP98. Changing input parameters induced clinically significant modifications of mean dose (up to a factor of 3.5), spatial dose distribution, and TCP predictions (up to factor of 2.6 for D_{50}). TCP predictions were found more sensitive to the parameter threshold dose (D_t) than to the biological parameters α and β. Additionally, an analytical expression was derived to correlate α, β and D_t, and has emphasized the importance of $\frac{D_t}{\alpha/\beta}$.
The study of the LEM I parameters on the prediction of the tumor control probability for prostate cancer was essential for the quantification of the sensitivity of LEM I. To our best knowledge, the present work on sensitivity analysis with TCP modeling for carbon-ion treatment based on the LEM I and on published α, β and D_t estimates for prostate cancer, was the first to be presented (Chanrion *et al.* (2014)).

Secondly, two methods were tested to find LEM I input parameters for prostate cancer based on NIRS published results data in term of absorbed dose profiles and bNED. To start with, a simple approach was chosen to obtain the RBE at the middle of the SOBP following the NIRS radiobiological model. This approach seemed to be a pragmatic way to make use of published

clinical protocols from NIRS, since the report of results in publications lacks details on the dose delivery of such protocols. Some dosimetric indexes of the absorbed dose or radiobiological indexes, such as the equivalent uniform biologically effective dose (EUBED, Jones and Hoban (2000)), could be reported.

Method A had the goal to find a D_{t} that would simulateneously tie-in LEM and NIRS protocol in term of prescribed and absorbed dose in the middle of the SOBP. In other words, we tried to parameterize LEM I so that the prescription of a biological dose based on LEM would be the same as NIRS while the absorbed dose profiles will be same as published by NIRS. Such parameterization was not found with α and β parameters from Brenner and Hall, and, as several authors concluded, there is no possibility to compare directly the figure of a biological dose prescribed with the NIRS model or with the LEM. Hence, depending on the institution, the treatment protocol and the radiobiological model used, the prescribed dose will have to be found and refine with the continual feedback from clinical results, for instance by initiating dose-escalation trials.

The method B was based on the reproduction of the NIRS irradiation fields. We chose a pragmatic and simple methodology to try to reproduce these fields with published HSG parameters for the input parameters of LEM I. Hence, profiles could be calculated for all NIRS published protocols. Based on published bNED and for defined boundary conditions (protocol and geometry), "optimized" D_{t} were proposed for the treatment of prostate cancer. One particular profile calculated with LEM I_{HSG} could be compared with a published profile from NIRS. After finding a difference in shape, the sensitivity of TCP to the dose profile was studied. Fortunately, this sensitivity was found to be low, and we believe that the "optimized" D_{t} we proposed seem acceptable when the treatment is delivered with two lateral opposed beams.

Our results also brought out that the presence of ADT with carbon-ion therapy has an influence on the set of the D_{t} value. Without a clinical estimation of the effect of ADT that could be expressed as S_{ADT}, it seems difficult to evaluate the combined effect of carbon-ion and ADT. Consequently, at this stage, it is not possible to conclude whether carbon-ion therapy has a higher cell killing efficiency depending on the tumor risk. Hence, we can not discuss the hypothesis formulated by Ishikawa *et al.* that carbon-ion therapy alone may have the same effect on the tumor control for any risk groups.

Besides this important conclusion, another result we found for the treatment of prostate is that there seem to be no differences in tumor control for treatments calculated with two lateral oppposed beams delivered per day or just one for the same prescription dose. If this hypothesis is later confirmed by clinical results, this has the potential of simplifying modelization studies and more generally data analysis.

Theoretical predictions of TCP for on-going CNAO and HIT trials can be calculated with the obtained "optimized" D_{t} we proposed. Our estimates and the methodology associated, will only be confirmed or infirmed when the clinical results become available. Furthermore, D_{t} estimates can still be refined by doing more treatment planning studies on several *in silico* patient cases.

Finally, our results have shown that α, β, N_0, D_{t} and the clinical protocol make a consistent whole. The clinical experience from conventional EBRT with photons is not enough to estimate α, β and D_{t}. Only feedback from carbon-ion treatments will improve the radiobiological

modeling of carbon-ion therapy with LEM I.

Promising therapy techniques can only become widely available when there are underpinned by several evidence-based medicine studies. This means, that world clinical experience in carbon-ion therapy should be fairly shared. However, this arcadian but ambitious idea faces several obstacles: the reporting of dose should be harmonized between institutions and reliable techniques to convert doses based on different radiobiological models should be found and approved. On the strict clinical point of view, well-defined patient groups should be included in future carbon-ion trials, with fractionation schemes and well-defined end-points. The improvement of radiobiological models for particle treatment planning systems will only be achieved after these obstacles have been overpassed.

Bibliography

Chanrion, M.-A., Sauerwein, W., Jelen, U., Wittig, A., Engenhart-Cabillic, R., *et al.* (2014). The influence of the local effect model parameters on the prediction of the tumor control probability for prostate cancer. *Phys Med Biol*, 59(12):3019–3040. 7

Jones, L. C. and Hoban, P. W. (2000). Treatment plan comparison using equivalent uniform biologically effective dose (eubed). *Phys Med Biol*, 45(1):159–170. 7